

Cite this: *Chem. Soc. Rev.*, 2012, **41**, 1218–1260

www.rsc.org/csr

CRITICAL REVIEW**P450_{BM3} (CYP102A1): connecting the dots****Christopher J. C. Whitehouse, Stephen G. Bell and Luet-Lok Wong****Received 18th July 2011*

DOI: 10.1039/c1cs15192d

P450_{BM3} (CYP102A1), a fatty acid hydroxylase from *Bacillus megaterium*, has been extensively studied over a period of almost forty years. The enzyme has been redesigned to catalyse the oxidation of non-natural substrates as diverse as pharmaceuticals, terpenes and gaseous alkanes using a variety of engineering strategies. Crystal structures have provided a basis for several of the catalytic effects brought about by mutagenesis, while changes to reduction potentials, inter-domain electron transfer rates and catalytic parameters have yielded functional insights. Areas of active research interest include drug metabolite production, the development of process-scale techniques, unravelling general mechanistic aspects of P450 chemistry, methane oxidation, and improving selectivity control to allow the synthesis of fine chemicals. This review draws together the disparate research themes and places them in a historical context with the aim of creating a resource that can be used as a gateway to the field.

1 Context**1.1 Introduction**

P450_{BM3} (CYP102A1) belongs to the P450 cytochrome (CYP) superfamily of haem *b*-dependent monooxygenases, members of which are found in virtually every organism. P450 enzymes have a highly conserved tertiary structure and share a characteristic protein fold, but only one amino acid is invariant—the cysteine residue to which the prosthetic group is axially ligated.¹

*Department of Chemistry, University of Oxford, Inorganic Chemistry Laboratory, South Parks Road, Oxford OX1 3QR, UK.
E-mail: luet.wong@chem.ox.ac.uk; Fax: (+44) 1865 272690;
Tel: (+44) 1865 272619*

**Christopher J. C. Whitehouse**

As an undergraduate at the University of Oxford, Christopher Whitehouse worked under Professor Allen Hill on the NMR of metal-substituted azurins. After more than twenty years away from science, he returned to Oxford to join the Cytochrome P450 team headed by Dr Luet Wong, completing a D. Phil on P450_{BM3} in 2010.

The CO-bound ferrous form of the enzyme has a distinctive 450 nm absorption band from which the superfamily takes its name. The human genome project has so far identified 63 human P450 genes, and there are as many as 286 in the plant *Arabidopsis thaliana*.² Prokaryotes are less well represented: *Escherichia coli*, in which P450s are usually expressed for research purposes, has none, while *Mycobacterium tuberculosis* has ca. 20.³ P450s are also found in archaea such as *Sulfolobus solfataricus*, suggesting they are of ancient origin.⁴ One possibility is that they evolved in response to the toxicity risk posed by rising planetary dioxygen levels and had functions that revolved around the lipids that formed the cell membranes of early microbes.

P450s catalyse the oxidation of a broad array of endogenous and exogenous organic substrates, allowing them to perform

**Stephen G. Bell**

Dr Stephen Bell was born in Belfast and obtained his BA (Chemistry, 1995) and D. Phil (Chemistry, 1999) from the University of Oxford. His research interests include bacterial cytochrome P450 enzymes and their electron transfer proteins for applications in biocatalysis. He has also studied zinc and copper binding human metallothioneins. He is currently the Inorganic Chemistry Lecturer at Brasenose College, University of Oxford, and takes up a lectureship at the University of Adelaide in January 2012.

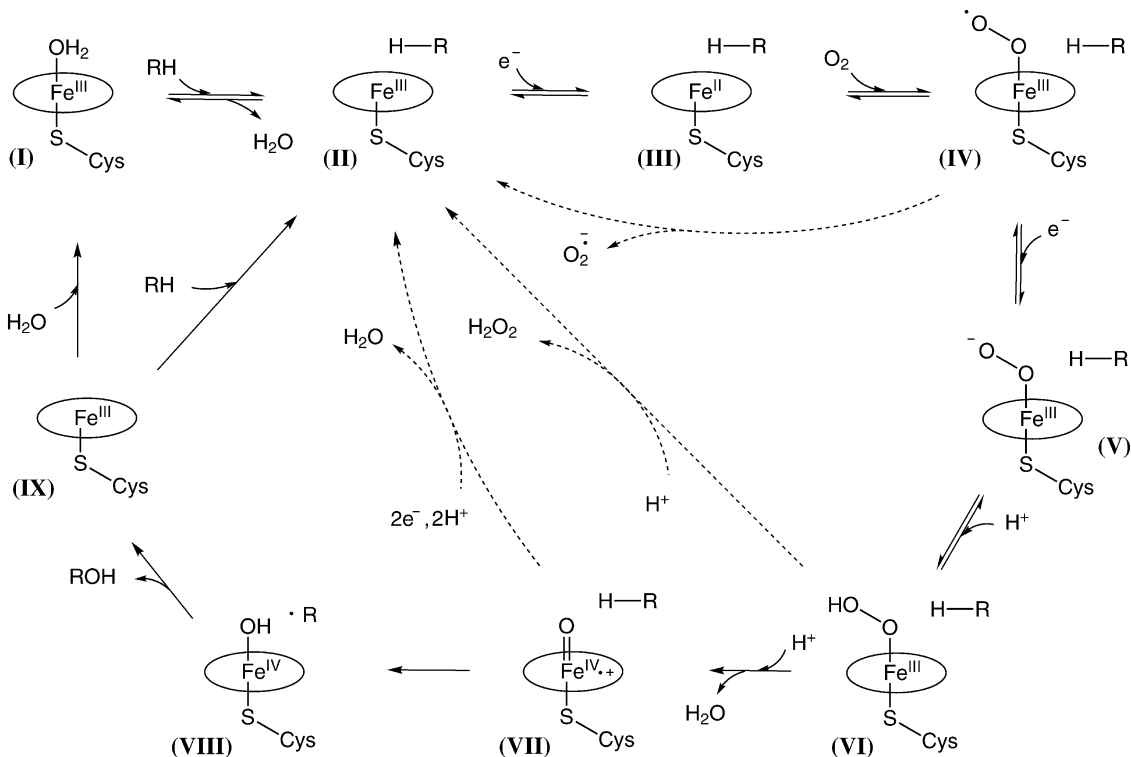


Fig. 1 The P450 catalytic cycle.

physiological roles as varied as steroid hormone synthesis in mammals, and herbicide resistance in plants. They are best known for breaking down xenobiotics—including pharmaceuticals—in humans, but also defend insects against plant toxins, feature prominently in the metabolic and synthetic pathways of bacteria where present, and are involved in the synthesis of antibiotics in bacteria and fungi. Those with anabolic functions are often substrate-specific, but others—notably those involved in the detoxification and metabolism of xenobiotics—are more promiscuous, versatility being an asset in such roles. The signature reaction of a P450 is the insertion of a single oxygen atom from molecular dioxygen into a carbon–hydrogen bond to give the corresponding alcohol, the second oxygen atom being reduced to water. Other activity types include olefin epoxidation, ring

expansion, heteroatom oxidation and dealkylation, and dehydrogenation across C–O, C–N and C–C bonds, as well as carbon–carbon bond formation and cleavage.⁵

1.2 The catalytic cycle

The P450 catalytic cycle, which is shown in Fig. 1, has been widely studied and extensively debated, as a result of which the details are now broadly agreed. In the resting state (I), the ferric iron atom is six-coordinate, the porphyrin system supplying four equatorial nitrogen ligands, while a water ligand occupies the axial position *trans* to the proximal thiolato ligand. The arrival of a viable substrate in the active site results in the loss of the axial water ligand (II), whether through direct displacement or in response to induced conformational changes. This causes the ferric spin state to increase from $S = 1/2$ (low-spin) to $S = 5/2$ (high-spin), a transition that can be monitored spectrophotometrically since the Soret band, which arises from a $\pi \rightarrow \pi^*$ electronic transition in the delocalised π system of the porphyrin ring, undergoes a blue or “type I” shift from *ca.* 418 nm to *ca.* 390 nm. At the same time, the haem reduction potential becomes more oxidising. A single electron supplied almost invariably by a reduced pyridine nucleotide (NADH or NADPH) is shuttled to the haem iron *via* electron transfer partners, reducing it to the ferrous state (III), whereupon dioxygen binds to yield an oxy-complex (IV). A second electron is transferred, creating a ferric peroxy complex (V). Protonation of the terminal oxygen atom gives “Compound 0”, a hydroperoxy adduct (VI). A second protonation triggers water loss *via* the heterolytic cleavage of the O–O bond to give “Compound I” (VII), a ferryl species thought to be the active entity in most P450 oxidations, which has recently been characterised.⁶



Luet-Lok Wong

Dr Luet Lok Wong is a University Lecturer in the Department of Chemistry and Fellow and Tutor in inorganic chemistry at St Hugh's College, University of Oxford, UK. His main research interests are in biocatalysis using metalloenzymes, specifically in the discovery, structural biology, mechanism, function, protein–protein recognition interactions and protein engineering of haem monooxygenase enzymes. The research work has implications and applications in alkane oxidation, fine chemical synthesis, drug metabolism and bioremediation.

NAD(P)H consumption is not necessarily fully coupled to product formation.⁷ If dioxygen binding is hindered, the second electron transfer may be too slow to prevent superoxide being lost from (**IV**) (superoxide uncoupling). If (**VI**) is protonated at the iron-bound oxygen because a loosely fitting substrate fails to prevent water encroachment, hydrogen peroxide loss is possible (peroxide uncoupling). If a substrate binds with no hydrogen atom conveniently positioned for abstraction, the oxygen “atom” in (**VII**) may be reduced to water (oxidase uncoupling). High peroxide concentrations cause the peroxide uncoupling pathway to reverse, a reaction known as the peroxide shunt. This allows oxidation to be driven using peroxide rather than NAD(P)H/O₂/H⁺ as in chloroperoxidase (CPO), a related haem enzyme with axial cysteine coordination, and the CYP152 family. In hydroxylation reactions, a hydrogen atom is abstracted from the substrate following the formation of Compound I to give (**VIII**), after which “radical rebound” sees OH[•] (including the abstracted atom) and the substrate radical combine, giving the impression that oxygen has been inserted into the C–H bond. The product leaves the active site, returning the enzyme to the pentacoordinate ferric state (**IX**). Hydrogen abstraction also initiates the desaturation pathway, but does not occur in the epoxidation of unsaturated linkages, including those of aromatic systems, which are attacked by (**VII**) directly.⁵ Mechanistic deviations from the principal pathway are known. The possible involvement of cationic intermediates has been probed using P450_{BM3}.^{8,9} The enzyme has also been the subject of studies undertaken to establish whether Compound 0 rather than Compound I is the reactive intermediate in certain oxidations,^{10–13} and to gain insight into the nature of Compound I.^{14,15}

1.3 Discovery and early history of CYP102A1 (P450_{BM3})

CYP102A1 was discovered in the early seventies by Fulco *et al.*, who identified it as a soluble medium- to long-chain fatty acid hydroxylase that required only NADPH and oxygen to function.^{16–19} As the third²⁰ P450 to be isolated from *B. megaterium*, the enzyme was designated P450_{BM3}, a name by which it continues to be widely known. Hydroxylation took

place exclusively at sub-terminal positions, a specificity shared by most bacterial P450s (the CYP153 family being a notable exception) but not by the CYP4A sub-family of microsomal fatty acid hydroxylases, which are ω-hydroxylators. Pentadecanoic acid was the preferred saturated straight-chain substrate, activity falling away as the chain-length increased or decreased.¹⁶ Fatty amides and alcohols,²¹ hydroxylated fatty acids^{22–24} and ω-oxo fatty acids²⁵ were also accepted as substrates, as were unsaturated fatty acids,^{16,21,26} which could also be epoxidised.^{27–29} The product profiles given by a selection of fatty acid substrates are shown in Table 1. With unsaturated fatty acids, the epoxidation/hydroxylation partition was sensitive to pH²⁸ and also to antibody binding.³⁰ Characterisation of the purified 119 500 Da^{31,32} enzyme revealed that the 55 kDa P450 (or “haem”) domain (BMP) was fused to a 65 kDa “reductase” domain (BMR) containing two prosthetic flavin groups, FAD and FMN, in an equimolar ratio.^{30,33,34} In addition to catalysing oxidative chemistry, the enzyme was therefore capable of effecting rapid reduction of artificial electron acceptors such as ferricyanide or cytochrome *c* via electron transfer from BMR. The *CYP102A1* gene was cloned into *E. coli*^{35,36} and sequenced.³⁷

Both domains resembled microsomal enzymes.³⁷ BMR, like sulphite reductases, shared sequence similarities with mammalian cytochrome P450 reductase (CPR).^{41,42} BMP aligned well with eukaryotic P450s such as the CYP2A sub-family and the CYP4A fatty acid hydroxylases, save for the deletion of a region at the N-terminus end assumed to code for membrane binding (typically 25–50 residues).⁴³ For a time it was used as a template for the sequence analysis of eukaryotic P450s^{44,45} and in homology modelling⁴⁶ as the crystal structure (section 3.1) became available at a relatively early stage. When compared to prokaryotic P450s, BMP exhibited minor topological differences and CO-binding behaviour.^{47–49} The most conspicuous contrast was that other bacterial isoforms typically received electrons from discrete protein partners rather than *via* an integrated flavin domain. The unprecedented self-sufficient structure of P450_{BM3} meant that electron transfer to the haem

Table 1 Product distributions in the oxidation of fatty acids by P450_{BM3}

Fatty acid	= or ≡ bonds	% Hydroxylation (% R or % de)			% Epoxide or carboxylic acid			Ref.
		(ω-1)	(ω-2)	(ω-3)	(% S, R)	location		
Lauric (C12)	0	36 (98)	30 (93)	34 (82)				21, 38
Tridecanoic (C13)	0	17	65	18				
Myristic (C14)	0	44 (94)	28 (93)	28 (87)				
Pentadecanoic (C15)	0	32 (93)	49 (95)	19 (74)				
Palmitic (C16)	0	31 (95)	48 (95)	21 (74)				
Heptadecanoic (C17)	0	49	35	16				
Octadecanoic (C18)	0	39	47	14				
Tridecanoic (C13)	1	0	97	0	3	12–13		26
Octadecenoic (C18)	1	0	95	0	5	17–18		
Octadecynoic (C18)	1	0	100	0	0	17–18		
Arachidonate (C20)	4	0	80 (96)	0	20 (99)	14–15		29
Eicosapentaenoic (C20)	5	0	0	0	100 (97)	17–18		
Eicosatrienoic (C20)	3	18	39	43	0			
12-Methylmyristic (C15) ^a	0	85 (98)	2	13 (92)				39
13-Methylmyristic (C15) ^a	0	15	83	2				
14-Methylpalmitic (C17)	0	85 (99)	2	13 (92)				
15-Methylpalmitic (C17)	0	9	89	2				

^a Contrasting product distributions have been reported by researchers using racemic substrates.⁴⁰

iron was not contingent on the enzyme encountering a redox partner, either in solution or bound at an adjoining position on a membrane. Partly for this reason, activity levels were up to three orders of magnitude higher than in other P450 fatty acid hydroxylases.⁵⁰

Other self-supporting P450s have since been identified, and these have been reviewed.⁵¹ CYP505 (P450_{foxy}), a sub-terminal fatty acid hydroxylase from the fungus *Fusarium oxysporum*, was the first to be recognised.^{52,53} Further examples include ferredoxin/flavin/P450 fusions from species of *Burkholderia* and *Ralstonia metallidurans*⁵⁴ and CYP116 family members such as those found in *Rhodococcus* sp. (P450_{RhF})⁵⁵ and *Rhodococcus ruber* DSM 44319.⁵⁶ Nitric oxide synthase (NOS), a soluble eukaryotic FAD- and FMN-containing haemoprotein that oxidises L-arginine to citrulline and nitric oxide,⁵⁷ and P450_{BM3} have remarkably similar architectures. Interest in P450_{BM3} began to widen in the early nineties.^{50,58–61} Alternative expression and purification methods were reported,^{50,62–66} and it was established that the porphyrin system could be removed from its binding site and replaced without impairing activity—a contrast to CYP101A1 (P450_{cam}),

the other widely researched bacterial P450 of the time.⁶⁷ Synopses of the early P450_{BM3} literature exist,^{20,68–70} but with 20–30 papers now appearing annually, a figure that has roughly doubled each decade since the enzyme's discovery, a formidable research archive has built up, and recent reviewers have preferred to focus on selected topics^{71–74} or place the enzyme into context within the wider P450 field.^{75–78}

1.4 Possible physiological roles

The precise physiological role of the enzyme is obscure. For many years, the natural substrates were assumed to be straight-chain fatty acids, and these have been copiously researched, with the result that over thirty different NADPH consumption rates (N , k_{cat} or V_{max}) have been published for lauric acid (C12), one of the more soluble exemplars, ranging from 1.4 s^{-1} to 86 s^{-1} (Table 2). However, NADPH utilisation is not fully coupled to product formation when saturated fatty acids are oxidised *in vitro*,^{30,79,80} as it is in camphor oxidation by P450_{cam}. Moreover, whereas P450_{cam} expression can be induced in *Pseudomonas putida* by camphor, the natural substrate, P450_{BM3} expression is not induced in *B. megaterium* by saturated straight-chain fatty acids⁸¹

Table 2 Fatty acid oxidation and binding by P450_{BM3}

Lauric acid (C12)				Myristic acid (C14)				Palmitic acid (C16)				Arachidonic acid (C20;4=)				Buffer	pH	$T\text{ (}^{\circ}\text{C)}$	Ref.
N	k_{cat}	K_M	K_D	N	k_{cat}	K_M	K_D	N	k_{cat}	K_M	K_D	N	k_{cat}	K_M	K_D				
26	77 ^a	110			77 ^a	10			77 ^a	2.0						P	8	19, 22, 23	
							0.5									P	7	20	30 ^b
6.7				26,38												P	8	58, 94	
1.4		40	256	23				78	27			10				P	7.4	79, 94	
												5	39–61	72	1.2–3	M/2	7.4	25/RT	50, 60, 95 ^b
								25							P/2	7.4	25	100	
15		28	250												P/2-K	7.4	RT	101	
20,21	33 ^a	115													P	8	30	61	
16			22												M/5-K	7.4	30	102–104	
68	86	288	241												M/5-K	7.4	25	105	
	84	322	370												95	285 ^c	4.7	3.6	
	46	87	89	81 ^c	37	6.9		77 ^c	12	11					273 ^c	5.1	0.6	M/5-K 7.4 30 108, 109	
	23 ^a	145		45 ^a	16										P	7.4	25	63	
25,26	130	290													P	8	23/27	67, 110	
26	136	270		55	7	23		81	1.4	5					P	8	27	31, 111	
				52	8										P	8	24		
18	28	265	270							0.1					P/2	8	30	112	
	33 ^a	180													P	7.6	25	113	
12	57 ^a							50,54	68 ^a						T	7.7	25	32, 114, 115	
															P	7.4	RT	92	
15			40,41					39,40							P	8		116, 117	
8,3,9,3			27,43				0.6,2.2								SP	8/8.3	25	116, 117	
	33	74	135												P/2	7.5		118, 119 ^c	
44															P	8	20	120	
3.2															P	7.4	37	121	
20			28												P/1000	7.4	30	122	
36															T	8.2		123	
															P	8		124 ^c	
46	17			1.3	27					0.2					P	7.4	37	80	
	73	239		94	79 ^d			72	87	52 ^d					T/2	7.4	30	125–127 ^c	
	82	170		138	70				122	83					P	7.4	30	127 ^c	
	77	230							91,98	42,65 ^d					P/2	7.4	30	125–127 ^c	
									32	31 ^d					P/10	7.4	30	127 ^c	

N: NADPH consumption rate (in nmol (nmol P450) $^{-1}$ s $^{-1}$). k_{cat} data are in units of s $^{-1}$; K_M and K_D are in μM . ^a V_{max} . ^b Based on O₂ consumption or product formation rather than NADPH consumption. ^c Substrate stock in organic co-solvent. ^d K_{H_2} . ^e Four binding sites indicated; RT: room temperature. Buffers at 100 mM unless otherwise specified (/2 = 50 mM etc.); P: phosphate; M: MOPS; T: Tris/HCl; K: KCl. Data grouped by research laboratory. See section 5.2.2 for discussion.

or monounsaturated acids. Polyunsaturated analogues such as linoleic and arachidonic acids, by contrast, do induce P450_{BM3} expression,^{82,83} binding 1000-fold more strongly to the repressor protein, Bm3R1.^{84–89} Given the important homeostatic role in the arachidonic acid cascade played by eukaryotic P450 monooxygenases,⁹⁰ it is interesting that P450_{BM3} appears to be more active towards arachidonic acid than other straight-chain analogues.²⁹ However, unsaturated fatty acids are toxic to *B. megaterium* if applied exogenously,⁸² and there is evidence to suggest that they are synthesised only as a transient response to cold, and even then in small quantities.⁹¹ This raises the possibility that one function of the enzyme may be to detoxify the xenobiotic lipids produced by plants. Branched-chain saturated fatty acids, which play a key role in the regulation of membrane fluidity, also induce P450_{BM3} expression,⁹² and it has been argued^{39,40} that these are more likely to be the enzyme's true substrates, since they account for almost 90% of the fatty acid content of *B. megaterium*.⁹³

Barbiturates, though not accepted as substrates by P450_{BM3},^{63,128} are also powerful inducers of the enzyme,^{81,128} particularly if lipophilic,¹²⁹ as are certain acetylureas^{130,131} and non-steroidal anti-inflammatory drugs such as 17 β -estradiol^{132,133} and ibuprofen.¹³⁴ Ibuprofen also induces other enzymes associated with oxidative stress response in *Bacillus*, including catalase and glucose-6-phosphate dehydrogenase (G6PDH).¹³⁵ However, barbiturate induction is inhibited by certain phytochemicals,¹³⁶ so it may be inappropriate to rely too heavily on such studies when seeking to interpret the function of the enzyme. In separate research, it has been established that *N*-acyl amino acids¹⁰⁰ and their homoserine and homoserine lactone derivatives¹⁰¹ bind more tightly to P450_{BM3} than the corresponding fatty acids, and are also rapidly oxidised. *N*-acyl homoserine lactones, which are used by bacteria to sense and signal population density, become *ca.* 20-fold less active when sub-terminally hydroxylated. Although it is unlikely that P450_{BM3} regulates density signalling in a physiological context, this finding has raised the possibility of the enzyme playing a part in a pathogen resistance system for use in genetically modified crops.¹³⁷

1.5 The CYP102A sub-family

Fulco trawled unsuccessfully for P450_{BM3}-like proteins in other species of *Bacillus*,¹³⁸ but showed good instincts in searching as current microbial genome databases reveal that there are more than fifty homologues of the *CYP102A1* gene distributed among bacteria (CYP102) and fungi (CYP505). Several of the corresponding CYP102A sub-family proteins have been expressed and characterised, including CYP102A2 and A3 from *B. subtilis*,^{139–141} A5 from *B. cereus*¹⁴² and A7 from *B. licheniformis*,¹⁴³ all of which were more active than A1 with preferred fatty acid substrates. A14 from an uncultured soil bacterium was less active than A1 with fatty acids, but accepted naphthalene and phenanthrene as substrates,¹⁴⁴ while A2 was significantly more active towards 1,4-naphthoquinone and sodium dodecyl sulphate than lauric acid.^{145,146} A2 and A3, unlike A1, did not appear to play a physiological role in fatty acid detoxification.¹⁴⁷ Publications have recently begun to appear on other CYP102 sub-family members.¹⁴⁸

Biophysical property contrasts were apparent within the 102A sub-family. A3 was less stable than A1 in saline solution,

hampering purification.¹³⁹ A7 was less thermostable than A1,¹⁴³ and the haem domains of A2 and A3 less stable than BMP,¹⁴⁹ but the A3 reductase domain was more thermostable than BMR.¹⁵⁰ A3¹³⁹ and A7¹⁴³ were more tolerant than A1 of DMSO, a co-solvent commonly employed to enhance substrate solubility.¹⁵¹ A2 was an inefficient haem incorporator.^{140,141} Preincubation with a substrate (section 5.2.2) caused no change to activity in A3,¹⁵² but resulted in a 60% activity increase in A1 and a 40% decrease in A2.¹⁴¹ Electron transfer through the reductase domain (section 2.2) was significantly faster in A5 than in A1 or A2.¹⁴² A2 and A3 have been engineered,^{139,145,152} as have A5 and A7.¹⁵³ The homologue of a desirable mutation discovered in A3 was subsequently found to be effective in A1,¹⁵⁴ so cross-engineering opportunities exist within the subfamily.

An alignment of the A1–A15 haem domain sequences (Fig. 2) shows that the F/G and G/H loops, the first half of the G-helix and the domain extremities (residues 1–32 and 447–473) are poorly conserved. It is probably no coincidence that these regions are relatively plastic.¹⁵⁵ This suggests that they interact weakly with other regions of the enzyme, potentially permitting a higher incidence of mutation. It is also worth bearing in mind that mammalian isoforms typically contain insertions at the N-terminus end and in the F/G and/or G/H loops relative to the CYP102A sub-family.⁴³ The same is true of the J/J' loop, where A6 and A10–A14 show a three-residue insertion relative to the other sub-family members. Highly conserved regions include the B'/C loop and the C-helix, the E-helix and most of the E/F loop, much of the I-helix and the β 5-sheet that precedes it, and the proximal loop together with the region to the N-terminus side (residues 391–402). The six regions identified as substrate recognition sites (SRSs) across the P450 superfamily using sequence alignment techniques¹⁵⁶ display a range of conservation levels. SRS4 (residues 253–271) is almost fully conserved, and there is relatively little variation in SRS6 (434–441). The C-terminus portion of SRS1 (69–92) is well conserved, but the N-terminus portion exhibits a number of discontinuities. Residues 72 and 73 are Glu-Gly or Arg-Gly in all but four isoforms, for instance, but Gly-Lys in A3 and A7 and Ser-Gln in A1, while proline is used at residue 74 in the B'-helix of A10 and A11 rather than the usual Ala or Gly. SRS2 (181–188) and SRS5 (325–335) each contain interesting anomalies. The C-terminus end of SRS5 has the consensus sequence Tyr-Gly-X-Ala-Pro in A6 and A10–A14, as against Phe-Ser-Leu-Tyr-Ala in the remaining isoforms, for instance. SRS3 (200–208), which is almost entirely unconserved, should probably not be viewed as an SRS in P450_{BM3}.⁴⁸

A recent study of a group of naturally occurring CP102A1 variants has provided some useful context for this field.¹⁵⁷ Divergences of >50-fold in palmitic acid (C16) binding affinity and >25-fold in lauric acid hydroxylation rates were recorded, while two of the nine distinguishable strain types showed slight activity towards phenacetin, a non-natural substrate. There were also significant contrasts in thermostability and in the rates of ferricyanide and cytochrome *c* reduction, reflecting the fact that the majority of the variable residues were in the reductase domain and the linker region.

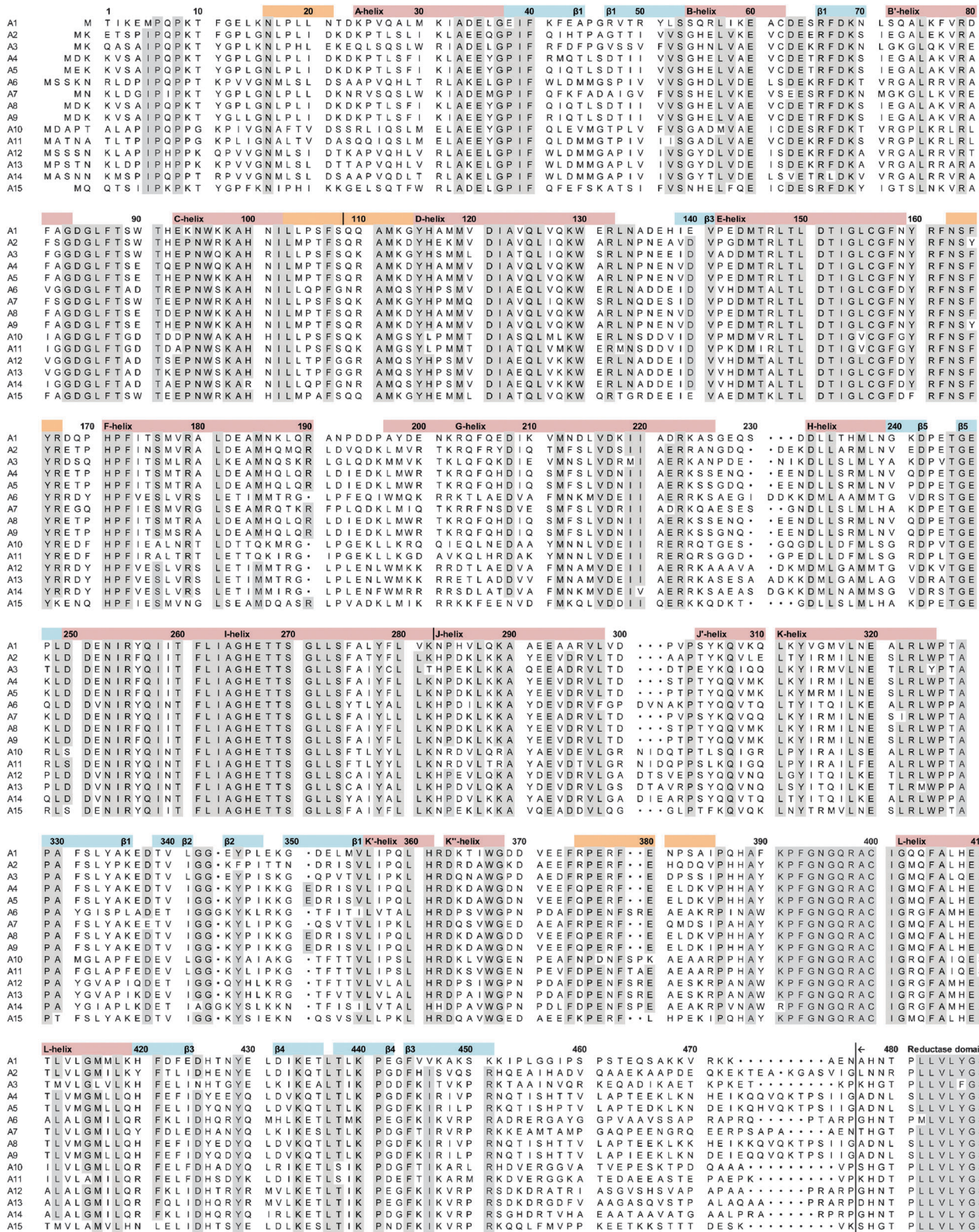


Fig. 2 Haem domain sequence alignments for the CYP102A sub-family. CYP102A1 numbering applies. Pink is used to delineate α -helices, orange for 3_{10} -helices, and blue for regions of β -sheet.⁴⁸ A1 was from *B. megaterium* (NCBI code: J04832); A2 from *B. subtilis* (D87979); A3 from *B. subtilis* (U93874); A4 from *B. anthracis* str. Ames (AAP27014); A5 from *B. cereus* ATCC 14579 (AAP10153); A6 from *Bradyrhizobium japonicum* USDA 110 (BAC48147); A7 from *B. licheniformis* ATCC 14580 (AAU24352); A8 from *B. thuringiensis* serovar konkukian str. 97-27 (AAT62301); A9 from *B. weihenstephanensis* KBAB4 (ZP_01184381); A10 from *Erythrobacter litoralis* HTCC2594 (YP_456909); A11 from *Erythrobacter* sp. NAP1 (ZP_01041731); A12 from *Rhodopseudomonas palustris* HaA2 (YP_487251); A13 from *Rhodopseudomonas palustris* HaA2 (YP_568957); A14 from an uncultured soil bacterium (ABD83817); and A15 from *B. pumilus* ATCC 7061 (ZP_03053227).

2 Function studies

2.1 Domains and the linker region

Once cleaved by trypic proteolysis, BMP and BMR showed little affinity for one another, and fatty acid hydroxylase activity could not be reconstituted.^{34,50} The same was generally the case when the domains were expressed and purified separately,^{58,61,67,103} though outcomes were impacted by the ratios in which they were mixed.⁹⁵ This revealed the importance of the region linking the two domains.¹⁰³ Deleting residues from the linker progressively inactivated the enzyme,⁷⁹ but mutagenesis resulted in a modest enhancement to myristic acid hydroxylation rates, particularly when proline and glycine substitutions were introduced to deter helix formation.⁹⁴ Whereas the linker region in NOS binds calmodulin in a helical conformation,¹⁵⁸ there is therefore no apparent incumbency on the P450_{BM3} linker to exist as a helix. The linker varies significantly in length across the CYP102A subfamily, being nine residues shorter in A1, A10 and A15 than in A4, A5, A8 and A9, which have the longest linkers so far discovered (Fig. 2).

Isolated BMR was less amenable to expression than isolated BMP,⁶² less stable,¹⁵⁹ and susceptible to temperature-induced activity loss.¹⁶⁰ When proteolysed, it yielded two sub-domains, an FMN-binding region and an FAD/NADPH-binding region,^{59,161} both of which could be expressed as separate entities.¹⁶² As in CPR,¹⁶³ the FMN-binding portion exhibited good homology with FMN-containing bacterial flavodoxins, while the FAD portion resembled the FAD-containing spinach ferredoxin reductase.¹⁶⁴ This suggested that the full-length protein had evolved *via* the fusion of at least three separate sub-entities. Neither the FAD domain nor the FMN domain was active individually as a cytochrome *c* reductase,¹⁶² but the FAD domain was 35–80% as active as the full-length enzyme as a ferricyanide reductase.^{162,164} The enzyme showed a lower binding affinity for FMN than for FAD,^{159,164} again as in CPR.¹⁶⁵ Myristic acid was slowly hydroxylated when BMP was mixed with NADPH and FMN,¹⁶⁶ and slight oxidase activity (*ca.* 5%) could be reconstituted with palmitic acid when BMP was mixed with the separated FMN and FAD domains.¹⁶⁷

2.2 Electron transfer^{70,168,169}

The ability of the isoalloxazine rings of the flavins in BMR to form semiquinones when reduced by one electron is central to their function, as it allows electrons to be shuttled singly to the iron centre. Semiquinone formation was not detected when P450_{BM3} was reductively titrated with NADPH or dithionite,¹⁷⁰ but could be demonstrated using EPR,¹⁰⁵ and was readily observed when the isolated FAD^{161,162} and BMR^{105,171} domains were reduced. As in microsomal CPR,^{165,172} electrons pass from NADPH to FAD and thence to FMN before being shuttled to the haem iron. In CPR, the final step entails the reoxidation of FMNH₂ to the FMNH semiquinone. In P450_{BM3}, by contrast, electrons are supplied to the haem iron *from* the FMNH semiquinone.^{42,171} The reduction potentials of the FMN semiquinone/hydroquinone couples in the two enzymes are accordingly very different.¹⁷³ The discrepancy can be traced to the absence of a single glycine residue between Tyr536 and Asn537 in the FMN binding loop.¹⁷⁴ The insertion of glycine at

this position gave rise to a protein with CPR-like redox behaviour,¹⁷⁵ while deletion of the corresponding glycine in NOS, which has a redox architecture similar to CPR, caused electrons to pass to the haem iron from FMNH rather than from FMNH₂.¹⁷⁶ In P450_{BM3}, the first electron transfer from FADH₂ to FMN results in the simultaneous formation of a red anionic FMNH[−] semiquinone, the haem-reducing species, and a neutral FADH semiquinone, which is blue.^{42,171} A proposal that the anionic semiquinone might be FADH[−] rather than FMNH[−]¹¹⁴ lost support when a red semiquinone was produced in the isolated FMN domain.¹⁷⁷ Reduction potentials were determined for the FMN/FMNH[−] and FMNH[−]/FMNH₂^{2−} couples to remove any residual uncertainty.¹⁷⁸ A significant decrease in palmitic acid hydroxylase activity took place when chloro- or amino-substituted FMN was employed in place of the natural co-factor to alter the FMN reduction potential and, to a lesser extent, in cytochrome *c* reductase activity.¹⁷⁹

That fatty acid oxidation rates were not lowered by the presence of cytochrome *c*, suggested that electron transfer through the BMR domain was not rate-limiting to hydroxylase activity.^{30,180} Stopped-flow spectrophotometry confirmed that the rates of flavin reduction and semiquinone formation on NADPH addition were rapid even at 5 °C,⁴² and considerably faster at ambient temperature.¹⁰⁵ Substrate binding^{105,113} and dioxygen binding⁴⁹ were also too fast to be rate-limiting—indeed, it is the rapidity with which gaseous diatomic ligands such as dioxygen or CO bind to the haem iron on reduction that allows *k*_f, the rate of the first FMN-to-haem electron transfer, to be determined. (An acceptable estimate for *k*_f can be obtained by measuring the rate at which absorbance at 450 nm increases as a result of Fe^{II}(CO) complex formation following NADPH addition to the substrate-bound enzyme in CO-saturated buffer using stopped-flow techniques.) *k*_f is rate-determining in P450_{cam} providing ferredoxin is in excess, but with P450_{BM3} the position is more complicated. *k*_f values diminished progressively as residues were deleted from the linker region, prompting a proportionate fall in the catalytic rate, *k*_{cat}, but the latter was roughly an order of magnitude lower than the former.⁷⁹ This suggested that a catalytic step influenced by related factors such as the second FMN-to-haem electron transfer might be rate-limiting. Electrons passed significantly more rapidly to the haem iron when bound with myristate than with laurate.¹⁰⁵ Again there was correlation between *k*_f and *k*_{cat}, and it was concluded that reaction rates might be influenced by a range of steps, including both FMN-to-haem electron transfer rates and also product release. A more detailed study indicated that *k*_f was largely rate-limiting with laurate, but substantially less influential with palmitate, myristate falling between the two extremes.¹²⁷

FMN-to-haem electron transfer at 18 s^{−1} was observed in a photolytically-driven CO-saturated substrate-free construct from which the FAD/NADPH domain had been removed, rising to 250 s^{−1} in the presence of myristate¹⁸¹—significantly faster than in many other P450 systems.¹⁸² Rates were [CO]-dependent in the myristate-bound form, indicating that CO entered the active site while the haem iron was still in the ferric state. Cytochrome *c* reductase activity was similarly stimulated in a [CO]-dependent fashion in the myristate-bound full-length enzyme, though ferricyanide activity remained unaffected,

implicating interaction between the FMN and BMP domains.¹¹³ However, electron transfer also exhibited [CO]-dependence when photoexcited NAD(P)H was used to reduce isolated BMP.¹⁸³ The kinetic behaviour of this system was biphasic, whether or not a substrate was bound, suggesting that CO associated with the enzyme prior to electron transfer. This presented a contrast with the monophasic kinetics observed in the full-length protein, where fatty acid binding had a markedly lower impact on CO binding than in other prokaryotic P450s.⁴⁹ Geminate CO rebinding to the ferrous haem iron following photo-induced dissociation showed biphasic kinetics in the substrate-free form of the full-length enzyme, but monophasic kinetics in the fatty acid-bound form.¹⁸⁴ Rebinding appeared to be preceded by transient CO docking to the enzyme, as in globins.¹⁸⁵ High-pressure stopped-flow studies showed that CO bound with similar rate constants to dioxygen in P450_{BM3} (though not in NOS), suggesting that the use of CO as a dioxygen proxy for this enzyme is not unreasonable.¹⁸⁶

P450_{BM3} loses fatty acid hydroxylase activity if incubated with NADPH (or NADH)¹¹⁴ in the absence of substrate.^{19,28,30} Inter-domain electron transfer is arrested within milliseconds,¹⁸⁷ and 70% inactivation takes place within two minutes, irrespective of dilution levels, though *ca.* 10% activity is retained for at least ninety minutes.³⁰ However, activity can be fully recovered *via* overnight dialysis. Incubation of BMP with NADPH does not have the same incapacitating effect as incubation of BMR,⁴² and the enzyme can be “rescued” by electron acceptors such as cytochrome *c*,^{113,188} confirming that the issue is BMR-related. The incapacitated form of the enzyme is commonly believed to be the “over-reduced” three-electron species, FADH⁻/FMNH₂²⁻^{113,114,171} which, though incapable of reducing the haem iron, remains able to reduce cytochrome *c*.¹⁸⁸ Fusions between BMR and mammalian P450s (section 4.4) do not share this susceptibility.¹⁸⁹ BMR activity can also be compromised by NADP⁺ (or NAD⁺) accumulation, the oxidised co-factor binding to a regulatory site and hindering the release of NADPH from the catalytic site.^{104,190,191} The conformational changes induced by the binding of NADPH or NADP⁺ are nevertheless integral to the efficient transfer of electrons through BMR.¹⁹⁰

The NADPH-reduced enzyme was unable to bind CO in the absence of substrate, showing that the reduction potential of the low-spin haem iron was less oxidising than that of BMR.⁵⁸ In the presence of substrate, the haem iron was reduced prior to BMR under CO, but under an argon atmosphere the opposite occurred, suggesting that CO was pulling the thermodynamically unfavourable Fe^{III}/Fe^{II} equilibrium across by altering the apparent potential of BMP.¹⁷⁰ The accuracy of this interpretation was confirmed when the FMN/FMNH⁻ potential was found to be more oxidising than that of substrate-bound BMP.¹⁷³ Like the first FMN-to-haem electron transfer rate, the potential varied according to the fatty acid bound, but it was always > 100 mV more oxidising than that of the substrate-free form, as in other P450s.¹⁸² It seems natural to draw the conclusion that this is a gating mechanism designed to prevent the futile cycling of electrons causing auto-degradative damage when no substrate is bound, but this may be overly simplistic. In the first place, reduction potentials do not, as thermodynamic parameters, correlate directly with FMN-to-haem electron transfer rates,

since the latter are kinetic in nature and therefore also reflect the reorganisation energies associated with electron transfer, as described by Marcus theory.¹⁹² To illustrate, the equilibrium constants associated with electron transfer through BMR differed from those calculated from equilibrium redox potentials by as much as two orders of magnitude.¹⁹⁰ Secondly, experimentally determined potentials do not reflect the impact of rapid dioxygen binding to the ferrous haem iron (which, like CO binding, alters the equilibrium potential), since they are necessarily measured under anaerobic conditions.^{178,192} Finally, P450_{BM3} variants that consume NADPH at < 1.5 nmol (nmol P450)⁻¹ s⁻¹ in the substrate-free form despite having first electron transfer rates of > 200 s⁻¹ have recently been identified^{193,194} (section 5.2). A method of estimating the reduction potentials of P450_{BM3} variants using UV-visible spectroscopy has been reported.¹⁹⁵

2.3 Dimerisation

The specific fatty acid oxidation activity of P450_{BM3} increased with increasing protein concentration, suggesting to early researchers that the functional form of the enzyme was a complex susceptible to dissociation on dilution.¹⁹ This impression strengthened when reductive titration with NADPH implied that electron transfer could be intermolecular.¹⁷⁰ Sedimentation velocity experiments indicated the presence of a mixture of monomers, dimers, trimers and tetramers, but incubation with DTT showed that the dominant aggregated form was dimeric, with a “1.45-mer” also prominent.¹⁹⁶ The 1.45-mer could in principle be a species comprising one full-length enzyme and one BMP domain formed as the result of partial proteolysis. Heterodimer constructs of this kind are known in NOS, which also loses activity when monomeric.¹⁹⁷ It was suggested that the activity loss observed when residues were deleted from the linker region might owe to the fact that it had become too short to allow a functional dimer to form.⁷⁹ The isolated FAD and BMR domains were found to dimerise *via* disulphide bridging.¹⁶⁴ The same applied to BMP, which required the mutagenesis of two solvent-exposed cysteine residues to maintain in a monomeric form.¹⁹⁸ However, the full-length protein dimerised *via* some other mechanism.^{164,196,199} Monomerisation was not fully reversible, and the monomer/dimer equilibrium was sensitive to the presence of substrate and to ionic strength.¹⁹⁹ Although dilution was deleterious to hydroxylation activity and also to cytochrome *c* reductase activity, it had the opposite effect on ferricyanide activity, presumably because the FAD domain was more accessible in the monomer.²⁰⁰ Fusions between P450_{BM3} and mammalian isoforms (section 4.4) can also exist as dimers, but electron transfer appears to be intramolecular rather than intermolecular.¹⁸⁹

In NOS, electrons pass from the reductase domain in one sub-unit of the dimer to the haem iron in the other sub-unit.¹⁹⁷ A mixture of two P450_{BM3} mutants, one with an inactivated BMP domain, the other with an FMN-deficient BMR domain, showed significant levels of hydroxylase activity reconstitution, implying that intermolecular electron transfer of an analogous nature occurred in P450_{BM3}.²⁰⁰ Experiments carried out with a three-component system comprising mutants with inactivated BMP, FMN and FAD domains invited a different

conclusion—namely, that electrons passed from the FAD domain of the first molecule to the FMN domain of the second, and thence to *either* of the two BMP units in the dimer, possibly because the linker between the FMN and FAD domains was too short for intramolecular FAD-to-FMN electron transfer to be feasible.¹⁹⁹ A significantly higher K_D value was obtained for the transition in this work: 327 nM vs. 1 nM. This was attributed to full allowance being made for the slow kinetics of monomerisation on dilution. There is experimental evidence in support of a proposal that the slow activity loss that occurs during extended periods of preincubation in dilute solution is due to FMN depletion rather than monomerisation,^{187,201} but also evidence that opposes it.^{199,200} (FMN depletion *via* dialysis plays a significant role in the activity loss suffered by the isolated BMR domain when incubated at 30 °C for *ca.* 30 min, but BMR is essentially stable at 4 °C.)¹⁶⁰

2.4 Spectroscopic approaches

Numerous spectroscopic techniques have been used to probe the full-length protein and its sub-domains. The equilibrium between the low-spin and high-spin forms of the ferric haem iron can be monitored using UV/visible spectroscopy, allowing the determination of substrate binding constants (Table 2). Resonance Raman, NMR, MCD and EPR have shed complementary light on spin equilibria and the conformational perturbations that result from the binding of substrates and exogenous ligands, mutagenesis and physical changes.^{61,202–214} High pressure returned the substrate-bound enzyme to the low-spin state, for example,^{215,216} as did high arachidonate concentrations (6 mM).²¹⁷ Resonance Raman showed that water has readier access to the iron centre in BMP than in the full-length protein, and that the enzyme was not fully high-spin in the presence of palmitate.²⁰⁸ According to NMR shift data at 27 °C, lauric acid docked 7.6 Å from the ferric haem iron, a distance too great to permit oxidation,¹¹⁰ suggesting that substrates approached more closely only on haem reduction.²¹⁸ Subsequently published crystal structures of longer-chain fatty acids and their derivatives conveyed a similar picture (section 3.1). However, UV/visible spectroscopy and solid-state NMR revealed that the substrate-bound enzyme underwent a high- to low-spin transition when cooled to the temperatures at which crystal structures are determined. This suggested that substrates were dynamic and might lie in closer proximity to the haem iron at physiological temperatures even in the ferric form.^{219,220} FTIR was used to probe the formation of the BMP–FMN domain complex.²²¹ EPR, MCD, Mössbauer and UV/visible spectroscopy have supplied insights into the reactive iron intermediates formed during the latter stages of the catalytic cycle,^{222–224} and also peroxynitrite inactivation.²²⁵ These include the oxy-ferrous form of the enzyme²²⁶ which, though significantly more susceptible to autoxidation than those of P450_{cam}⁴⁹ and NOS,²²⁶ was fully stable at –55 °C even in the full-length protein.²¹⁷

2.5 Effectors, competitive binding and allosteric regulation

BMP is sensitive to conformational changes in, or induced by, the BMR domain, and *vice versa*.⁶⁹ The rate of cytochrome *c*

reduction by BMR was stimulated by myristate binding to the BMP domain, for example.¹⁸⁰ Laurate binding was tighter in the presence of BMR, the dissociation constant for the full-length protein being 256 μM vs. 909 μM for the isolated BMP domain.⁹⁵ Flavin fluorescence levels in the reductase domain doubled on laurate addition, while laurate binding and CO binding in the presence of laurate enhanced cytochrome *c* reductase activity by 60% and 3- to 4-fold respectively, but did not stimulate ferricyanide activity, implicating conformational change in the FMN domain.¹¹³ The cytochrome *c* reductase activity of the full-length protein was higher than that of isolated BMR even in the substrate-free form, suggesting that BMP and cytochrome *c* do not compete for the same FMN binding site.¹⁸⁸ Because of the complex relationships that exist between the various domains, it can be difficult to pinpoint the origins of behavioural changes brought about by mutagenesis or alterations to experimental conditions.

The first FMN-to-haem electron transfer rate has been shown to be broadly independent of ionic strength.^{127,188} Catalytic rates, on the other hand, were almost four-fold higher at 300 mM potassium phosphate than at 10 mM.¹²⁷ The remarkable activity levels of which the enzyme is capable are therefore not reached under physiological conditions even though inter-domain electron transfer remains rapid. High ionic strengths also have an adverse effect. *N*-palmitoyl glycine (NPG) oxidation was roughly half as rapid in 1000 mM KCl as in 100 mM KCl, for example.¹⁹⁹ In P450_{cam}, camphor binding tightens in the presence of potassium ions, and a potassium binding site has been identified,^{227,228} but experiments with a variety of buffer types showed that ionic strength rather than potassium-dependency was responsible for the behaviour observed in P450_{BM3}.¹²⁷ And yet buffer composition can have a significant influence on FMN-to haem electron transfer rates, which were *ca.* 100% higher in potassium phosphate than in Tris/HCl for the laurate- and myristate-bound enzyme, irrespective of ionic strength.¹²⁷ It is worth noting in this context that that the oxy-ferrous form of the enzyme is more stable in Tris/HCl than in phosphate.²¹⁷

Binding between the isolated BMP and BMR domains, though weak, tightened as ionic strength increased, as did binding between BMP and CPR.²²⁹ This was indicative of electrostatic inter-domain repulsion, and potentially explained the requirement for BMP and BMR to be covalently linked. The opposite effect was observed for the binding of CYP2B4 to CPR or BMR. Unlike the unmodified enzyme, P450_{BM3} fusion proteins (section 4.4) accordingly exhibited ionic strength-dependent electron transfer behaviour. Electron transfer rates doubled in a flavodoxin/BMP construct as KCl concentrations were raised from 50 mM to 250 mM, for instance, underpinned by a significant tightening in binding between the two proteins, but then decreased on a further increase to 400 mM.^{230,231} It was postulated that constructive reorganisation of the electrostatic complex accounted for the initial response, but that dissociation took place when ionic strength became excessive, as observed with other redox partner systems.²³¹ The *N*-demethylation of erythromycin by three separate fusions also displayed ionic strength-dependence across the 0–500 mM NaCl concentration range, peaking at 500 mM.¹⁸⁹

Kinetic titrations with palmitic acid became sigmoidal as ionic strength was reduced, the point at which Michaelis–Menten

kinetics ceased to apply being higher in Tris/HCl (50 mM) than in phosphate (25 mM).¹²⁷ This effect appeared to originate in the BMP domain, since ionic strength-sensitive behaviour with a similar transition point was also apparent in binding titrations. At low phosphate concentrations, a minimum of four palmitate binding sites was indicated, the fourth binding event being strong ($K_D \leq 2 \mu\text{M}$) and cooperative, but the third weak, and both the second and third inhibitory. At higher phosphate concentrations, the data fitted a two binding-site model and no longer displayed cooperativity. Whether phosphate and palmitate competed for the same binding site was unclear. While it is possible for two fatty acid molecules to co-occupy the active site (*vide infra*), it seems unlikely that as many as four could be accommodated. Two palmitate molecules are seen to be complexed at the dimer interface in the crystal structure of human CYP2C8.²³² Such a binding event could in principle explain the P450_{BMP3} data if it caused conformational changes that led to the displacement of the axial water ligand. However, it is unclear why palmitate would bring this about, but not myristate or laurate. Moreover, four-site binding was observed in the full-length protein as well as in the isolated BMP domain. Non-hyperbolic behaviour has also been observed in titrations of fatty acids and related substrates with CYP102A2 and, to a lesser extent, A3,^{140,141,146} while CYP102A5 showed sigmoidal kinetics in the oxidation of linoleic acid.¹⁴² Saturated fatty acids incorporating a single methyl branch were particularly susceptible.

Spectroscopic evidence of various types suggests that fatty acid substrates can co-occupy the active site with tightly binding inhibitors such as pyridine,¹¹⁰ metyrapone²⁰⁴ and ω -imidazolyl fatty acids,²³³ as well as their derivatives.²³⁴ Binding of the latter tightened in the presence of laurate but weakened in the presence of arachidonate, suggesting that, although the majority of the funnel-shaped access channel was sufficiently spacious to allow co-occupation, there was competition between the inhibitor and the longer-chain substrate at the haem end. Binding titrations with the inhibitor alone showed non-hyperbolic behaviour only when a space-creating mutation was introduced close to the haem iron, reinforcing this impression.^{233,234} Palmitic acid hydroxylation rates more than doubled when an equal quantity of lauric acid was added to incubations, and the accompanying changes to product distributions suggested that the two substrates could occupy the active site simultaneously.¹²²

Co-occupation of the active site may explain the homotropic cooperativity observed in the metabolism of testosterone by an engineered P450_{BMP3} variant, though conformational change induced by binding at an external site would also be consistent with these data.²³⁵ Heterotropic cooperativity was encountered in the metabolism of 3,4-methylenedioxymethylamphetamine (MDMA) and acetaminophen by the same variant, activity being stimulated up to 70-fold by caffeine, which could bind to an allosteric site. Both forms of cooperativity are known in the CYP3A sub-family, and caffeine is an activator of rat CYP3A2. Interestingly, while caffeine stimulates certain P450_{BMP3} variants, it acts as an inhibitor with others.²³⁶ The researchers who carried out this work noted that deploying a co-ligand could be a viable means of enhancing oxidase activity and/or altering product distributions, to be used instead of (or in conjunction with) mutagenesis.²³⁵ Non-hyperbolic kinetics have been observed in the oxidation of cyclohexane²³⁷ and, under alkaline conditions,

indole²³⁸—though, with indole, a single active-site mutation was sufficient to bring about a reversion to Michaelis–Menten kinetics. The binding of trichloroethane,¹²⁰ indole¹¹² and styrene²³⁹ exhibited non-hyperbolic behaviour. Heterotropic cooperativity was observed in cumene hydroperoxide-driven indole oxidation (section 7.3), NADPH consumption rates being enhanced by the presence of cumene hydroperoxide as indole binding tightened, but neither *t*-butyl hydroperoxide nor hydrogen peroxide brought about comparable effects.²³⁸ Cyanide binding was cooperative in two glutamate mutants.¹⁹³

BMR is also sensitive to ambient conditions. NADPH binding was twofold less rapid in 50 mM phosphate than in 50 mM MOPS, possibly because the higher ionic strength of the former (130 mM) was not conducive to charge-transfer complex formation.¹⁸⁸ However, onward electron transfer to FMN was more rapid at high ionic strength. The rate of ferricyanide reduction by the FAD/NADPH domain varied with ionic strength, being 90% slower at 1 mM phosphate than at 50 mM.¹⁶⁴ Cytochrome *c* reductase activity also varied with ionic strength, but in a more complex fashion, peaking at phosphate concentrations of *ca.* 25 mM.¹⁸⁸ Cytochrome *b*₅ reductase activity was different again, being almost 20-fold higher in 500 mM KCl than in 100 mM KCl, whereas cytochrome *c* reductase activity was 75% lower.²⁴⁰

3 Structure

3.1 Crystal structures

The asymmetric unit in the *P*2₁ structure of the first BMP crystal structure to be published (Protein Data Bank (PDB) code 2HPD)^{241,242} contained a closely associated pair of molecules, one in a more “open” conformation than the other. The F/G loop and the F- and G-helices aligned poorly when the two molecules were overlaid, the *B* factor for this region being 80 Å² vs. 25 Å² for the structure as a whole. This suggested the loop was flexible, a property subsequently found to be common to other P450 structures.⁴⁸ In contrast to the only previously published P450 structure—that of P450_{cam},²²⁷ which failed to reveal how substrates reached the haem iron—the P450_{BMP3} structure showed a long, hydrophobic, largely non-aromatic substrate access channel. A structure determined independently to the same resolution (2.0-Å, PDB code 2BMH)²⁴³ overlaid closely onto 2HPD if the F/G loop was excluded from the comparison, the root mean square deviation (rmsd) for the backbone C_α atoms being 0.23 Å. Here, however, both molecules in the asymmetric unit were in the open conformation, partly on account of intermolecular crystal packing constraints. Energy minimisation calculations showed that the open conformation was too spacious to bind myristic acid effectively, but suggested that the access channel would reshape in response to substrate binding, producing a closed conformation in which protein-substrate interactions would be enhanced. Structures at resolutions of 1.65-Å (1BU7)¹⁷⁴ and 1.2-Å (2IJ2)²⁴⁴ followed. The latter is one of several in which the porphyrin unit is found to incorporate in either of two conformations related by a 180° rotation,^{126,194} a phenomenon that also occurs in other P450 structures.²⁴⁵

The first structure to be solved with a substrate *in situ*, that of palmitoleate-bound BMP (1FAG),^{155,246} contained four

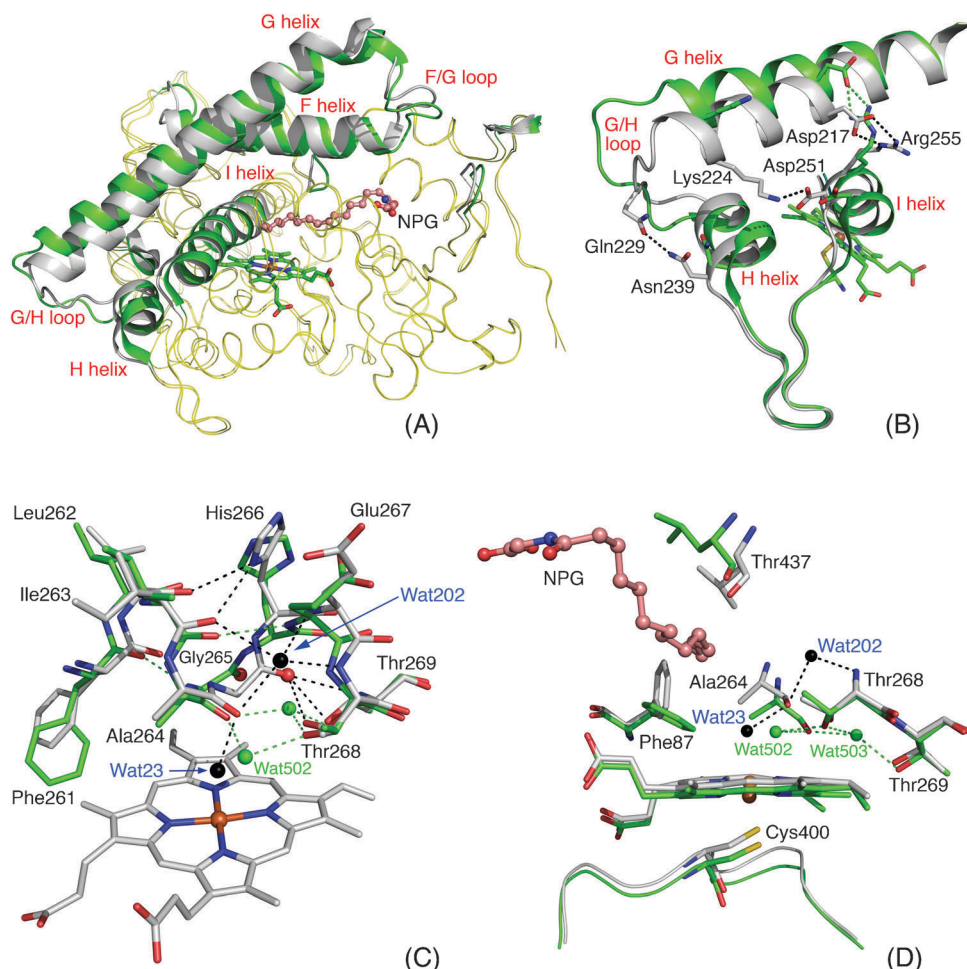


Fig. 3 Substrate-induced structural changes in P450_{BM3}. The substrate-free BMP structure (PDB code 1BU7)¹⁷⁴ is in grey, with waters and hydrogen bonds in black, and the haem iron in orange. The NPG-bound structure (PDB code 1JPZ)²⁰¹ is in green, including waters and hydrogen bonds, with the haem iron in brown, and NPG in salmon. (A) Complete overlay, showing the movements of the F-, G- and H-helices and the F/G and G/H loops on substrate binding, and the disruption to the turn pattern of the I-helix. In regions that show little or no change on substrate binding the NPG structure is in yellow. The Table of Contents entry shows a complementary representation of this movement. (B) Regions of the G-, H- and I-helices, showing (i) scission of the Lys224–Asp251 salt bridge and extension of the Asp217–Arg255 salt bridge, which together reshape the I-helix, causing the turn pattern to translocate; (ii) scission of the Gln229–Asn239 salt bridge, either caused by, or as a response to, increased flexibility in the G/H loop (a region not fully resolved in molecule A of the NPG structure), which may contribute to the destabilisation of the Lys224–Asp251 salt bridge. (C) The kink region of the I-helix, where hydrogen-bonding networks are extensively redistributed, primarily as a result of the repositioning of Gly265, the rotation of His266, and the loss of Wat202. The rotation of the Phe261 side-chain is a response to movements at Ile 219 and Phe158.¹⁹⁴ (D) The active site, showing (i) the sinking of the proximal loop where the proximal cysteine ligand, Cys400 is situated, which causes the haem iron to lie below the porphyrin plane; (ii) displacement of the axial water ligand (Wat23), which remains hydrogen-bonded to Ala264, to the “alternative” binding site (Wat502) as the I-helix recedes; (iii) loss of Wat202, which allows the I-helix kink angle to contract from 13° to 5°; (iv) rotation at Phe87 and the associated retreat of the Leu437 side-chain.

molecules in the asymmetric unit. The most conspicuous difference between the substrate-bound (SB) and substrate-free (SF) forms was the positioning of the F- and G-helices and the F/G loop (Fig. 3A). Both helices tilted and were translated along their axes by approximately half a turn, closing the access channel and disrupting contacts with the I-helix, including a salt bridge (Fig. 3B). Electron density was clearer in this region of the structure than in the SF form, showing that the loop was less disordered. The most widely cited SB structure is that of the complex formed with NPG (1JPZ),²⁰¹ a substrate that is more soluble than fatty acids of equivalent chain length and also binds an order of magnitude more tightly. Water molecules were clearly resolved in this structure. Only three remained in

the active site and access channel, as compared to 17–21 in SF structures. Amongst those no longer present was Wat202 (Fig. 3C) which had interrupted the I-helix in the SF form, creating the kink or groove where dioxygen binding is believed to take place by preventing the formation of a hydrogen bond. With Wat202 absent, a normal intrahelical hydrogen bond was formed, reducing the I-helix kink angle from 13° to 5°. In addition, the turn pattern of the helix was translated, with the result that the associated network of hydrogen bonds was extensively rearranged (Fig. 3C). The water molecule closest to the haem iron was displaced to an off-axial position by the movement of the I-helix, to which it remained hydrogen-bonded, leaving the iron centre pentacoordinate. It was proposed

that the spin state equilibrium of the ferric haem iron arose from partitioning of this water molecule between the “alternative” binding site (Wat502, Fig. 3D) and the iron-bound axial site (Wat23). The *N*-palmitoyl methionine-bound structure (1ZO9)¹⁰⁰ was broadly similar to the NPG-bound structure. The structure of the enzyme has been compared to, and contrasted with, those of other P450 structures.¹⁶⁹

An artificial construct of BMP complexed with the proteolysed FMN domain has been crystallised (1BVY).¹⁷⁴ The asymmetric unit contained a pair of tightly associated BMP units, as in the majority of P450_{BM3} structures, and a single FMN domain docked on the proximal side of one of the iron centres, disrupting the Pro382–Gln387 region. Given that the Asn381–Ala389 insertion characteristic of eukaryotic P450s is not found in other bacterial P450 families, it was suggested that these residues might be critical to inter-domain binding. The crystal structure of the FAD/NADPH domain has been solved.⁷¹ A structure of BMP bound with the inhibitor *N*-(12-imidazolyldecadecanoyl) L-leucine (3BEN)²³⁴ overlaid poorly with other SB structures but closely with the SF structure. This disparity is the antithesis of that displayed by the SF structures of certain variants that are more active as oxidases than the wild-type enzyme (WT), which resemble SB forms of WT more closely than SF WT (section 5.1). Structures have also been determined for two DMSO-permeated forms of BMP with the object of establishing why high concentrations of this co-solvent inactivate the enzyme.²⁴⁷ Crystals were grown at 14% v/v and 28% v/v DMSO (LD and HD, PDB codes 2J4S and 2J1M respectively). In LD, the nearest water molecule to the haem iron lay at a Fe–O distance of 3.75 Å vs. 2.6 Å in SF WT and was off-axial as in SB WT—yet the iron atom, which moves to the proximal side of the porphyrin system in SB WT (Fig. 3D), lay 0.16 Å to the distal side. In HD, DMSO became a sixth ligand, coordinating to the haem iron through the sulphur atom rather than the oxygen. This reconciled with spectroscopic analysis, which showed the enzyme to be partially high-spin at 14% (v/v) DMSO, but fully low-spin at higher DMSO concentrations.

3.2 Key residues

Like certain mammalian P450s,²⁴⁸ P450_{BM3} crystallises in a “precatalytic” conformation in which no substrate atom lies sufficiently close to the haem iron for oxidation to take place. It is thus unclear whether the conformations in which the residues lining the access channel are depicted are catalytically relevant, complicating the task of engineering the enzyme. Most have nonetheless been subjected to site-specific mutagenesis with a view to clarifying the roles that they play in the catalytic process—typically *via* comparison of the fatty acid oxidation rates and product distributions given by the mutants generated with those of the wild-type enzyme. The substrate access channel portion of the NPG-bound structure is shown in Fig. 4.

3.2.1. Arg47 and Tyr51. Fulco’s prognosis that a hydrophilic binding region must tether the carboxylate groups of fatty acid substrates many Ångströms from the haem iron²¹ was proved correct when the palmitoleate-bound crystal structure showed the substrate closely associated with two polar residues close to the mouth of the substrate access

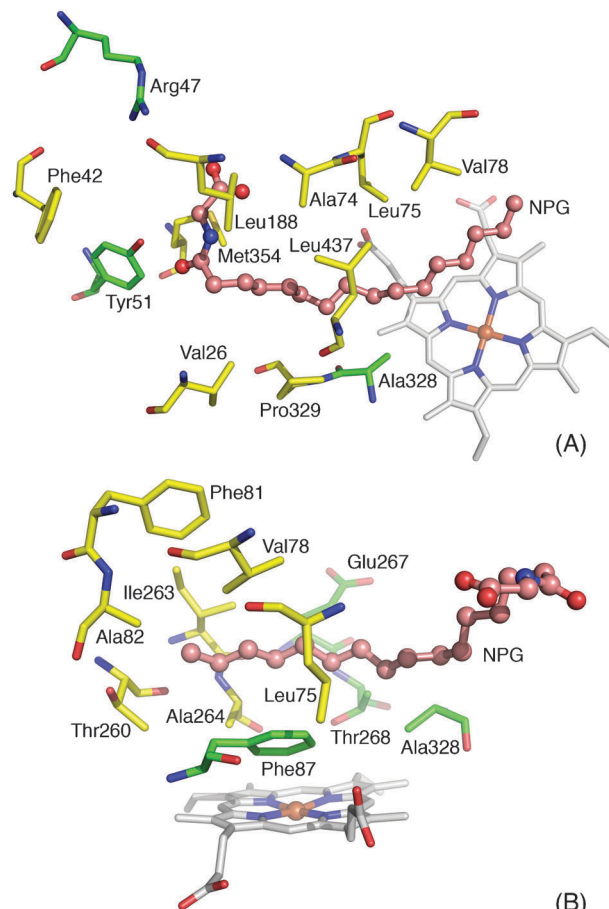


Fig. 4 The substrate access channel and active site of NPG-bound P450_{BM3}.²⁰¹

channel, Arg47 and Tyr51¹⁵⁵ (Fig. 4A), potentially explaining the dependence of product partitioning on pH.²⁸ The R47E mutant was inactive towards arachidonic acid⁹⁸ but retained some activity towards shorter-chain fatty acids, and efficiently hydroxylated C12–C16 trimethylammonium compounds, the polarity reversal enabling the enzyme to accept a substrate of the opposite ionic character.³¹ Mutagenesis of either residue generally lowered fatty acid hydroxylase activity and raised binding constants, suggesting that they acted jointly as gate-keepers to the active site.^{99,106} Together, the two residues may regulate not only the admission of substrates, but also water²⁴⁹ and co-solvents.¹⁵¹ That the R47A/Y51F double substitution reduced catalytic efficiency by two thirds even with a short-chain substrate such as hexanoate suggested that, in addition to functioning as a binding site, the couplet was responsible for luring substrates to the access channel opening.²⁵⁰ Arg47, which lies at the enzyme surface and is unusually variable in its position in crystal structures (and sometimes ill-defined),^{155,246} seems likely to be more influential in this role than Tyr51. Arg47 does not form a hydrogen bond with the substrate in the NPG-bound²⁰¹ or *N*-palmitoyl methionine-bound¹⁰⁰ crystal structures. Possibly fatty acid substrates tether instead to Tyr51 and Ser72 when binding closer to the haem iron, as suggested by recent modelling studies on perfluorocaprate.²⁵¹ However, position 47 is undoubtedly important for the binding of *N*-acyl homoserines and their lactone derivatives in solution, since the R47S mutant

enhanced the affinity of the enzyme for the latter relative to the former by almost 250-fold.¹³⁷

Although the tyrosine residue is conserved in microsomal fatty acid ω -hydroxylases, the arginine residue is not,⁶⁹ and neither residue is conserved in P450_{foxy}, which otherwise has the same key active-site residues as P450_{BM3} (Phe42 excepted).⁵³ P450_{foxy} is inactivated by myristic acid and longer-chain analogues but metabolises fatty acid esters such as monopalmitoyl glycerol,^{53,252} suggesting that the primary function of the Arg47/Tyr51duet in P450_{BM3} may be to control substrate specificity. Strikingly, P450_{BM3} is the only CYP102A sub-family member with a polar residue at position 51 or its equivalent, and also the only one with a positively charged residue at position 47 (Fig. 2). This has obliged researchers to re-examine some long-standing assumptions. Although fatty acid binding is tighter in A1 than in A2, A3 or A5,^{140,142} hydroxylase activity levels with unsaturated fatty acids are lower in A1 than in A2 and A3.¹⁴³ Does this indicate that over-tight binding is counter-productive? And how is it that activity levels in A2, A3 and A7 are broadly similar to those in A1 with saturated fatty acids irrespective of chain-length, even though they lack the Arg/Tyr couplet?¹⁴³ A likely explanation is that other sub-family members incorporate substrate tethers at different locations. Positions 352_{A1}¹⁴¹ and 435_{A1}¹⁴⁹ have been suggested as possible binding sites in A2, for example, where Arg and Gln are employed respectively. Position 72_{A1} (*vide supra*), where most sub-family members use arginine or glutamate, is another contender, given that the S72Y mutant brought about a substantial selectivity shift in lauric acid hydroxylation relative to WT in A1.¹¹⁹ A deeper-set binding site would also be consistent with the capacity of A3 to hydroxylate fatty acids at the (ω -8) position.¹⁴³

3.2.2. Phe87. The side-chain of Phe87 extends into the lumen of the substrate access channel, close to the haem iron. In the SF crystal structure, it lies roughly perpendicular to the porphyrin system, but in SB crystal structures it is rotated through *ca.* 90° and occupies a position between the iron centre and the substrate tail¹⁵⁵ (Fig. 3D and 4B). It has been proposed that this motion, as distinct from substrate binding, is responsible for displacing the axial water ligand from its coordination site, since it reduces the distance of closest approach to just 3.1 Å.²⁰¹ It may also trigger other aspects of active site reorganisation.²⁵³ Early researchers hypothesised that Phe87 might be responsible for the sub-terminal oxidation specificity shown by P450_{BM3}, since microsomal fatty acid ω -hydroxylases typically employ leucine in the homologous position.⁶⁹ The idea was strongly supported by a report that mutant F87A gave >90% ω -hydroxylation with lauric and myristic acids.¹¹¹ A popular rationalisation was that the termini of fatty acid substrates were sequestered,²¹ a process in which the phenylalanine side-chain played a role.^{26,155,242} However, primary alcohol formation could seldom be reproduced in subsequent studies.^{71,99,119,123,125,253} It has been suggested that faulty derivatisation protocols could be to blame,^{122,254} but this seems unlikely, given the number of different investigations involved. Interestingly, small quantities of ω -hydroxylation (*ca.* 3.5%) were reported with lauric acid as recently as 2008 by researchers who not only agreed with the consensus that mutation F87A shifts the focus of attack towards the centre of

the substrate relative to WT rather than towards the terminus, but also observed no ω -hydroxylation in turnovers with palmitic acid or farnesol, which has the same chain length as lauric acid.³²

It is now accepted that the sub-terminal hydroxylation specificity generally displayed by P450_{BM3}—with or without the F87A mutation present—owes to the fact that most substrates are sufficiently dynamic, even when bound, to allow the enzyme to discriminate between closely situated C–H bonds on the basis of reactivity (sections 3.3, 5.3). But it is also the case that Phe87 possesses powerful specificity-influencing and activity-regulating properties. With arachidonic acid, the F87V mutant gave 100% 14(S)-15(R)-epoxidation *vs.* 20% for WT, which also gave *ca.* 80% 18(R)-hydroxylation⁹⁸ (Table 1). The same mutation caused a sharp increase in peroxide uncoupling relative to WT with lauric acid.⁹⁹ The F87Y mutant was fully uncoupled in turnovers with arachidonic acid,⁹⁸ but gave significantly higher k_{cat}/K_M values than WT and a selection of other single-site mutants during the early stages of lauric acid oxidation.¹⁰⁶ However, the F87Y and F87G mutants both exhibited first FMN-to-haem electron transfer rates that were 80–90% lower in the laurate-bound form than that shown by WT.¹⁰⁶ Phe87 is the most commonly mutated residue in the protein. Residues with less bulky side-chains than the naturally occurring phenylalanine are typically introduced, creating incremental space in the vicinity of the haem iron and elevating the active-site water population. Although this can increase peroxide uncoupling levels with small, loosely-fitting non-natural substrates, it is often beneficial to the oxidation of larger substrates as well as those with hydrophilic character. The F87V mutation is thus a common component of drug-metabolising variants (section 6.1), while the F87A mutant is often deployed when dealkylation is the objective.

3.2.3. Glu267 and Thr268. The P450 superfamily has a highly conserved acid-alcohol pairing close to the kink region of the I-helix—typically Asp-Thr or Glu-Thr. In P450_{BM3}, the residues in question are Glu267 and Thr268 (Fig. 3C and 4D). Thr268, one of the few polar features of the active site, has been implicated in various roles including proton delivery, dioxygen activation, and the stabilisation of the oxy-ferrous or hydroperoxy catalytic intermediate (**IV** and **VI**, Fig. 1).^{10,11,107} The T268A mutation caused NADPH consumption rates and coupling levels to collapse in the oxidation of lauric,²⁵⁵ palmitic^{96,255} and arachidonic⁹⁶ acids, implying that the threonine side-chain might position a critical active-site water molecule in WT.⁹⁶ This interpretation was supported by the subsequently published NPG-bound crystal structure, which showed the side-chain OH group of Thr268 stabilising the “alternative” binding site for the water molecule closest to the haem iron²⁰¹ (Fig. 3C and D). With pentadecanoic acid, however, coupling was unaltered at *ca.* 90%, indicating that the conserved threonine was *not* in fact essential for efficient catalysis.⁸⁰ Since the mutant converted 68% of the reducing equivalents to peroxide in palmitic acid turnovers, as against 1% for WT, it was postulated that uncoupling was a function of substrate chain-length-driven variations in the active-site water population, on which the positioning of individual water molecules would be expected to depend. The first FMN-to-haem electron transfer rate was found to be $\geq 70\%$ lower in

the arachidonate-bound form of T268A than in WT,¹⁰⁷ consistent with the 80% reduction in the NADPH consumption rate observed in the oxidation of palmitic acid.⁸⁰ However, the myristic acid rate was 30% higher with T268A than with WT, mirroring the uncoupling trends.⁸⁰

The E267Q mutant also had an adverse impact on fatty acid oxidation activity, proving just 5% as active as WT with palmitic acid, and raising uncoupling levels in lauric acid oxidation.¹¹⁶ The Glu267 side-chain is typically hydrogen-bonded to at least one water molecule in SF crystal structures, and it was suggested that even a relatively conservative substitution such as Gln for Glu could be sufficient to disrupt proton delivery pathways. With this mutation, however, uncoupling came largely *via* the oxidase pathway rather than through peroxide formation, and (ω -1)-hydroxylation levels halved from *ca.* 45% in myristic acid oxidation while (ω -3)-hydroxylation levels doubled to *ca.* 55%. This suggests that compromised substrate positioning made at least some contribution to the activity loss. The E267V mutation, by contrast, enhanced coupling efficiency relative to WT with certain substrates.²⁵⁶ Whereas the E267Q mutant was fully low-spin in the SF form,²⁵⁵ E267V-containing variants were partially high-spin. Computer simulations (section 3.3) suggested that the active-site water content was relatively low when this mutation was present,²⁵⁶ influenced presumably by the removal of the glutamate side-chain. This could impact the partition between the binding sites available to the water molecule closest to the haem iron, potentially explaining the mixed spin state, and would also be expected to mitigate peroxide uncoupling levels if carried through to the SB form.

3.2.4. Other residues. The carbonyl oxygen of Ala264, which is part of the I-helix, is hydrogen-bonded to the water molecule closest to the haem iron in almost all the crystal structures published to date, irrespective of whether or not a substrate is bound and whether the water molecule is axially coordinated or at the “alternative” site. It therefore appears to be instrumental in drawing the water ligand away from the axial binding site when the I-helix retreats from the haem iron on substrate binding²⁰¹ (Fig. 3D).

It has been suggested that access channel residue Leu437 acts as a “safety catch” for Phe87, preventing rotation of the side-chain to the SB position when no substrate is bound¹¹² (Fig. 3D). While there is good evidence to suggest that the two residues move in tandem,¹⁹⁴ the distance of closest approach is 4.7 Å, which appears too high for steric interaction to be directly responsible.

Another proposal is that Phe42 caps the access channel once a substrate has entered and bound,²⁴² supporting evidence coming from a study showing that catalytic efficiency with lauric acid was 15-fold lower in the F42A mutant than in WT, and the first FMN-to-haem electron transfer $\geq 90\%$ slower.¹⁰⁶ However, the position of the phenylalanine side-chain does not alter significantly on substrate binding according to the crystal structure, and although this residue is conserved in CYP102A3, A7 and A15 it is not present across the remainder of the sub-family or in P450_{foxy}.

Ph393, which lies to the proximal side of the porphyrin system, may tune the rate of haem reduction to optimise the

oxygen binding rate.^{213,257,258} This residue is highly conserved across the P450 superfamily, and most of the isoforms that do not employ it catalyse isomerisation or rearrangement, processes for which dioxygen activation is not required²⁵⁹ (CYP101C1 being a notable exception). The role played by Trp96 (originally reported as Trp97), another conserved residue, is more obscure.¹⁰²

Two reductase domain residues worthy of note are Gly570, which is important for FMN binding,²⁶⁰ and Trp1046 which shields the prosthetic FAD group and controls co-factor specificity.²⁰⁰

3.3 Computational methods

Computational techniques are routinely used to rationalise experimental findings or prepare the ground for new research, most commonly molecular dynamics (MD) simulations based on crystal structure data. In an early example, it was confirmed that the enzyme structure was dynamic and could adopt open or closed conformations.²⁶¹ Docking studies suggested that substrate capture should bring about a transition to the closed conformation, after which the F/G helix domain would rotate.²⁶² Random expulsion simulations suggested that the products from fatty acid oxidation left the active site *via* an opening close to the point of entry, with scission of the Arg47/Tyr51 tether being the final step in the catalytic process.^{263,264} Because non-natural substrates cannot tether in the same fashion, it is unclear how the products from non-natural substrate oxidation are expelled. The existence of a possible exit route on the proximal side of the haem iron has been mooted.²⁵⁶ In CYP2C5, products seem likely to depart through a solvent channel that reaches the protein surface between the F-, E- and I-helices and the β 4 sheet.²⁶⁵ This channel (which is not to be confused with the water channel on the proximal side of the haem)²⁶⁶ closes in substrate-bound crystal structures of wild-type P450_{BM3},²⁰¹ and may also be partially closed in the substrate-free forms of certain variants with low active-site water contents according to computer simulations.²⁵⁶ However, there is as yet no evidence to suggest that it doubles as an exit channel in P450_{BM3}.

Computational solvent mapping implied that the active sites of mammalian P450s could reshape to accommodate substrates of different shapes and sizes more readily than that of P450_{BM3}.²⁶⁷ Modelling studies suggested that the P450_{BM3} active site was less cramped than that of human CYP4A11, a terminal fatty acid hydroxylase, giving the tails of substrates such as lauric acid room to pass the haem iron.²⁶⁸ This tallied with the enzyme’s trademark reluctance to effect terminal hydroxylation. A combination of computational techniques was used to show that substrate-protein interactions could promote ω -hydroxylation by modulating intrinsic bond reactivities.²⁶⁹ Lauric acid appeared less susceptible to ω -hydroxylation than octane unless the charge at the carboxylate group was neutralised. Replica exchange MD simulations suggested that the termini of substrates such as NPG approached the ferric haem iron more closely at higher temperatures,^{270,271} corroborating NMR evidence to the same effect predicated on the temperature sensitivity of spin shift equilibria.²¹⁹ Corroboration was important because other spectroscopic evidence and mutant crystal structures were increasingly indicating that displacement of the axial water ligand to the haem iron and the related conformational change were not necessarily substrate-induced,

meaning that changes to the spin equilibrium might or might not be substrate-driven.^{71,112,125,194} At least three distinct substrate conformations existed in a dynamic equilibrium, undermining the idea that the termini of fatty acid substrates were rigidly sequestered by the protein.

MD simulations indicated that the E/F loop and the E- and F-helices were liable to be disrupted by high concentrations of DMSO,¹⁵¹ by which the enzyme is inactivated, a process in which the linker region and BMR probably also play important roles.²⁷² Simulations on the F87A mutant suggested that its anomalously low DMSO tolerance could stem from the axial water molecule being more susceptible to displacement than in the wild-type enzyme.²⁷³ MD simulations have also been employed to assist in the design of chimeric proteins¹⁴⁹ (section 4.4), to identify appropriate mutation sites,²⁷⁴ and to account for product distributions.²⁷⁵ One study suggested that a conformational change to one of the haem propionate groups could be responsible for the distinctive product profiles given by a drug-metabolising mutant, a possibility consistent with resonance Raman data.²⁵⁶

4 Engineering and redesign^{77,276–281}

4.1 Objectives

There is widespread interest in developing P450 variants suitable for biocatalysis,^{282,283} a technique that has already been successfully applied to ketone reduction, Baeyer–Villiger oxidation, enantioselective transesterification, and epoxide opening.²⁸⁴ Chemical C–H bond oxidation methods typically require harsh conditions, produce undesirable side-products and give racemic outcomes, often in low yields. Lucrative synthetic opportunities therefore await any new technology that can offer environmentally friendly regio- and stereo-specific hydroxylation and/or epoxidation routes.²⁸⁵ Eukaryotic P450s oxidise an impressive range of substrates and are already used to produce hydrocortisone, but these can be challenging to isolate and are slow-acting. Much of the research in this area has therefore focused on the soluble and more tractable bacterial isoforms, and particularly on P450_{BM3}, with its self-sufficient electron transport system. A few of the enzyme's natural substrates are precursors to desirable oxidation products: linoleic acid is metabolised to leukotoxin, whose derivatives are implicated in a variety of pathophysiological responses;²⁸⁶ certain linolenic acid derivatives may possess antifungal properties,²⁸⁷ and it is possible to produce precursors to δ - and γ -lactones, which find applications as fragrance components and antibiotics, from fatty acid substrates.¹¹⁹ But the majority of the products that are of interest to researchers have precursors that are not natural substrates for the wild-type enzyme. By and large, these do not fit the active site well and are unable to saturate it, meaning oxidation takes place slowly, if at all. Substrate specificity can be radically altered via mutagenesis, however, leading to significant activity enhancement, and this is a primary engineering aim. As with any catalyst, robustness and longevity are also important considerations, and stability management constitutes a secondary engineering goal.

Selectivity control is also critical, given that most organic substrates contain a variety of possible oxidation sites. *Ceteris paribus*, oxidation should take place at the most highly activated carbon centre, but in practice P450 product profiles are generally

influenced to a greater or lesser extent by protein-substrate interactions. P450_{cam} oxidises camphor to 5-*exo*-hydroxycamphor with 100% regioselectivity and 100% stereoselectivity,²⁸⁸ for example, demonstrating the exquisite specificity of which these enzymes are capable. Although P450_{BM3} occasionally delivers high levels of regio- and/or stereo-selectivity^{38,97,98,289,290} (Table 1), the active site is more spacious than that of P450_{cam}, allowing greater substrate mobility, and mixtures of oxidation products are more typical. For a specific product to be formed in high percentages, the substrate from which it originates must be constrained to bind in a particular orientation. This will normally require active site redesign—the introduction of a polar residue or the removal of a bulky side-chain, for example. Selectivity control is a more demanding challenge than activity enhancement, partly because the number of residues that contact the substrate is relatively small, and partly because individual mutations do not have predictable or generic effects, meaning that substrates must generally be dealt with on a case-by-case basis.

Directed evolution,^{291–293} in which mutations are introduced at random positions using error-prone PCR, is a valuable complementary tool to site-directed mutagenesis. This approach has the advantage of being able to generate desirable mutations at residues that do not appear at first sight to be of any obvious importance. The benefits of the two strategies can be combined using rational evolution, in which selected residues are subjected to random or semi-random mutagenesis. Alternatively, directed evolution can be used to identify sites suitable for targeting, followed by site-saturation mutagenesis to establish which mutations are most effective in those positions. A streamlined method for site-saturating P450_{BM3} and other enzymes has been developed.²⁹⁴ An increasingly favoured approach is to use directed-evolution variants with enhanced activity and/or stability profiles as a development platform, and incorporate site-specific mutations (sometimes chosen on the basis of site-saturation studies) on a substrate-by-substrate basis to bias selectivity in the intended fashion. Directed-evolution variants that display enhanced activity can also be combined with activity-enhancing site-specific mutations to obtain incremental activity enhancement, but this methodology is not always reliable.²⁹⁵ Table 3 catalogues the mutations reported in P450_{BM3} as of June 2011, the overriding majority of which are in the BMP domain.

4.2 Site-directed mutagenesis

The earliest reports of non-natural substrate oxidation using engineered variants involved mutations at Ala328, Thr268 and Phe87 and substrates that included 1,1,2,2-tetrachloroethane³²⁹ and 2-phenylpropanal.³⁴¹ Intractable polyaromatic hydrocarbons (PAHs) were targeted by introducing two space-creating mutations close to the haem iron, F87A and A264G, and by neutralising the polar binding site at the mouth of the access channel using the R47L/Y51F double substitution.²⁴⁹ This resulted in product formation rate (PFR) enhancements of more than two orders of magnitude. The impact of the hydrophobic R47L/Y51F couplet appears to be generic, and it is now widely employed to expedite the oxidation of apolar substrates.^{126,295,302–304} Substrate recognition improves, and water may also be deterred from entering the active site.²⁴⁹

Table 3 Directory of reported P450_{BM3} mutations

Glu4	Asp ²⁹⁶	Lys9	unknown ²⁰
Leu19	Phe ²³⁰	Lys24	Arg ^{296,297}
Pro25	Gln ¹¹⁷ Ser ²⁹⁸ SS ²⁹⁹	Val26	Thr ^a SS ²⁹⁹
Phe42	Ala ¹⁰⁶		
Arg47	Ala ^{98,99,106,250,298} Cys ^{b,c} Gln ^{100,137} Glu ^{31,98} Gly ^{106,149,233} His ^{296,297} Leu ^{126,235,237,249,295,298,300–305,d,e} Phe ^{306,307,a} Ser ^{100,137,308} Tyr ³⁰⁶ SS ^{299,306}		
Thr49	Ala ³⁰⁹		
Tyr51	Ala ⁹⁹ Ile ³¹⁰ Leu ³¹⁰ Phe ^{106,126,237,249,250,295,298,300,302–305,310,311,e} SS ^{299,310}		
Leu52	Ile ^{312,313,f}	Ile58	Val ^{f,g}
Cys62	Ala ³¹⁴ Ser ¹⁹⁸	Glu64	Gly ^{e,h} Val ³⁰⁹
Asp68	Gly ²⁹⁶	Lys69	Ala ³¹⁵
Asn70	Tyr ³⁰⁸	Ser72	Asp ³¹⁶ Glu ^{316,317} Gly ²⁹⁹ Tyr ¹¹⁹ SS ²⁹⁹
Gln73	Tyr ^{32,115}		
Ala74	Asp ³¹⁶ Glu ^{32,72,115,237,295,312,316,318} Gln ³¹² Gly ^{a,e,i} Ser ³¹² Val ^{296,297} SS ^{297,299,312,319–322}		
Leu75	Ala ³¹⁵ Arg ³⁰⁹ His ^{296,297} Ile ^{296,320,322} Lys ²⁵⁰ Pro ³²³ Ser ³²¹ Thr ²⁵⁰ Trp ^{296,320,322} Tyr ^{32,115} SS ^{297,312,320–322}		
Lys76	Ser ^{32,115}		
Val78	Ala ^{119,b,j} Glu ^{296,297} Leu ^{32,115,308,324} Phe ^{296,320,322,c} Ser ^{296,322} Thr ^{296,320,322} SS ^{297,312,320–322,325}		
Arg79	Phe ^{32,115,324}	Asp80	Pro ^{32,115,324}
Phe81	Ile ^{e,h,k} Leu ³²³ Pro ³¹³ Trp ^{32,115,324} SS ^{297,320–322}		
Ala82	Cys ^{296,316,320,322} Gly ^{296,312,313,320,322} Ile ^{112,296,320,322,326} Leu ^{32,115,296,297,313,320–322,324,326–328} Phe ^{112,239,296,320–322,326} Pro ^{296,297}		
Asp84	Thr ^{32,115}	Leu86	Glu ¹⁹³ Ile ^{e,l}
Phe87	Ala ^{10,32,72,111,119,122,123,154,194,201,237,249,254,269,272,273,295,296,300,303–308,310,313,316,317,324,325,328–340,e,f,g,m,PDB codes 3DGI, 2X7Y & 2X80} Arg ^{316,340}		
	Asn ³⁴⁰ Asp ³⁴⁰ Cys ^{316,340} Gln ^{316,340} Glu ^{316,340} Gly ^{72,106,119,121,220,223,233,237,275,295–297,308,316,329,332,334,340–343} His ^{316,340}		
	Ile ^{154,274,296,308,313,316,320–322,340} Leu ^{32,154,194,274,296,316,320–322,324,340} Lys ^{316,340} Met ^{316,340} Pro ^{316,340} Ser ^{119,340} Thr ^{316,340} Trp ^{316,340}		
	Tyr ^{98,106,199,233,316,340,344} Val ^{98,99,119,154,235,238,286,296,301,308,313,315,320–322,332,334,339,345,346,d,e,i,n} SS ^{297,304,306,312,319–322,340}		
Thr88	Cys ^{320,322} Leu ²⁹⁶ SS ^{297,312,320–322}	His92	Gln ²⁹⁶
Lys94	Ile ^{b,c}	Trp96	Ala ¹⁰² Arg ³⁰⁸ Phe ¹⁰² Tyr ^{102,210}
Lys97	Cys ³¹⁴	Ala99	Val ²³⁰
His100	Arg ^{f,g}	Ile102	Thr ^{296,297}
Leu104	Cys ¹⁷⁷	Ser106	Arg ^f
Phe107	Leu ^{f,g}	Gln109	Leu ³⁰⁹
Gln110	His ³⁰⁹	Ala111	Val ³⁰⁸
Met112	Thr ³⁰⁸	Ile122	Val ³⁰⁹
Ala135	Ser ^{f,g}	His138	Tyr ^{230,j}
Glu140	Gly ³⁰⁹	Val141	Ile ³⁰⁸
Pro142	Ser ^{b,c}	Glu143	Gly ^{309,e,h}
Met145	Ala ^{296,297,312} Val ^g	Leu148	Ile ³⁴⁷
Cys156	Ser ^{177,198,314,348}	Gly157	Cys ³²⁷
Phe158	Leu ³⁰⁸	Asn159	Asp ³⁰⁸
Phe162	Ile ^{309,347} Leu ³²⁷	Phe165	Leu ³⁴⁷
Asp168	Asn ^{327,349} His ³⁴⁹ SS ³⁴⁹	Pro170	Ser ³⁰⁹ Thr ³⁰⁹
His171	Leu ^{303,305,337}	Ile174	Asn ³⁰⁸
Thr175	Ile ^{b,e,j}	Met177	Ala ³¹⁵ Thr ³⁴⁷
Val178	Ile ^j	Ala180	Thr ³¹³ Val ³⁰⁸
Leu181	Ala ³¹⁵ Arg ²⁵⁰ Gln ²³⁰ Lys ²⁵⁰ SS ³¹²	Asp182	Val ³⁰⁹
Ala184	Arg ³²⁵ His ³²⁵ Ile ³²⁷ Lys ³²⁵ Ser ³¹² Thr ^{308,312} Val ^{b,c,f,j} SS ^{312,325}	Asn186	Asp ³²⁷
Met185	Lys ³⁰⁹ Thr ³³⁷		
Lys187	Glu ³⁴⁷		
Leu188	Ala ²⁹⁹ Arg ²⁹⁹ Asn ²⁹⁹ Gln ^{235,299,301,d,e,i} Gly ²⁹⁹ Lys ^a Pro ^{312,347} Ser ²⁹⁹ Trp ^{299,309} SS ^{299,306,312,319}		
Gln189	Arg ³²³	Ala191	Thr ^{194,303,305}
Ala197	Val ³¹³	Tyr198	Cys ^{236,316,317,350}
Ph205	Arg ²⁹⁶ Cys ^{b,c}	Lys210	Met ³⁰⁸
Asp214	Gly ²³⁰	Asp217	Val ³²⁷
Asp222	Glu ³²⁷	Ala225	Gln ³⁴⁹ Gly ³⁴⁹ Phe ³⁴⁹ Pro ³⁴⁹ Val ³⁴⁹ SS ³⁴⁹
Ser226	Arg ^{b,c}	Gly227	Ser ³²⁷
Glu228	Lys ³⁴⁷	Asp231	Gly ³⁰⁹
Asp232	Glu ³⁰⁹	Thr235	Ala ^{272,325} SS ²⁷²
His236	Arg ^{327,347} Gln ^{351,b,c,j}	Met237	Ile ³⁴⁷
Asn239	His ^{194,303,305,f,g}	Lys241	Arg ³⁰⁸ Glu ³³⁶
Asp251	Gly ²³⁰	Glu252	Gly ^{b,c,j}
Arg255	Ser ^{b,c,j}	Ile259	Val ^{194,303,305}
Thr260	Ala ³¹⁵ Asn ^{296,320,322} Leu ^{296,320,322} Ser ^{296,322} SS ^{312,320–322}	Leu262	Phe ²³⁰
Ph261	Glu ¹⁹³		
Ile263	Ala ^{119,300,315,321,323} Gly ¹¹⁹ Lys ²⁵⁰ Met ³⁰⁸ Thr ³²³ SS ^{304,320–322}		
Ala264	Cys ^{109,298} Gln ¹⁰⁹ Glu ^{108,109,352} Gly ^{249,e} His ^{109,200,244} Lys ^{109,244} Met ¹⁰⁹ Val ²⁷⁴ SS ^{304,312,320–322}		
Gly265	SS ³¹²	His266	Gln ³⁰⁸
Glu267	Gln ¹¹⁶ Val ^{e,h,o}		
Thr268	Ala ^{10,11,38,80,96,107,255,315,323,PDB code 3DGI} Asn ¹⁰⁷ Ser ³²⁹ Val ³²⁹ SS ³¹²		
Ser274	Thr ^{f,g}	Ala276	Thr ^{194,303,305}
Val281	Ala ³²⁷ Gly ³⁰⁷	Asn283	Tyr ³⁰⁸
His285	Tyr ^{236,316,317,350}	Val286	Ala ³⁰⁹ ; Glu ³²³
Ala290	Val ^{b,c,j}	Glu293	Asp ³⁰⁹

Table 3 (continued)

Ala294	Val ²³⁰		Ala295	Thr ^j
Ser304	Arg ³⁰⁹		Tyr305	His ³²³
Gln307	His ^{230,303,305,337}		Gly315	Ser ³⁰⁸
Asn319	Ser ²³⁰ Thr ^j Tyr ^{303,305,337}			
Leu324	Ile ^{296,297,312,f}		Thr327	Val ³²⁴
Ala328	Asn ³⁰⁴ Ile ^{154,274,339} Leu ^{154,274,296,304,313,320,322,339} Met ^{296,320,322} Phe ^{154,296,309,322,339,353,c} Ser ^{329,PDB code 1ZOA}	SS ^{304,312,320-322}		
Pro329	SS ³⁰⁶		Ala330	Leu ³²⁴ Pro ^{126,303,305,337} Val ³⁰⁸
Phe331	Ile ³²⁴		Ser332	Ala ³²⁴
Asp338	Gly ²⁹⁶		Val340	Met ^{312,f}
Tyr345	Cys ³⁰⁸		Lys349	Asn ³¹³
Leu353	Ile ^{194,303,305} Val ^{b,c,j}		Met354	Ala ²⁴⁹ Ser ³⁰⁷ Thr ²⁹⁹ SS ^{299,306,307}
Asp363	His ³⁰⁷		Ile366	Val ^{296,297,312,313,315,323,f}
Glu372	Cys ¹⁷⁷		Glu377	Ala ^{303,305,337}
Pro386	Ser ^{72,237,295,318}		Gln387	Cys ^{177,348,354}
Phe393	Ala ^{213,257,258} His ^{107,186,195,213,257-259,311} Trp ^{195,213,258} Tyr ^{213,257,258}			
Gly396	Met ³²⁷		Arg398	His ³⁰⁹
Ile401	Glu ¹⁹³ Pro ^{125,126} SS ³¹²		Gln403	Lys ^{PDB code 2NNB} Pro ³⁵⁵
His408	Gln ³⁰⁹		Thr411	Ala ³²⁷
Val413	Ile ³⁰⁹		Gly415	Ser ^{h,o}
Asp425	Asn ^{303,305,337}		Lys434	Arg ³⁴⁹ Glu ^{f,g} Gly ³⁴⁹ SS ³⁴⁹
Glu435	Asp ³⁴⁹ Gln ¹⁴⁹ Thr ³⁴⁹ SS ³⁴⁹			
Leu437	Ala ^{249,274,315} Arg ²⁵⁰ Asn ³¹⁶ Glu ³¹⁶ Ile ²⁷⁴ Lys ²⁵⁰ Phe ²⁷⁴ Ser ^{316,317} Thr ³¹⁶ Val ²⁷⁴ SS ^{306,312}			
Thr438	Ile ²³⁹ Leu ²³⁹ Phe ²³⁹ Val ²³⁹ SS ³¹²		Lys440	Asn ³⁴⁹ SS ³⁴⁹
Glu442	Lys ^{296,297,312,315,f}		Gly443	Ala ³¹² Asp ³¹² SS ³¹²
Val445	Arg ³¹² Met ³¹² SS ³¹²		Val446	Ile ^{f,g}
Glu464	Gly ^c		Arg471	Ala ^{272,325} Cys ²⁷² SS ²⁷²
Thr480	Met ³¹² SS ³¹²		Glu494	Lys ^{272,325}
Thr515	Met ³¹² SS ³¹²		Tyr536	Asp ²⁶⁰ Gly ²⁶⁰ Gly insertion ¹⁷⁵
Gly570	Ala ^{180,260} Asn ²⁶⁰ Asp ^{114,190,199,200,209,260}			
Trp574	Asp ^{233,260} Gly ^{114,190,260} Phe ^{180,260} Tyr ^{180,190,260}			
Pro654	Gln ³¹² Lys ³¹² SS ³¹²		Thr664	Gly ³¹² Met ³¹² SS ³¹²
Asp698	Gly ³¹² SS ³¹²		Ile710	Thr ^c
Ala963	Val ^{236,316,317}		Ser965	Ala ³⁵⁶ Asp ⁷²
Arg966	Ala ³⁵⁶ Asn ³⁵⁷ Asp ^{72,237,298,358}		Lys972	Ala ³⁵⁶ His ³⁵⁷ SS ³⁵⁷
	Met ⁷² SS ³⁵⁷			
Tyr974	Phe ³⁵⁷ SS ³⁵⁷		Cys999	Ala ¹⁹¹
Ser1024	Arg ²⁷² Glu ^{272,325} Lys ²⁷² Thr ²⁷² SS ²⁷²		Glu1037	Gly ³¹² SS ³¹²
Trp1046	Ala ^{72,187,199,237,356,359} Asp ³⁵⁷ His ³⁵⁹ Ser ^{72,237,298,358} SS ³⁵⁷			
Gly1048	Glu ^{236,316}			

SS: site saturation. Mutations generated in research carried out to assess evolutionary forces³⁶⁰⁻³⁶² are not included.^a Component of LARV and QM.^{298,299,363-366} ^b Component of 9-10A.^{296,308,309,313,315,320-322,326-328} ^c Component of 35E11.^{312,313,320} ^d Component of M01, M02, M05 & M11.^{236,256,316,317,340,350,367} ^e Drug panel component.³⁶⁸⁻³⁷¹ ^f Component of 5H6.^{309,372,373} ^g Component of 21B3.^{296,297,335,372} ^h Component of M11.^{236,316,317,340,350,367,374} ⁱ Component of GVQ.^{40,72,118,237,269,275,295,298,302,303,318,319,337,349,353,375-378} ^j Component of 139-3.^{124,296,313,325-327,379,380} ^k Component of M05.^{236,256,316,367} ^l Component of M02.^{236,256,316,317,367} ^m Component of LARV.^{298,299,363} ⁿ Component of QM.³⁶³⁻³⁶⁶ ^o Component of M01 & M05.^{236,256,316,367}

Mutations F87G and F87V raised activity with propylbenzene and 3-chlorostyrene relative to WT.³³⁴ F87A, by contrast, lowered activity but was more effective in a selectivity-altering capacity, giving 54% β-hydroxylation with propylbenzene where WT gave 99% α-hydroxylation and <1% β-hydroxylation. Alterations to optical purity levels were also observed. Even the wild-type enzyme gave an NADPH consumption rate of 13 nmol (nmol-P450)⁻¹ s⁻¹ (henceforth abbreviated to s⁻¹) with propylbenzene—40% higher than that observed with lauric acid.¹¹⁸

Like fatty acids, n-alkanes are oxidised at sub-terminal positions by P450_{BM3}. Researchers have sought to create variants with the ability to convert such substrates instead to primary alcohols, which are high-value products and synthetic intermediates. Mutation A328V figured prominently in a variant that gave 82% 2-octanol and 5% 1-octanol from octane³²⁶ where WT

gave 17%, and zero respectively, preferring to oxidise the 3- and 4-positions.¹²⁴ A82L played a lesser role in the selectivity shift, but enhanced coupling levels and doubled the total turnover number (TTN).³²⁶ The F87V/A328F double mutant gave 92% 2-octanol.³³⁹ A328L was the crucial mutation in a variant that gave 52% 1-octanol from octane, with V78T and A82G in SRS1 also making significant contributions.³²² The oxidation of valencene to nootkatone, a prized grapefruit flavouring not formed by WT, was accomplished by creating space in the active site using mutations F87A and I263A.³⁰⁰ The F87V mutant was found to oxidise phenols, a compound type accepted only reluctantly by WT.³⁴⁵ Hydroxylation typically took place *para* to the phenolic group at PFRs between two and three orders of magnitude higher than those given by WT. The F87V mutation has also been used in an activity-enhancing capacity with β-ionone²⁹⁵ and monoterpenes.³⁰² Mutations A82F,

F87V, I263A and A328V were used to raise epoxidation levels at the expense of allylic hydroxylation with terminal alkenes.³²¹ F87L has been employed in a selectivity-directing capacity with octane³²² and n-butylbenzene.¹⁹⁴ The F87L mutation also proved useful in drug metabolism.²⁹⁶ Mutation A82F raised the PFR with indole 170-fold by rendering the active site less spacious,¹¹² and enhanced the stereospecificity of styrene epoxidation when combined with T438F, giving 64% (*R*)-styrene oxide.²³⁹ The F87G mutant gave 92% of the (*R*)-oxide with the same substrate.⁷²

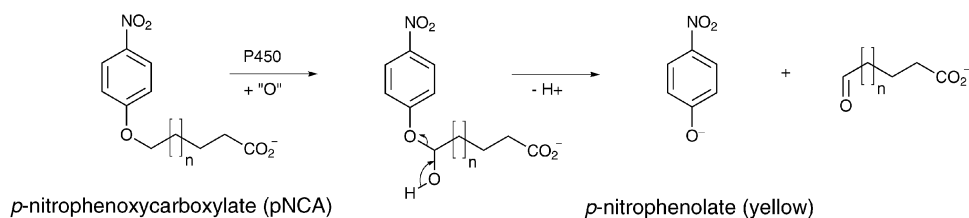
The enzyme was engineered to accept short-chain fatty acids by installing a polar couplet modelled on the Arg47/Tyr51 duet midway down the access channel (L75T/L181K).²⁵⁰ This double mutant gave a k_{cat} value of 43 s⁻¹ with hexanoic acid as against 3.8 s⁻¹ for WT, and also a lower K_M value. Using the same principle, tyrosine was introduced at Ser72 to help bias selectivity in lauric acid oxidation with a view to preparing γ - and δ -lactone precursors, the S72Y/V78A/F87A triple mutant giving 55% hydroxylation between the (ω -6)- and (ω -9)-positions where WT gave nil.¹¹⁹ I263G and I263A gave less dramatic shifts. An F87G triple mutant gave 77% verbenol, a precursor to the flavouring additive verbenone, from (−)- α -pinene, a significant improvement over the 20% given by the F87V analogue.²⁷⁵ F87Y enhanced the activity of certain variants towards non-natural substrates such as testosterone.^{316,340} A portfolio of double mutants capable of manipulating product distributions in the oxidation of sundry terpenes,^{154,381} alkanes and cycloalkanes³³⁹ was created from permutations of five hydrophobic mutations at two specific sites, Phe87 and Ala328. Extension of this focused library to two further sites, Ala264 and Leu437, allowed still greater selectivity control.²⁷⁴ In a comparable strategy, alanine was incorporated at permutations of eight targeted active-site positions to expedite the oxidation of bulky substrates such as substituted monosaccharides and 11- α -hydroxyprogesterone, leading to activity enhancements of up to eightfold.³¹⁵ Finally, the introduction of proline at the residue immediately to the C-terminus side of the cysteine ligand gave a mutant that exhibited remarkably high PFRs with non-natural substrates (e.g. 60 s⁻¹ with propylbenzene vs. 11 s⁻¹ for WT).^{125,126} Unlike the other substitutions detailed here, I401P lies to the proximal side of the haem iron. Mutation Q403P exhibited similar, albeit more modest, rate-accelerating properties (39 s⁻¹ with propylbenzene).³⁵⁵

4.3 Random mutagenesis, directed evolution and rational evolution

P25Q, the first randomly generated P450_{BM3} mutation to be reported, was found to weaken fatty acid binding and alter product profiles,¹¹⁷ but limited interest was shown in this

approach prior to the discovery that active P450 variants turned complex media cultures blue by oxidising the indole produced from tryptophan degradation to indigo.³⁸² This provided researchers with an efficient and cost-effective method for screening libraries containing many hundreds of randomly created variants for enhanced oxidase activity. In a pioneering “rational evolution” study, error-prone PCR was used to generate a small number of indigo-producing P450_{BM3} mutants. All proved to contain mutations at three specific residues, and a highly active second-generation variant was created by site-saturating these in turn: A74G/F87V/L188Q (GVQ).³¹⁹ This oxidised a range of non-natural substrates¹¹⁸ including PAHs,³⁷⁵ organophosphorus pesticides^{376,383} and chlorinated dioxins,³⁷⁷ as well as branched fatty acids.⁴⁰ The GVQ variant and its component mutations have since been applied in diverse contexts.^{237,269,275,295,298,318,349} The CYP102A3 homologue showed dramatically enhanced activity relative to WT_{A3} (e.g. 35 s⁻¹ with capric acid vs. 0.8 s⁻¹).¹³⁹ More surprisingly, it displayed slight ω -hydroxylase activity, on which basis it was itself subjected to directed evolution with the object of leveraging this capability, leading to the identification of the A330V_{A3} mutation. When this was used in place of the original glutamine substitution in GVQ_{A3}, 1-octanol formation from octane rose to ca. 50% of the product mix.¹⁵² This dovetailed with earlier site-specific mutagenesis research in which the A1 homologue, A328V_{A1} had been successfully deployed in a similar role³²⁶ (section 4.2).

The PFR-enhancing properties of the GVQ variant extend to substrates that bear almost no structural resemblance to indole (e.g. 9.8 s⁻¹ with pentane vs. 0.3 s⁻¹ for WT),³⁰³ as do those of other variants identified via indigo screening.³⁰³ However, the chances of engineering successful variants clearly improve if customised high-throughput screens involving substrates more closely related to those being targeted are employed. The P450-mediated *O*-dealkylation of *p*-nitrophenoxycarboxylic acids (pNCAs) has been widely exploited in this capacity as the yellow chromophore produced is readily detectable (Scheme 1). This assay was first used to identify rational-evolution variants with enhanced activity towards shorter-chain (C8–C10) fatty acids.³³⁰ Starting from an F87A platform, libraries with mutations at eight other sites of known or likely importance were randomly generated and screened. The most promising mutations were then combined in a stepwise fashion to generate the V26T/R47F/A74G/F87A/L188K variant.²⁹⁹ Activity was further enhanced when the F87A base mutation was replaced with F87V.³⁶³ Both these variants have been used in the development of improved preparative-scale protocols.^{298,364,366} The assay was subsequently customised for *in vivo* use to allow more efficient, cost-effective throughput.³³³ A medium-throughput version



Scheme 1 The colorimetric pNCA assay.

has been created to allow the identification of variants with superior performance in a zinc-driven system (section 7.3).³⁰⁶

Other customised screening methods have been created to assay for the formation of phenols,^{310,384} epoxides^{325,379} and primary alcohols.¹⁵² An alkoxyresorufin fluorescence assay for *O*-dealkylation was able to distinguish variants with an aptitude for metabolising pharmaceuticals,³⁰¹ and a continuous-flow version with cost and efficiency advantages based on allyloxyresorufin fluorescence detection has been used to cross-screen a library of mutants against 30 different substrates.³¹⁶ One of the earliest P450_{BM3} libraries of variants to be reported²³⁰ was screened using an assay for the formation of NADP⁺, which can be detected either fluorometrically or spectroscopically when treated with strong alkali.¹²⁰ Screening has been addressed as a review topic in its own right.^{385,386}

In a variation to the pNCA protocol, *p*-nitrophenoxo octane dealkylation was used to screen for medium-chain alkane hydroxylase activity. Successive rounds of directed evolution yielded a variant capable of hydroxylating octane at enhanced rates.³⁵¹ Three further rounds gave rise to an 11-mutation variant, 139-3, which oxidised alkanes as short as butane and propane, substrates towards which WT showed negligible activity.¹²⁴ 9-10A, a 13-mutation variant containing eight of the substitutions from 139-3, showed enhanced activity towards propane when two designed mutations were introduced (A82L and A328V, section 4.2).³²⁶ Screening from this stage on was carried out using dimethylether as a propane surrogate. Further modifications produced PMO, a variant containing 24-mutations, including three in the BMR domain, that showed 95% coupling efficiency with propane *in vitro* and gave a TTN of 36 000.³¹² A well summarised account of this work is available.³⁸⁷ Variant 35E11, which contained twelve of the mutations in 9-10A, oxidised ethane at a PFR of 0.007 s⁻¹.³²⁰ In spite of the specialised screening techniques employed, the rate-improving properties of the directed-evolution mutations discovered were (like those of the GVQ variant) generic in scope, 139-3 showing enhanced activity towards substrates structurally unrelated to *n*-alkanes such as valencene and limonene, as well as fatty acids.³⁸⁷ Specificity for short-chain alkanes developed only when an important mutation was discovered at an access channel residue (L188P).³⁸⁷ Though destabilising, this increased coupling efficiency with propane from 15% to 44%. Analogous directed evolution techniques were used to create variants with enhanced peroxygenase activity (“21B3”),^{123,335} thermostability (“5H6”)³⁷² and co-solvent tolerance.²⁷² This research has been reviewed.³⁸⁸

Variants with the ability to metabolise pharmaceuticals were developed using the alkoxyresorufin fluorescence screen described above.³⁰¹ Known site-specific mutations were first combined to give a triple mutant with activity 900-fold higher than WT: R47L/F87V/L188Q. Activity towards drugs such as acetaminophen and MDMA was still up to two orders of magnitude lower than that shown by human P450s,²³⁵ but a variant with 90-fold higher initial activity than human CYP2D6 towards dextromethorphan was produced by subjecting this platform to directed evolution.³⁶⁷ Three influential new mutations were identified—all at, or adjacent to, active-site residues: F81I, L86I and E267V. Indigo screening of an unrelated directed-evolution library followed by fluorescence

screening for coumarin oxidation activity identified another family of variants with an ability to metabolise pharmaceuticals such as acetaminophen.³⁴⁷ The most promising of those generated in the first round of evolution, F162I/E228K, was used as a template for the succeeding round, from which the L188P mutation once more emerged as significant. Docking studies showed that Thr260 and Thr268 played important roles in orientating coumarin in the active site by interacting with the carbonyl oxygen, and suggested that these interactions were stronger and more influential in the second-generation variants.

One of the more unusual directed-evolution variants to emerge to date is the single-site proline mutant, A330P.³⁰³ Though identified *via* indigo screening, this was selectively active towards small non-natural substrates such as toluene and pentane relative to WT. It also possessed selectivity-altering properties, giving 30% *o*-propylphenol from propylbenzene *vs.* 1% for WT, which gave 99% 1-phenyl-1-propanol. Again the mutated residue was adjacent to an access-channel residue (Pro329). Variant KT5, a four-mutation variant containing both F87A and A330P identified in the same screen, gave contrasting selectivity profiles, producing 78% 2-phenyl-1-propanol from propylbenzene, *vs.* nil for WT. KSK19 and KT2, which contained four and five mutations respectively, were more typical directed-evolution variants from the same library, enhancing PFRs by an order of magnitude relative to the respective base variants even though none of the introduced mutations was in the active site. A directed-evolution library created using an F87A/R47L/M354S platform yielded two activity-enhancing mutations for use in zinc-driven systems, V281G and D363H, the latter being the more influential.³⁰⁷

Site-saturation mutagenesis has been carried out on key residues in the substrate pocket and along the access channel. As early as 1993, the I-helix was targeted with the object of altering substrate specificity.³⁸⁹ Variants with enhanced activity have been created by targeting Arg47, Tyr51, Pro329, Met354 and Leu437 using an F87A template.^{306,307,310} Val78 and Ala184 were site-saturated during the development of a screen for variants with epoxygenase activity.³²⁵ A variant suitable for playing a role in a multi-step synthesis of artemisinin, an anti-malarial drug, was developed from the R47L/Y51F/F87A template by site-saturating Phe87, Ile263, Ala264, and Ala328, leading to the inclusion of the A328L mutation.³⁰⁴ The majority of the residues shown in Fig. 4 were site-saturated during the further development of two directed-evolution variants, 9-10A and 21B3, for more specialised purposes, including sites adjacent to key active-site residues such as Phe81, Thr88, Thr260, Ile401 and Thr438.^{297,312,320–322} Site-saturation mutagenesis confirmed that the L188P mutation discovered *via* error-prone PCR was the optimum substitution at this position for conversion of the enzyme into a propane hydroxylase.³⁸⁷ Phe87 was site-saturated as a means of exploring the importance of F87V to a potent drug-metabolising variant.³⁴⁰ Finally, five residues outside the active site (again identified by error-prone PCR) were targeted during the creation of an indole hydroxylase: Asp168, Ala225, Lys434, Glu435 and Lys440.³⁴⁹

4.4 Chimeragenesis and protein fusions³⁹⁰

In an imaginative and distinctive approach to reengineering the protein, short sections of CYP4C7 from *Diploptera punctata*

(cockroach), a P450 of unknown structure that ω -hydroxylates farnesol, were substituted into P450_{BM3} in two key substrate recognition regions, SRS1 and SRS5. One recombinant showed a six-fold activity enhancement, while another gave the terminal hydroxylation product, which is not formed by WT P450_{BM3}, in > 50% yields. F87L, A328V and A330L were the most influential mutations.^{32,115,324} This strategy was redolent of earlier research in which a soluble form of CYP2E1 had been created by substituting the majority of the CYP2E1 sequence into BMP, while retaining the BMR domain.²³⁰ The same researchers also fused BMP to a flavodoxin from *Desulfovibrio vulgaris* to improve the electrochemical properties of the enzyme^{230,391} (section 7.3). Detailed studies of the interactions between the two partners in the latter hybrid have been carried out.²³¹ Other microsomal P450 domains have been fused to BMR, allowing the *in vitro* oxidation of substrates oxidised by mammalian P450s.^{189,392,393} Approximately 10% oxygenase activity was retained when BMR was fused to the NOS haem domain.³⁹⁴

Chimeras comprising sections of CYP102A1, A2 and A3 have been reported.^{149,336,395} Two were active towards verapamil and astemizole, substrates towards which none of the parents was active. Surprisingly, perhaps, the reductase component was able to influence substrate specificity. A1 was *ca.* threefold more active towards 2-phenoxyethanol if BMR was replaced with the A2 reductase domain, for instance, but *ca.* threefold less active towards 12-pNCA.³⁹⁵ This approach has proved more effective than directed evolution for producing variants with enhanced thermostability profiles, and a method for predicting chimeric thermostability from the sequence fragments involved has been developed.³⁹⁶ Unfortunately, there often appears to be a trade-off with activity.³⁹⁹ Thus, although a fusion of BMP to a thermostable reductase domain from a sulphite reductase was stable at 49 °C, fatty acid oxidation rates and coupling efficiency were significantly compromised.⁷² Similarly, a fusion between BMP and the A3 reductase domain offered superior process stability but gave a TTN roughly one third as high as the A1 parent.¹⁵⁰ Finally, thermostability has been enhanced by fusing an archaeal *cis-trans* isomerase known to function as a molecular chaperone to full-length P450_{BM3} at the N-terminus.³⁴⁶

4.5 Practical applications

A number of purposes can be served by altering the phenylalanine side-chain of Phe87. Mutation F87Y has been employed to probe peroxy nitrite inactivation, which was found to take place selectively at Tyr334 in the wild-type enzyme.³⁴⁴ The F87G mutant deformed aldehydes, leading to the formation of haem adducts,³⁴² though the enzyme retained some oxidase activity, which does not occur when the reaction is performed with other isoforms.¹²¹ The same mutant was used to explore P450 reaction intermediates,²²³ and in a study of spin state equilibria.²²⁰ The F87A mutant played roles in investigations into the binding of multiple substrates in the active site,¹²² and co-solvent inactivation, to which it was more susceptible than WT.²⁷³ It has been a popular platform for rational and directed evolution,^{272,299,303,304,335} and was prominent in the development of the pNCA screen.³³⁰ This research was guided

by a report (since questioned, section 3.2.2) that the F87A mutant ω -hydroxylated fatty acids, which implied that the dealkylation of medium-chain pNCAs might be favoured by F87A over competing sub-terminal hydroxylation pathways. The mutant duly proved superior to WT in the assay, but in practice this probably owed a good deal to the enhanced active-site water presence, which is conducive to the binding of polar substrates.³²⁸ It is no coincidence that the pNCA assay is also effective at identifying variants with enhanced peroxygenase activity¹²³ (section 7.3), which almost invariably contain F87A (or F87G).^{123,332} The F87A mutation has since been employed in the development of other dealkylation-based assays.^{306,310}

Other residues have been mutated for a variety of unconnected reasons. The Y51F mutant was used to demonstrate that Tyr51 was a principal nitration site following the binding and subsequent dissociation of NO.³¹¹ Cysteine was introduced at Leu104, and Gln387, two sites implicated in FMN/BMP binding, prior to dansylation. The impact on inter-domain electron transfer was then assessed, the E372C mutant being employed as a control.¹⁷⁷ Rapid haem reduction could be effected photochemically ($2.5 \times 10^6 \text{ s}^{-1}$ and $4.6 \times 10^5 \text{ s}^{-1}$ with and without substrate bound) by tethering a ruthenium complex to Q387C.³⁴⁸ A ruthenium photosensitiser was linked to a K97C variant to allow the high-valent iron intermediates generated by photoexcitation to be studied.³¹⁴ In all cases, the naturally occurring cysteine at residue 156 was blocked using serine. C156S was subsequently used as part of a protocol to immobilise the protein on a gold electrode (section 7.3), together with C62S.¹⁹⁸ BMP was “wired” to a graphite electrode by attaching pyrene to the Q387C mutant.³⁵⁴ All thirteen methionine residues in BMP were replaced with norleucine, with the aim of limiting inactivation *via* methionine oxidation, resulting in a small increase in peroxygenase activity but a decrease in thermostability.³⁹⁷ Surprisingly, perhaps, applications have also been found for randomly generated P450_{BM3} mutations. Stability was shown to enhance an enzyme’s capacity to evolve;³⁶⁰ and genetic drift was explored as a general topic by evolving the enzyme under conditions designed to enhance a specific activity type and monitoring the impact on other, unrelated activity types.^{361,362} Various mutations not detailed in Table 3 were generated in this work. On a similar theme, the enzyme has been the subject of an investigation into whether transversion mutations (purine to pyrimidine, or *vice versa*) are adaptively superior to transition mutations (purine to purine, or pyrimidine to pyrimidine).³⁹⁸

5 Exploring mutants and variants

5.1 Crystal structures

Several of the earliest mutant crystal structures to be published were broadly identical to the SF WT structure, including those of SF T268A (PDB codes 1FAH²⁵⁵ and 1YQO),¹⁰⁷ T268N (1YQP),¹⁰⁷ F393H (1JME),²⁵⁹ F393A, F393W and F393Y (1P0V, 1P0W and 1P0X).²⁵⁸ The highly plastic F/G loop and the final turns of the helices to either side (residues 189–200) were unresolved in all but one of these structures. In the T268A structure, the carbonyl oxygen of Ala264, though unable to hydrogen-bond to the side-chain of the

mutated residue, remained hydrogen-bonded to the axial water molecule.²⁵⁵ In the T268N mutant, the introduced residue was hydrogen-bonded to the Thr438 side-chain.¹⁰⁷ In the F393A mutant, the Gln403 side-chain was displaced into the space vacated by the phenyl ring of the substituted residue.²⁵⁸

SF and palmitoleate-bound structures have been published for the A264E mutant (1SMI and 1SMJ),³⁵² which was prepared with the idea of improving stability by linking the prosthetic haem group covalently to the protein. A conserved glutamate residue at the homologous position performs this function in eukaryotic CYP4 isoforms.³⁹⁹ Rather than esterifying with the porphyrin system, however, the introduced residue displayed a capacity to coordinate to the haem iron in place of the axial water ligand. In the palmitoleate-bound structure, it was ligated in both molecules of the asymmetric unit, while in the SF structure it was “on” in molecule A and “off” in molecule B, where the axial site was instead occupied by a water ligand. According to spectroscopic data, the “off” conformation was 75–80% populated in solution. The same ambivalent coordinative tendencies were observed in the structures of A264H, A264K (2IJ3 and 2IJ4),²⁴⁴ A264C, A264M and A264Q (3EKB, 3EKD and 3EKF).¹⁰⁹ A fatty acid was bound in one molecule of the A264M asymmetric unit, but the other mutants were crystallised in the SF form. With the exception of A264H, all these structures nonetheless overlaid more closely onto the SB form of WT than onto the SF form (rmsd: 0.5 Å vs. 1.4 Å for A264E, for example). The structures of L86E, F261E and I401E (3KX3, 3KX5 and 3KX4), which were created with similar aims to the A264E mutant, have also been solved.¹⁹³ These showed the introduced glutamate linking neither to the porphyrin nor to the haem iron, though EPR studies suggested some haem ligation in the two distal-side mutants. The water molecule closest to the haem iron in the L86E mutant, which was crystallised in the NPG-bound form, was partitioned between the axial ligation site (*ca.* 35% occupancy) and the “alternative”, off-centre water site, showing that the presence of substrate and axial water ligation were not mutually incompatible.

Tenacious substrate binding meant that two high-activity variants, A82F and 139-3, could be crystallised only in an SB condition. The A82F structure (2UWH)¹¹² showed palmitic acid bound with the carboxylate group closer to the protein surface than in WT, and the hydrogen bond to Tyr51 disrupted. It appeared that active-site residues such as Ile263 and Leu437 adopted SB orientations not as a result of the presence of substrate but on account of the bulky substitution, and it was suggested that the mutant would probably exist in the SB conformation even in the absence of substrate. A water molecule lay within 3.5 Å of the haem iron in only one of the six molecules in the asymmetric unit, showing that occupation of the “alternative” water binding site was not a mandatory feature of the SB or high-spin form, and consistent with the unusual inability of the SB mutant to move to the low-spin form on temperature reduction. NPG-bound 139-3 (3CBD)³⁸⁷ superposed relatively well onto the NPG-bound WT structure (rmsd = 0.5 Å), the greatest deviations being at the N-terminus end and residues 45–47, 243–247 and 380–383. The hydrophobic pocket enclosing the haem iron was 29 Å³ more capacious than in WT, primarily on account of the V78A substitution.

Leu437 was in contact with the A184V substitution across the substrate access channel. Models based on this structure suggested that mutation A328F, which was subsequently incorporated into 139-3 to create a more effective alkane hydroxylase, would compartmentalise the active site, creating a more tightly enclosed inner pocket. 22A3, a precursor of directed-evolution variants with enhanced activity towards substrates metabolised by human CYP2C9, was crystallised in the SF form (3Q18).³⁰⁹ This structure overlaid closely onto SB WT structures and those of A264 mutants, which exist in SB conformations (*vide supra*), but poorly onto SF structures. The B' helix was more flexible than in SF WT due to the L75R mutation, which appeared to contribute significantly to the altered substrate specificity.

Three further high-activity variants were crystallised in the SF form: A330P (3M4V), I401P (3HF2) and KT2 (3PSX). In all three structures, the F/G loop was unresolved in at least one molecule, as were portions of the flanking helices. In the A330P structure,¹²⁶ the positions of the backbone atoms of the mutated residue were relatively little changed, but Pro329, the adjoining residue was displaced into the substrate access channel, possibly because this was less disruptive to the β1 sheet. The resulting constriction to the area around the haem iron provided a structural basis for the selectivity-altering properties displayed by the variant and the enhanced activity shown towards smaller substrates relative to WT. I401P^{125,126} and KT2,¹⁹⁴ by contrast, exhibited little disruption in the immediate vicinity of the mutated residues, but resembled SB forms of the enzyme in key respects. In both structures, the proximal loop dropped away from the active site, drawing the haem iron to the proximal side of the porphyrin plane (*cf.* Fig. 3D). The I-helix kink angle was reduced due to changes in hydrogen-bonding patterns in the dioxygen activation region, the reorientation of the carbonyl oxygen of Gly265 being particularly influential (*cf.* Fig. 3C). In addition, each variant possessed SB-like characteristics not shared by the other. Thus the nearest water molecule to the haem iron in I401P lay 3.6 Å distant, off-axial and close to the “alternative” site identified in SB WT, whereas the KT2 structure instead showed a water molecule 2.6 Å from the haem iron, as in SF WT—albeit too far from the I-helix to hydrogen bond to Ala264. At the same time, the two ion pairs linking the G- and I-helices were disrupted in KT2, as was the ion pair pinning the H-helix to the F/G loop (*cf.* Fig. 3B), and the side-chains of Phe87, Phe158, Phe261 and His266 were in SB WT conformations (*cf.* Fig. 3C and D), changes that were not apparent in the I401P structure. It was suggested that these two variants—particularly KT2—were in catalytically primed conformations in which the reorganisation energy barrier associated with the first flavin-to-haem electron transfer was lower than in WT—*i.e.* the role of substrate-induced conformational change was reduced. How the introduced mutations had brought about the changes was unclear. Another structure that resembles SB WT even though crystallised in the SF form is that of the ruthenium photosensitiser-linked C62A/K97C/C156S variant (3NPL).³¹⁴

Other mutant structures deposited in the Protein Data Bank but as yet undiscussed in publications by the providers include A328S (1ZO4), NPG-bound A328V (1ZOA), Q403K (2NNB), F87A/T268A (3DGI) and DMSO-bound F87A (2X7Y and 2X80).

5.2 Biophysical properties, catalytic parameters and binding constants

5.2.1. Reduction potentials. Reduction potentials (E) have been determined for several families of mutants, both in the SF form and when bound with different substrates (Table 4). E generally becomes more oxidising on substrate binding due to displacement of the axial water ligand, the extent of the shift being substrate-dependent. Thus arachidonate, a preferred substrate, induces larger increases in the reduction potential than palmitate, which in turn induces larger increases than propylbenzene, a non-natural substrate. However, the potentials shown by A264E,¹⁰⁸ A264M²⁴⁴ and I401P¹²⁵ showed little change on substrate binding, as they were already significantly more oxidising than that of WT in the SF form. In the case of the Ala264 mutants, the unusual ligand sets involved may have been responsible. With I401P, a possible explanation was provided by the crystal structure, which showed the nearest water molecule to the haem iron to be remote and off-axial, consistent with the fact that the haem domain was already *ca.* 90% high-spin in the SF form. More challenging to account for are the elevated SF E values exhibited by three other proximal-side mutants F393A, F393H²⁵⁸ and I401E,¹⁹³ whose water ligands lay in conventional axial SF positions in the corresponding crystal structures. The reduction potentials of these variants increased still further on substrate binding, accompanied by normal type I spin shifts from $\geq 90\%$ low-spin resting states. It was believed for a time that potentials could be influenced by the network of hydrogen bonds formed by the sulphur atom of the axial cysteine ligand.⁴⁰⁰ This network can be disrupted by proximal-side mutations, potentially explaining the observed potential shifts. However, the Fe–S stretching frequency remained unaltered when Phe393 was mutated,²¹³ while the I401P mutation had the opposite effect on the reduction potential to its P450_{cam} homologue,¹²⁶ so arguments along such lines do not appear to provide a satisfactory explanation for these data. An alternative suggestion is that potentials reflect the extent to which the vinyl groups of the porphyrin system are in-plane, as well as the conformations adopted by the propionate groups.²¹³

As discussed in section 2.2, the physiological relevance of thermodynamic parameters determined under anaerobic conditions is open to debate. Moreover, it is apparent from Table 4 that little or no indication of a variant's catalytic activity can be obtained either from its SF reduction potential or from the shift in potential that a substrate induces.²⁵⁸ Closer attention is therefore paid to FMN-to-haem electron transfer rates, kinetic parameters measured in the full-length protein that have a direct bearing on k_{cat} values.

5.2.2. Electron transfer rates. The rate of the first FMN-to-haem electron transfer, k_f has been determined in various full-length SF and SB mutants (Table 4). k_f is generally $\leq 5 \text{ s}^{-1}$ in the absence of substrate, but significantly higher when a viable substrate is bound. As with the reduction potential, the extent of the increase is substrate-dependent. k_f values of 226 s^{-1} and 38.5 s^{-1} were determined for WT bound with palmitic acid and propylbenzene respectively, for example.¹⁹⁴ The correlation between E and k_f is reasonable for SB variants with

relatively low reduction potentials, as with P450_{cam},⁴⁰² but less good for variants with more oxidising potentials (Fig. 5). The glutamate mutants, L86E, F261E and I401E have potentials between -166 mV and -197 mV in the arachidonate-bound form, but k_f values that range from 58 to 473 s^{-1} , for instance.¹⁹³ Such dichotomies are wholly consistent with Marcus theory, which indicates that the activation energy associated with electron transfer is a function not only of the reduction potential but also of the energies associated with the accompanying inner-sphere (*e.g.* Fe–OH₂ bond cleavage) and outer-sphere (*e.g.* changes in protein conformation) reorganisation.¹⁹² An illustration of how dominant the structural component can be is provided by the substrate-free form of variant KT2, which displayed an E value of -405 mV (*vs.* -449 mV for SF WT), but a k_f value of 209 s^{-1} (*vs.* 1.5 s^{-1}).¹⁹⁴ The crystal structure of this variant showed a close resemblance to those of substrate-bound forms of WT (section 5.1), indicating that the level of reorganization associated with substrate binding would be significantly lower than in WT.

KT2 is not the only variant to exhibit a high k_f value in the SF form. Similar behaviour has been observed in I401E, L86E¹⁹³ and I401P.¹²⁶ Each of these variants showed a higher rate of NADPH consumption in the absence of substrate (leak rate) than WT. (Early research on WT suggested that such leakage takes place exclusively from the BMR domain.)¹⁰⁴ The I401P leak rate (7.6 s^{-1} *in vitro* *vs.* 0.5 s^{-1} for WT),¹²⁶ though just 3% of the respective k_f value, was probably sufficient to place any expression host under metabolic stress, but in KT2 the leak rate was an order of magnitude lower at 0.8 s^{-1} (0.4% of k_f).¹⁹⁴ The first electron transfer is therefore not the only step “gating” the catalytic cycle to guard against futile electron cycling and the associated generation of unwanted reactive oxygen species. Evidently a mechanism exists in these mutants for preventing the rapid reduction of dioxygen to water or peroxide by NADPH in the absence of substrate even if FMN-to-haem electron transfer has already taken place, and it seems likely that the same applies in WT. This throws up a perplexing paradox: KT2 is active towards substrates that do not fit the active site particularly well, apparently because substrate-induced conformational change is no longer essential for rapid FMN-to-haem electron transfer; yet NADPH consumption rates are negligible in the SF form, in which the first electron transfer is also rapid, showing that the variant commits to catalysis only if a substrate is present—*i.e.* substrate-induced conformational change of some description appears to be as crucial to subsequent steps in the catalytic cycle in this variant as it is in WT.

Discussion of the relationship between k_f and k_{cat} is complicated by the fact that the data published for the wild-type enzyme with fatty acid substrates lack consistency (Tables 2 and 4). This is partly because different research groups employ different experimental conditions. k_f is sensitive to temperature, buffer composition¹²⁷ and NADPH preincubation times,¹⁸⁷ all of which can therefore influence k_{cat} values. pH is important,^{19,34} as are the length of time for which a substrate is preincubated with the enzyme prior to NADPH addition,^{19,113,199} and the solvent in which it is prepared. The K_D value given by WT with aqueous lauric acid is 150% higher than that obtained if an organic co-solvent is used to make up the stock solution, for instance,¹⁰⁶ and there are corresponding

Table 4 Biophysical parameters for P450_{BM3} variants

Substrate-free <i>E</i> (mV)	<i>k</i> _f (s ⁻¹)	Mutant	Substrate-bound				Ref.
			<i>E</i> (mV)	<i>k</i> _f (s ⁻¹)	<i>k</i> _{cat} (s ⁻¹)	<i>T</i> ^a (°C)	
14	1.5	Lauric acid					
		WT		130		25	105
		WT		107	82	30	127
		WT		291			187
		WT		139	86	30	106, 240
		F42A		10	41		
		R47A		28	66		
		R47G		29	46		
		Y51F		62	102		
		F87G		15	13		
		F87Y		27	27		
		WT		172	86	30	257 ^b
		F393A		468	29		
		F393H		439	37		
		F393Y		215	65		
−368	0.7	Myristic acid					
		WT		111	46	25	109, 200
		A264H		7	0.004		
		Palmitic acid					
		WT	−265				
		WT		77		30	108, 173
		WT		303	122	30	127
		WT	−317	226	91	25,30	126
		I401P	−274	191	76		126
		KT2 ^d	−303	277	111		194
		Arachidonic acid					
		WT	−239	290	285	25,30	106, 173, 401
		WT		348	285	30	257 ^b
		F393A		1176	21		
		F393H		832	33		
−449	2.6	F393Y		366	143		
		WT	−289	99	67	15	257, 258
		F393A	−151	240	18		
		F393H	−176	205	21		
		F393W	−360	29	41		
		F393Y	−295	94	66		
		WT	−289	101	95	15	107 ^c
		T268A	−355	28	31		
		T268A/F393H	−255	116	19		
		T268N	−358	15	28		
		T268N/F393H	−270	52	7.2		
		F393H	−176	232	31		
		WT	−289		285	30	108
		A264E	−314		29		
−392	1.1	WT	−283		273	25	109
		A264C	−240		0.01		
		A264H			0.01		
		A264K			0.05		
		A264M	−227		1.9		
		A264Q	−35		13		
		WT	−285	250	273	25	193 ^b
		L86E	−176	213	126		
		F261E	−197	58	0.3		
		I401E	−166	473	33		
		Propylbenzene					
		WT	−400	39	13.1	25,30	194
		KT2 ^d	−334	200	121		

Each group of mutants is shown with data obtained for WT under identical conditions.^a Temperatures relate only to *k*_f and *k*_{cat} data (RT: Room temperature)—all reduction potentials were determined at 25 °C. ^b *k*_{lim} data in lieu of *k*_f data. ^c *k*_{sat} data in lieu of *k*_{cat} data. ^d KT2 = A191T/N239H/I259V/A276T/L353I.

increases to *K*_M and *k*_{cat} values. An apparent *k*_{cat} value of ca. 280 s⁻¹ has been reported for WT with arachidonic acid,

the preferred straight-chain substrate,^{106,109} but this has proved difficult to emulate,¹⁴² the next highest value in the

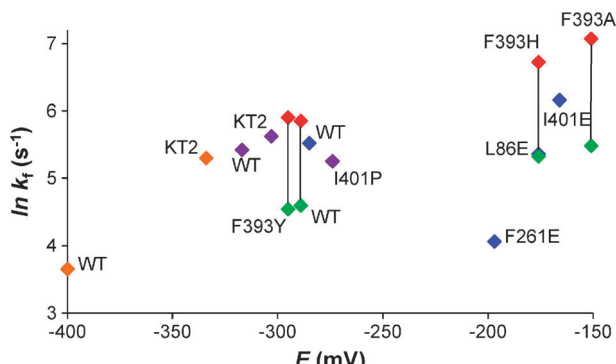


Fig. 5 Reduction potentials and first electron transfer rates for SB P450_{BM3} and variants. Data are from Table 4. Reduction potentials were determined at 25 °C. k_f values were determined at 25 °C other than those for F393 variants, represented by red (30 °C) and green (15 °C) points. Points coloured violet relate to palmitic acid, orange points to propylbenzene, and other points to arachidonic acid.

literature being 139 s $^{-1}$ for tetradecyltrimethylammonium bromide oxidation.⁶³ Being generally more rapid in P450_{BM3} than other isoforms,¹⁸² k_f is not necessarily rate-determining, as it is, for example, in P450_{cam} when putidaredoxin is in excess.⁴⁰³ Subsequent steps in the cycle such as the second FMN-to-haem electron transfer, dioxygen activation and product release play a more significant role in rate limitation,¹⁰⁵ though the extent to which this occurs varies by substrate and by mutant. Apparent k_{cat}/k_f values were respectively 77%, 62% and 40% for the oxidation of lauric, myristic and palmitic acids by WT, for instance.¹²⁷

Against this background, P450_{BM3} variants fall loosely into three categories when k_f and k_{cat} values are compared. k_f exceeded k_{cat} by an order of magnitude or more in arachidonate-bound variants containing F393A, F393H^{107,258} and I401E,¹⁹³ suggesting that a subsequent step in the cycle was rate-limiting.²⁵⁸ These mutations increased the substrate-bound first electron transfer rate two- to three-fold relative to WT, implying that accelerated haem reduction was catalytically undesirable, and it was suggested that there could be a trade-off between the rate at which this took place and the dioxygen binding rate.²⁵⁷ Variants in the second category gave catalytic rates approximately half as fast as the corresponding first electron transfer rate. Examples include L86E, F393Y, I401P and KT2—the latter whether bound with palmitic acid or with propylbenzene. In several data sets, WT also fitted this paradigm. Here, both the first electron transfer rate and one or more subsequent steps in the catalytic cycle played roles in limiting the catalytic rate. Variants in the third category gave apparent k_{cat} values equal to, or greater than, the corresponding k_f values. Most of these were investigated only in the laurate-bound form, where k_{cat} significantly exceeded the NADPH consumption rate observed at the laurate concentration used to determine k_f because the associated K_M values were relatively high. Mutant F42A gave k_f and k_{cat} values of 10 s $^{-1}$ and 41 s $^{-1}$ respectively, for example, but an NADPH consumption rate of just 11 s $^{-1}$ since the K_M value was 2.1 mM.¹⁰⁶ However, arachidonate-bound T268A, T268N¹⁰⁷ and F393W²⁵⁸ also fell under this heading, as k_f was significantly below the WT value at <30 s $^{-1}$. This suggests that k_f becomes rate-limiting only if it is severely curtailed.

Why k_f should be rate-limiting for WT with arachidonic acid is therefore something of a mystery ($k_f = 250$ s $^{-1}$, $k_{cat} = 273$ s $^{-1}$ at 25 °C),¹⁹³ particularly given that k_{cat}/k_f ratios decrease as active site saturation becomes more facile across the lauric/myristic/palmitic acid series (*vide supra*). As to which steps in the cycle contribute to rate-limitation in other circumstances, there is an implication that the collapse in catalytic rates that occurs as ionic strength is reduced¹²⁷ is not related to the second electron transfer. This is because the latter is probably governed by considerations similar to those that govern k_f , such as the ease with which the haem iron is able to move in and out of the porphyrin plane, which may in turn be influenced by the positioning of the proximal loop, to which the axial cysteine ligand belongs.¹⁹⁴ It would be surprising if one was ionic strength-dependent but not the other.

5.2.3. Catalytic parameters. Apparent k_{cat} and K_M values have been determined for numerous variants. With fatty acid substrates, mutagenesis has frequently had the effect of lowering catalytic efficiency (k_{cat}/K_M), confirming the importance of the role played by the naturally occurring residue (Table 5). Interestingly, the four proximal-side mutants with elevated SF reduction potentials (F393A, F393H, I401E and I401P) all showed higher catalytic efficiency than WT with lauric acid by virtue of giving lower apparent K_M values. With arachidonic acid, which saturates the active site more readily, however, the K_M effect was outweighed by the impact of a reduction in the associated k_{cat} value, and catalytic efficiency decreases were recorded.

With non-natural substrates, by contrast, engineered alterations have often brought about catalytic efficiency enhancements, whether as a result of increased k_{cat} values, a lowering of K_M values, or a combination of the two (Table 6). Reductions in K_M often bring about more dramatic activity increases under standard turnover conditions, as it is the inability of non-natural substrates to saturate the active site that is primarily responsible for the desultory rates of oxidation observed with WT. The K_M value associated with *p*-nitrophenol oxidation is dauntingly high, for example: 16 mM, rising to 22 mM in the presence of superoxide dismutase and catalase.¹²¹ However, this value fell to 2.8 mM when the F87G mutation was introduced. If activity enhancement is the sole objective, reductions to K_M and enhancements to k_{cat} should ideally be engineered in concert. This paradigm was successfully followed through successive generations of evolution targeted at creating a propane hydroxylase. The finished variant exhibited k_{cat} and K_M values of 7.6 s $^{-1}$ and 170 μM for propane, as against 0.03 s $^{-1}$ and 30 mM for the base variant, 139-3, which was itself significantly more efficient than the wild-type enzyme.³⁸⁷ If selectivity control and activity enhancement are both required in a variant, however, the case for engineering reductions to K_M is less compelling, since structural modifications that allow a substrate to saturate the active site more readily may achieve this end by enabling it to bind in a wider range of orientations.

Mutagenesis at Phe87 had little impact on apparent K_M values with hydrophobic substrates, but typically lowered them with substrates containing an element of polarity such as phenols³⁴⁵ and β-ionone,²⁹⁵ while the R47L/Y51F double substitution had the opposite effect. These differences seem

Table 5 Fatty acid oxidation and binding by WT P450_{BM3} and variants

Mutant	<i>k</i> _{cat} (s ⁻¹)	<i>K</i> _M (μM)	<i>k</i> _{cat} / <i>K</i> _M (s ⁻¹ mM ⁻¹)	<i>K</i> _D (μM)	Ref.
Lauric acid					
WT	33 ^a	115	287		102
W96A	33 ^a	110	300		
W96F	21 ^a	125	168		
W96Y	46 ^a	85	541		
WT	26	136	191	270	111
R47E	29	2000	15		31
F87A	25	167	150	103	111
WT				43	116
E267Q				29	
WT	86	288	299	241	106, 250
F42A	41	2080	20		106
R47A	66	859	77		106
R47A/Y51F	35	514	68		250
R47G	46	648	71		106
Y51F	102	432	236		106
Y51F	98	310	316		311
L75K	18				250
L75T/L181K	4.5	316	14	297	250
F87G	13	476	27		106
F87Y	27	42	643		106
L181K	12	134	90	255	250
I263K	17				250
F393A	29	19	1526	230	257
F393H	37	60	617	525	257
F393W				578	258
F393Y	65	274	237	520	250
WT	84	322	261	370	107 ^b
T268A	29	777	37	413	
T268A/F393H	22	85	259	285	
T268N	29	318	91		
T268N/F393H	9.8	13	754		
F393H	36	190	189		
WT	28	265	106	270	112
A82F	26	<20	>1300	0.3	112
A82F/T438F				46	239
A82F/T438I		89		35	239
A82F/T438V	28	112	250	86	239
A82I	45	320	141	240	112
A82W	43	<20	>2150	0.4	112
WT	46	87	529	89	108, 109
L86E	67	32	2094	1.0	193
F261E	10	1563	6.4	>1000	193
A264C	0.001				109
A264E	12	114	105		108
A264H	0.004				109
A264K	0.006				109
A264M	3.3	5.2	625	18	109
A264Q	0.03				109
I401E	15	23	652	12	193
WT	77	230	335		125
I401P	71	21	3381		
Myristic acid					
WT	55	7	7857	23	31
R47E	7	18	389		
WT				0.6	116
E267Q				0.6	
WT	81	37	2189	6.9	108
A264E	17	11	1545		
WT				1.3	80
T268A				0.2	
Palmitic acid					
WT	81	1.4	57857	5	31
R47E	12	4	3000		
WT				0.1	116
E267Q				0.1	
WT	77	12	6417	11	108
A264E	16	16	1000		
WT				0.1	112
A82I				0.3	

Table 5 (continued)

	k_{cat} (s ⁻¹)	K_M (μM)	k_{cat}/K_M (s ⁻¹ mM ⁻¹)	K_D (μM)	Ref.
A82F				<0.1	
A82W				<0.1	
WT				0.2	80
T268A				0.2	
WT	91	42	2167		126
I401P	76	17	4471		126
KT2 ^c	111	66	1682		194
Arachidonic acid					
WT				2.4, 3	98, 99
R47A				11	98
R47A/Y51A				14	99
R47A/Y51A/F87V				81	99
Y51A				12	99
F87V				1.7	98
WT				1.2	96
T268A				5.5	
WT	285	4.7	60 638	3.6	106
F42A	244	35	6971	19	106
R47A	177	19	9316		106
R47A/Y51F	54	33	1636	5.3	250
R47G	81	9.8	8265	7.1	106
Y51F	234	15	15 600	0.7	106
L75K	23				250
L75T/L181K	233	9.3	25 054	14	250
L181K	51	6.3	8095	2	250
I263K	24				250
A264E	29	0.7	44 615	0.2	108
F393A	21	2.7	7778	2.6	257
F393H	33	3.8	8684	7.6	257
F393W				2.0	258
F393Y	143	9.5	15 053	4.2	257
WT	67				258 ^b
F393A	18				
F393H	21				
F393W	41				
F393Y	67				
WT	95			3.6	107 ^{b,d}
T268A	31			6.9	
T268A/F393H	19			5.0	
T268N	28			4.0	
T268N/F393H	7.2				
F393H	31				
WT	273	5.1	53 529	0.6	109
L86E	126	12	1000	0.02	193
F261E	0.3 ^e			0.9	193
A264C	0.01			6.4	109
A264H	0.01				109
A264K	0.05				109
A264M	1.9	10	190	0.4	109
A264Q	13	1.9	6842	18	109
I401E	33	4.7	7021	0.3	193

Each group of mutants is shown with data obtained for WT under identical conditions.^a V_{max} . ^b k_{cat} and K_M determined at 15 °C. ^c KT2 = A191T/N239H/I259V/A276T/L353I. ^d k_{sat} data in lieu of k_{cat} data. ^e Second order rate constant. Data have also been published for eicosapentaenoic,⁹⁸ palmitoleic,⁹⁹ butanoic, hexanoic, octanoic and decanoic^{250,343} acids.

likely to derive from changes to the active-site water population, which increases relative to WT when space is created by introducing a smaller residue in place of Phe87, but may decrease when the polar couplet at the mouth of the substrate access channel is neutralised. The E267V mutation was particularly effective at reducing the K_M values associated with the oxidation of pharmaceuticals.^{368,369}

5.2.4. Dissociation constants and spin shifts. The tenacity with which a substrate or inhibitor binds to the enzyme varies between mutants (Tables 5 and 6), as does the shift in the spin

state equilibrium induced by substrate binding. Like reduction potentials, however, these parameters are not always good indicators of catalytic performance. To illustrate, arachidonic acid binding was tightened by a factor of 25 in the L86E mutant relative to WT, yet catalytic efficiency was diminished by a factor of 5, in part because the K_M value more than doubled.¹⁹³ With lauric acid, on the other hand, the same mutant enhanced catalytic efficiency by a factor of 4 on the back of a 90-fold tightening in binding, albeit from a lower level. There is an inference that excessively tight binding may be counterproductive. The spin shifts given by non-natural substrates are not

Table 6 Non-natural substrate oxidation and binding by WT P450_{BM3} and variants

Substrate	Mutant ^a	<i>k</i> _{cat} (s ⁻¹)	<i>K</i> _M (μM)	<i>k</i> _{cat} / <i>K</i> _M (s ⁻¹ mM ⁻¹)	<i>K</i> _D (μM)	Ref.
Acenaphthene	WT				6.8	375
	F87V				24	
	VQ				22	
	GVQ				24	
Acenaphthylene	WT		29		245	345, 375
	F87V		31		31	
	VQ				18	
	GVQ				30	
Aniline (4-hydroxylation)	WT	0.16 ^b	2523	0.06		404
2-Benzoyloxyphenol	WT		380			345
	F87V		320			
3-Chlorostyrene	WT				107	334
	F87A				73	
	F87G				66	
	F87V				91	
Chloroxazone (6-hydroxylation)	WT	0.77 ^b	1211	0.64		404
Coumarin ^c (3-hydroxylation)	II/M185T/L188P	0.27	1200	0.23		347
	L148I/F162I	0.2	15 000	0.01		
	II/M185T/L188P	0.07	1100	0.06		
	L148I/F162I	0.04	13 000	0.003		
Dextromethorphan	LVQ/N319T				1063	256
Fluorene	LVQ/IV/G415S				1233	
	WT				7.2	375
	F87V				6.8	
	VQ				6.4	
7-Ethoxycoumarin ^c (<i>O</i> -deethylation)	GVQ				12	
	L148I/F162I	0.23	340	0.68		347, 368
	LVQ	0.03	1220	0.02		
	LVQ/E267V	0.11	81	1.4		
7-Ethoxyresorufin ^c	R47L/L86I/QV	0.03	427	0.07		370
	LVQ/L86I	0.08	3.0	27		
	LVQ/IG/QV	0.03	4.6	6.5		
	Hexane	WT	0.63			343
1-Hexyne	F87G	0.8				
	WT	6.2	31 000	0.2		343
Indole	F87G	2.4	2000	1.2		
	F87V	2.0	17 000	0.12		319
	VQ	2.3	4200	0.55		
	GVQ	2.7	2000	1.4		319
	GVQ	2.9	2200	1.3		349
	GVQ/D168H	10	1200	8.3		349
	GVQ/K434G	1.5	3900	0.38		349
	GVQ/K434R	2.9	2000	1.5		349
	GVQ/E435D	3.0	1900	1.6		349
	GVQ/E435T	7.5	800	9.4		349
β -Ionone	GVQ/NVN	3.1	1500	2.1		349
	WT		1139			295
	F87A		704		75	
	F87G		476		139	
	F87V		305		85	
	LF		4545			
	LF/F87V		1611		152	
	VS		350		143	
	A74E/VS		769		100	
	LF/A74E/VS		540		115	
Lovastatin (6'- β -hydroxylation)	GVQ		1346		160	
	LVQ/GG/IV	0.23	44 000	0.005		371
	LVQ/IV/E143G	0.32	41 000	0.008		
Naphthalene	WT		160		143	345, 375
	F87V		150		150	
	VQ				162	
	GVQ				141	
4-Nitrophenol	WT	0.37	16 000	0.02		121
	WT + SOD,CAT	0.48	22 000	0.02		
	F87G	0.71	2800	0.25		
	F87G + SOD,CAT	0.75	3100	0.24		
12- <i>p</i> -Nitrophenoxy-	WT	2.5	12	208		299

Table 6 (continued)

Substrate	Mutant ^a	<i>k</i> _{cat} (s ⁻¹)	<i>K</i> _M (μM)	<i>k</i> _{cat} / <i>K</i> _M (s ⁻¹ mM ⁻¹)	<i>K</i> _D (μM)	Ref.
carboxylic acid ^d	F87A	6.2	8.1	765		299
	F87A/L188K	8.5	41	207		299
	F87A/GQ	13	141	92		299
	F87A/GQ/R47F	14	55	255		299
	LARV	9.5	40	238		299
	WT	1.7	7.2	236		363
	F87A	3.5	4.4	795		363
	F87V	0.7	3.8	184		363
	F87V/L188K	2.8	6.4	438		363
	F87V/GQ	2.2	15	147		363
	F87V/GQ/R47F	1.4	8.9	157		363
	QM	1.4	12	117		363
	QM	0.6	25	24		364
	QM + inhibitors	0.8	246	3.3		364
Octane	WT	0.7	20	35		351
	WT	0.38				343
	F87G	0.32				
1-Octyne	WT	24	12 700	1.9		343
	F87G	3.4	1300	2.6		
Perfluorolaurate					2.2	405
Phenacetin ^c	LVQ/GG/E267V	0.10	506	0.19		370
	LF/L86I/QV	0.09	2090	0.04		
Phenanthrene	LF		48			249
	LF/A264G		9.2			
α-Pinene	QM		46			364
Propane	139-3 ^e	0.17	30 000	0.006		387
	PMO ^e	7.5	170	44		
Propanolol (<i>N</i> -dealkylation)	WT	0.13 ^b	805	0.16		404
Propylbenzene	WT				74	334
	F87A				35	
	F87G				20	
	F87V				45	
Propylbenzene	WT	13	218	60		194
	KT2	121	1558	78		
Resveratrol ^c	LVQ/L86I	0.11	15	7.3		369
(3'-hydroxylation)	LF/L86I/QV	0.002	54	0.04		
Simvastatin	LVQ/GG/IV	0.17	37 000	0.005		371
(6'-hydroxylation)	LVQ/IV/E143G	0.25	42 000	0.006		

^a GG = E64G/E143G; GQ = A74G/L188Q; GVQ = A74G/F87V/L188Q; IG = F81I/E143G; II = F162I/M237I; IV = F81I/E267V; KT2 = A191T/N239H/I259V/A276T/L353I; LARV = V26T/R47F/A74G/F87A/L188K; LF = R47L/Y51F; LVQ = R47L/F87V/L188Q; NVN = D168N/A225V/K440N; QM = V26T/R47F/A74G/F87V/L188K; QV = L188Q/E267V; VQ = F87V/L188Q; VS = F87V/P386S. ^b *V*_{max}. ^c Data for other variants were also published—only those with the highest and lowest catalytic efficiency are tabulated. ^d Data were also published for 8- and 10-pNCA. ^e 139-3¹²⁴ and PMO³¹² are 11- and 24-mutation variants respectively. CAT: catalase; SOD: superoxide dismutase.

a reliable guide to binding avidity. With naphthalene, for example, the F87V mutant gave a spin shift of 73%, vs. 15% for WT, but the dissociation constants of the two enzymes fell within 5% of one another.³⁷⁵ The correlation between spin shifts and catalytic activity can also be poor. For example, F87A variants gave higher spin shifts than WT with a range of non-natural substrates—possibly because the enhanced active-site water presence stabilised the “alternative” water binding site—while those given by A330P variants were lower, yet activity trends ran in the opposite sense.³⁰³ Other variants that show enhanced activity relative to WT despite giving meagre spin shifts on substrate addition have been reported.^{249,256,380} Where polar substrates are involved, the binding of a heteroatom atom close to the haem iron may in fact enhance the stability of the axial water binding site rather than diminishing it.²⁵⁶ These observations serve as a reminder that displacement of the axial water ligand is merely one of the events that the arrival of a substrate in the active site may bring about. Substrate-induced structural change to the dioxygen-binding region of the enzyme is also

important, and the preferred substrate binding mode must also be conducive to efficient product expulsion following oxidation if efficient catalysis is to take place.

5.3 Structure-function studies

Intimate insights into aspects of P450 chemistry such as the interplay between competing reaction pathways have been obtained through investigations into the oxidation of structurally related substrates by different P450_{BM3} variants. Studies of non-natural substrate oxidation typically require the involvement of high-activity variants to ensure that NADPH consumption rates reach practicable levels. Selectivity-altering mutations are then incorporated to produce a variety of product outcomes. In the oxidation of 3- to 8-carbon *n*-alkanes by directed-evolution variants, activity was highest for the 6-carbon compound, falling away as the chain lengthened or shortened.¹²⁴ This contrasted with straight-chain fatty acid oxidation, where activity was highest for the 15-carbon compound.¹⁶

The specificity for sub-terminal hydroxylation was retained, however, ω -hydroxylation accounting for $\leq 2\%$ of the products formed by 6- to 10-carbon alkanes.³²⁶ With hexane, variant 139-3 gave similar 2-hexanol:3-hexanol ratios to WT (20% : 80%), but with octane, 2-octanol formation ran at 66%, as compared to 17% for WT.¹²⁴ With decane, on the other hand, 139-3 gave just 15% 2-decanol. Introduction of the A328V mutation drove the focus of attack towards the ω - and (ω -1)-positions across the full gamut of substrates,³²⁶ octane and decane both giving *ca.* 80% (ω -1)-hydroxylation, and further mutagenesis resulted in a variant capable of producing 52% 1-octanol from octane.³²² However, the same variant gave just 5% 1-decanol from decane, illustrating the measure of the challenge faced by selectivity engineers. High-activity variants may be generic in reach, but selectivity alteration typically needs to be addressed on a substrate-by-substrate basis, particularly where unfunctionalised substrates are concerned.

The desaturation of alkylbenzenes has been probed using an unrelated family of directed-evolution variants.³³⁷ Those containing the F87A mutation, which creates space in the active site, gave the highest desaturation/hydroxylation ratios. The alkyl side-chain structure also influenced product profiles, $\alpha\beta$ -desaturation being most favoured when the α carbon was branched and the β carbon primary. Cumene (isopropylbenzene) gave almost 30% desaturation with F87A variants, for example, while *n*-propylbenzene gave $\leq 1\%$. α -Hydroxylation was the principal competing pathway in most instances, but one variant gave $> 75\%$ β -hydroxylation with *n*-propylbenzene, and small quantities of β -hydroxylation (up to 4%) even when the β carbon was primary. These patterns suggested that the first of the two hydrogen abstractions required to accomplish desaturation might take place from the β carbon rather than the more activated α carbon, with electron transfer followed by rearrangement to the more stable α carbocation completing the mechanism, as in certain microsomal P450s.⁴⁰⁶ However, isotope studies showed that the first abstraction in fact took place from the α carbon, making the role played by the side-chain branch more challenging to explain. One possibility is that it causes substrates to adopt different binding orientations to those favoured by straight-chain analogues.

An unusually vivid demonstration of metabolic switching came to light during this investigation, the oxidation of α -D-cumene by WT yielding 48% α - α -D-isopropylphenol, as compared to 9% for the non-deuterated substrate. This illustrated the delicacy of the balance that exists between the different competing oxidative pathways and delineated the extent to which the enzyme was capable of distinguishing between C–H bonds of differing reactivity. Density functional theory calculations have been carried out to rationalise an example of the same phenomenon in the oxidation of ethylbenzene by a microsomal isoform.⁴⁰⁷ Yet the level of switching in that instance was $< 3\%$, showing that oxidation outcomes depend crucially on the isoform and substrate involved. Moreover, F87A-containing P450_{BM3} variants gave no α -hydroxylation with cumene or any other alkylbenzene substrate, making it clear that bond activation levels only influence outcomes if the architecture of the active site allows. Similar considerations apply to the partition between desaturation and hydroxylation. Theoreticians have suggested that desaturation

takes place *via* a cationic pathway that operates only when radical rebound is inhibited both electronically and sterically.⁴⁰⁸ It is therefore interesting that desaturation in P450_{BM3}, which is initiated by α -abstraction, should be favoured in substrates capable of stabilising an α carbocation intermediate. While this strengthens the impression that a cationic pathway is involved, desaturation appears to compete freely with α -, β - and ω -hydroxylation, and it is far from clear that inhibition of α radical rebound is required if it is to take place. P450_{BM3} variants make particularly suitable test systems for mechanistic hypotheses of this kind,^{8,9} allowing a clearer understanding of the extent to which steric considerations or experimental conditions compromise the assumptions on which they are predicated.

Isotope effects have been used to probe the oxidation of 7-ethoxycoumarin by a panel of P450_{BM3} variants.³⁶⁸ Perdeuteration of the methylene group led to a reduction in the k_{cat} values associated with *O*-deethylation of roughly an order of magnitude across all variants, but little change to those associated with the competing 3-hydroxylation reaction. Metabolic switching was therefore not evident in this instance, probably because this would have required full rotation of the substrate in the active site, the hydroxylation and deethylation sites being situated at opposite ends of the bicyclic structure. However, the partition between the two products was sensitive to the mutations employed, A264G-containing variants giving *O*-deethylation percentages close to or above 50%, while F86I-containing variants gave percentages as low as 15%. Activity was greatest for those variants that showed a bias towards 3-hydroxylation, which is the same bias as that shown by human CYP1A2 and 2E1. Isotope effects have been cleverly used to ascertain how compact a substrate needs to be for rotation in the P450_{BM3} active site to be sufficiently rapid to influence product distributions.²⁵⁴ *p*-Xylene (1,4-dimethylbenzene) showed a full isotope effect when one methyl group was perdeuterated, demonstrating that rapid rotation of the substrate allowed hydroxylation to take place predominantly at the non-deuterated methyl group. With 4,4'-dimethylbiphenyl, however, an isotope effect of just 2.5 was observed when one methyl group was perdeuterated, showing that rotation was restricted—albeit not to the extent seen in the 7-ethoxycoumarin investigation described above. When this experiment was repeated with the F87A mutant, a full isotope effect was restored, by implication in response to the additional space created in the active site.

Outcomes in the oxidation of alkylbenzenes with single-carbon side-chains were significantly impacted by active-site mutations. WT gave 98% α -cresol (2-methylphenol) from toluene, but KT5, a variant containing mutations F87A and A330P, gave 95% benzylalcohol.³⁰³ A possible explanation is that the reshaped active site of KT5 allowed the substrate sufficient freedom to find a binding orientation in which the activated benzylic carbon could be presented to the haem iron for oxidation. However, this does not reconcile with the corresponding results for propylbenzene, where benzylic hydroxylation levels dropped from 99% in WT to 20% in KT5. A more satisfactory interpretation is therefore that the substituent plays a role in orientating alkylbenzene substrates in the active site. The product profiles obtained in the oxidation of different xylene isomers by WT and assorted variants showed that the relative positioning of multiple substituents

on an aromatic ring is also important. *m*-Xylene, like toluene, gave 98% aromatic hydroxylation with WT, but *o*-xylene gave 53%³⁰⁵ while *p*-xylene gave only benzylic hydroxylation.²⁵⁴ With F87A variants, benzylic hydroxylation percentages were significantly higher for *m*- and *o*-xylene, such that product distributions resembled those given by microsomal P450s. This adds to the growing body of evidence that P450_{BM3} can be a relevant and useful model for the metabolism of xenobiotics by higher organisms, particularly when judiciously mutated. Five oxidation products were formed by *o*-xylene, including two that entailed the NIH shifting of one of the methyl substituents, in one case leading to dearomatisation, a reaction seldom encountered beyond the confines of esoteric text books. These findings highlight the usefulness of the enzyme as a probe for unusual P450 reactivity types and the mechanistic pathways by which they proceed.

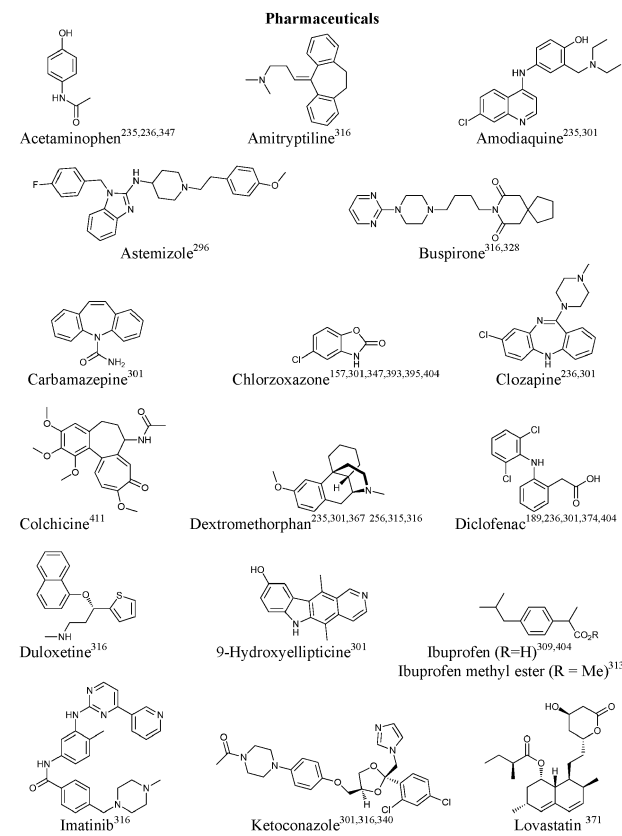
6 The oxidation of non-natural substrates

6.1 Pharmaceuticals and other biomolecules⁷⁴

With the enzyme now firmly established as an adaptable oxidation platform, attention is focusing increasingly on the development of dedicated applications for specific non-natural substrate categories. Pharmaceuticals have been particularly heavily targeted. Understanding the degradation and clearance behaviour of new products is critical as drug metabolites can often be pharmacologically active, and are as likely to cause adverse side-effects as the drugs from which they originate by reacting with endogenous or unconnected exogenous molecules.^{309,409} In most countries, information about which human P450s are responsible for metabolism is required before a drug candidate can be submitted for approval. Although human enzymes can be expressed in yeast and *E. coli*, they do not lend themselves readily to metabolite production as they are relatively unstable and exhibit low activity. Researchers have therefore turned to surrogate P450s for solutions. Early investigations involving wild-type P450_{BM3} suggested that compounds such as progesterone,¹⁹ benzphetamine, cocaine and 7-ethoxycoumarin (an *O*-dealkylation probe)⁶³ were not accepted as substrates, though other work indicated that coumarins and steroids might be viable targets.²⁴ Against this background, chimeragenesis (section 4.4) was used to create enzymes capable of oxidising chlorzoxazone,³⁹³ diclofenac,¹⁸⁹ omeprazole¹⁸⁹ and erythromycin,¹⁸⁹ BMR being fused to CYP2E1, 2C9, 2C19 and 3A4 respectively. Subsequent studies showed that WT P450_{BM3} was in fact capable of oxidising selected drugs,⁴⁰⁴ and CYP102A7 was found to be active towards 7-ethoxycoumarin.¹⁴³ The enzyme is more active towards drugs metabolised by human 3A4 and 2E1 isoforms, with which it shares higher levels of sequence similarity, than those processed by the 1A2, 2C9 and 2D6 sub-families.⁴⁰⁴ This is potentially advantageous, since 3A4 is involved in the metabolism of approximately 50% of the drugs currently on the market, while other P450s collectively metabolise just 25%.⁴¹⁰

The demethylation metabolite from colchicine, a 3A4 substrate, has been produced in a bioreactor using a CYP102A1 gene isolated from a wild *B. megaterium* strain.⁴¹¹ Engineered P450_{BM3} variants have given product arrays broadly similar

to those given by microsomal P450s (though in altered proportions) with 7-ethoxycoumarin³⁶⁸ and numerous different pharmaceuticals,^{235,236,297,309,328,350,369,371,374} often in enhanced yields. CYP102A5 and A7 have been engineered to oxidise chlorzoxazone and diclofenac.¹⁵³ Novel metabolites have been identified during these studies, as well as several overlooked in earlier work carried out with more “appropriate” P450s. Such investigations are typically conducted using a portfolio of variants rather than a single customised catalyst, partly because pharmaceuticals are structurally diverse and do not respond in a common fashion to particular mutations, and partly because this improves the probability of generating all the necessary metabolites, since different variants give contrasting and sometimes complementary product profiles. With verapamil, for example, one variant gave five metabolites at a high overall conversion (78%), while five additional metabolites could be generated using less productive variants, two in high percentages.^{296,396} Portfolios may consist exclusively of variants developed for drug metabolism.^{236,256,316,340,350,367} Alternatively, a mixture of customised and non-customised variants can be employed. Customised variants performed more effectively than mutants developed for PAH oxidation with several substrates,^{368–371} but non-customised variants gave superior performance with pharmaceuticals such as astemizole, an anti-histamine,²⁹⁶ showing that a flexible approach can pay worthwhile dividends. Fig. 6 depicts a selection of the drugs towards which WT or engineered variants have been reported as showing activity. Metabolites have been produced from several of these.



Fluorinated pharmaceuticals, which offer various benefits including enhanced membrane permeability, have been produced by regioselective hydroxylation of a substrate

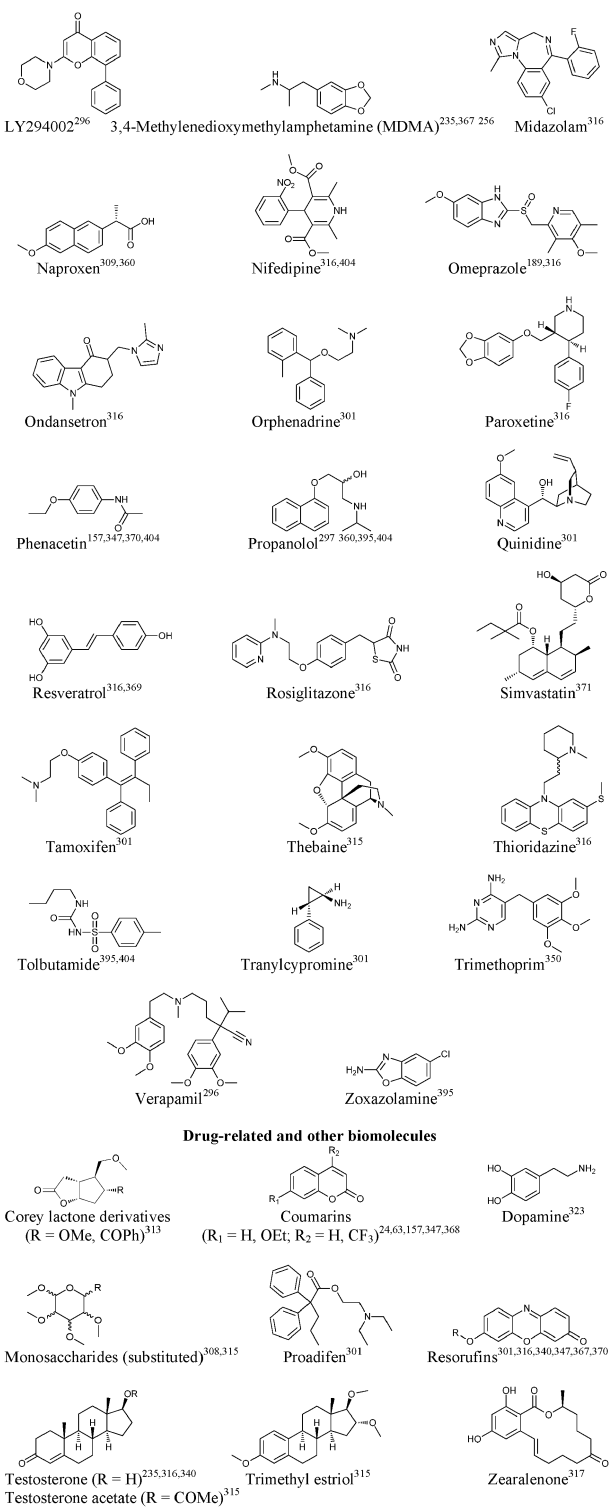


Fig. 6 Drugs and other biomolecules towards which WT P450_{BM3} or engineered variants are reported to show activity. Compounds investigated towards which activity was not observed or reported include adriamycin,³⁰¹ aripiprazole,³¹⁶ barbital,³⁰¹ benzphetamine,⁶³ caffeine,^{236,301,404} cholestan,³¹⁰ cloxacillin,³⁰¹ cocaine,⁶³ codeine,³⁰¹ dacarbazine,³⁰¹ debrisoquine,^{301,404} dexamethasone,³⁰¹ disulfiram,³⁰¹ erythromycin,^{189,404} estrone,³¹⁶ flucloxacillin,³⁰¹ furosemide,³⁰¹ glipizide,³¹³ indomethacin,³⁰¹ metyrapone,³⁰¹ mianserin,³⁰¹ nabumetone,³¹³ perhexiline,⁴⁰⁴ phenobarbital,^{63,301} phenylbutazone,³¹³ progesterone,¹⁹ propafenone,⁴⁰⁴ raloxifene,³⁰¹ sparteine,^{301,404} sulfamethoxazole,⁴⁰⁴ sulfaphenazole,³⁰¹ tacrine,³⁰¹ terfenadine,⁴⁰⁴ theophylline,^{301,404} tramadol,³¹⁶ troleandomycin,³⁰¹ warfarin⁴⁰⁴ and xylocaine.³⁰¹

followed by displacement of the introduced hydroxyl group using diethylaminosulphur trifluoride.³¹³ The enzyme has been used in multi-step drug synthesis pathways. Artemisinic acid was produced *via* the selective epoxidation of one of the two unsaturated linkages in amorpha-4,11-diene using a P450_{BM3} variant.³⁰⁴ Chemical methods were then employed to generate artemisinin, an anti-malarial agent. Other biomolecules have been targeted. The oxidation of bilirubin was stimulated by the presence of perfluorolauric acid.⁴⁰⁵ As with the stimulation of CYP1 oxidation by polychlorinated biphenyls, this appeared to result from co-occupation of the active site by the two substrates. Co-incubation with lauric acid, the unsubstituted analogue, stimulated NADPH consumption rates but not bilirubin oxidation, presumably because the co-substrate could itself be oxidised. The enzyme has been engineered to accept and demethylate permethylated saccharides.³⁰⁸ This potentially facilitates saccharide synthesis by allowing protecting groups to be removed *en bloc* without compromising regioselectivity. A BMP variant capable of functioning as a dopamine-sensitive MRI contrast agent has been engineered.³²³ The contrast effects achieved were weaker than those of synthetic agents, but could be augmented by employing the Mn³⁺-substituted variant in place of the ferric variant.⁴¹² Finally, a variant has been shown to give the same catechol metabolites from zearalenone as human P450s.³¹⁷

6.2 Flavouring, fragrance and pheromone precursors

Alcoholic functionality is common in flavour and fragrance compounds, making them natural targets for P450 engineers. Several are potentially available *via* the oxidation of naturally occurring terpenes. More often than not, epoxides are side-products in such reactions, but these too can be of value, being pheromones, fragrances and constituents of juvenile hormones in insects. They are also useful as synthetic intermediates³⁰²—in the production of the aggregation pheromone of the Colorado potato beetle, for example.⁴¹³ α -Ionone was one of the first non-natural substrates to be oxidised by a P450_{BM3} variant.¹¹⁸ With β -ionone (which is an important floral scent component in its own right), allylic oxidation was strongly favoured over other pathways, as with many terpenoids, and product distributions were difficult to manipulate, most variants giving >95% 4-hydroxy- β -ionone.²⁹⁵ However, coupling and activity were both enhanced relative to WT, and some variants showed improved enantioselectivity. Variants were found to discriminate surprisingly cleanly between different forms of geranylacetone, oxidising the *Z*-isomers to mixtures of products that included allylic alcohols, but epoxidising the *E*-isomers with high levels of regio- and enantio-specificity.³⁰² Farnesol has been oxidised to ω -hydroxyfarnesol, the primary CYP4C7 metabolite, by variants that also oxidised geraniol and geranylgeraniol, and a methyl ester derivative to 10,11-epoxymethylfarnesoate, a juvenile hormone.^{32,115,324} Fig. 7 shows the substrates in this category on which research has been carried out, many of which are also oxidised by CYP102A7.¹⁴³

The oxidation of (+)-valencene to nootkatone, a highly prized grapefruit flavouring not produced by WT, has attracted considerable interest.^{154,300,387} Part of the awkwardness of this challenge is the readiness with which nootkatone is itself accepted

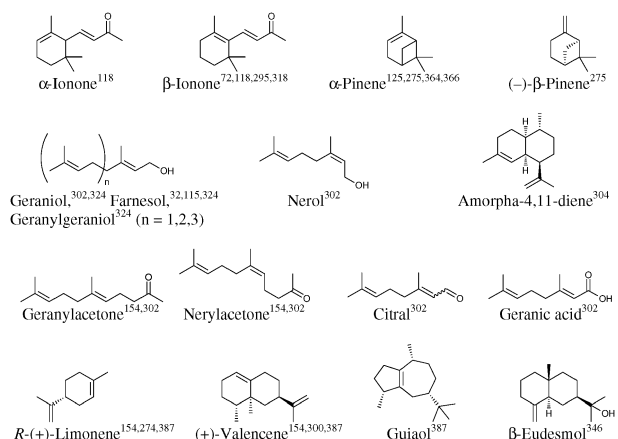


Fig. 7 Terpenoids targeted for oxidation by WT P450_{BM3} and variants.

as a substrate by P450_{BM3} variants. Nootkatone production was first achieved by deploying mutations F87A and I263A.³⁰⁰ Three A328I-containing mutants that gave $\geq 90\%$ nootkatol/nootkatone were subsequently identified by screening a library of variants combining mutations at two specific residues—Ala328 in the influential SRS5 region and Phe87 in SRS1.^{154,381} This was a vindication for the engineering strategy, since the stand-alone A328I mutant was inactive towards (+)-valencene. A TTN of 5750 has been reported for limonene oxidation.³⁸⁷ (*R*)-8,9-limonene epoxide accounted for 95% of the products formed by (*R*)-limonene when oxidised by A328F-containing variants (*vs.* 7% for WT),¹⁵⁴ but biasing selectivity in favour of the more desirable potential end-products (carveol, carvone and perillyl alcohol) proved more challenging, and for several years P450_{BM3} engineers viewed the 100% yields of (+)-*trans*-carveol⁴¹⁴ and (+)-perillyl alcohol⁴¹⁵ achieved using other bacterial P450s with some envy. Within the past few months, however, 97% perillyl alcohol formation has been demonstrated using the A264V/A328V/L437F triple mutant.²⁷⁴

6.3 Aliphatic hydrocarbons

6.3.1 Alkanes. Enzymes capable of alkane oxidation occur naturally, examples being the terminal alkane hydroxylases from *Rhodococcus rhodochrous* and *Acinetobacter calcoaceticus*, the membrane-bound non-haem iron alkane monooxygenase AlkB, and methane monooxygenase (MMO).^{416,417} Numerous bacterial, yeast and mammalian fatty acid hydroxylase systems are also active towards alkyl hydrocarbons²¹—indeed, *B. megaterium* hydroxylates a range of alkanes and cycloalkanes *in vivo*.⁴¹⁸ AlkB is used to produce 1-octanol from octane on an industrial scale, and variants with modestly improved activity towards butane and propane have been engineered.⁴¹⁹ Like MMO, however, this enzyme is difficult to express in a robust form capable of biotransformation over extended periods in a heterologous host. Similar considerations apply to CYP153A6.⁴¹⁹ Potential applications for other engineered P450s therefore exist in this field, most notably in the oxidation of methane. The development of a viable process for the conversion of this freely available and underutilised natural resource to methanol would be of enormous significance, transforming a biogenic greenhouse gas at least twenty times as potent as CO₂ into a readily transportable fuel additive.

Researchers have approached the task by developing variants capable of oxidising medium-chain alkanes, before further engineering these to accept progressively shorter-chain analogues. Hexane and octane were among the earliest non-natural substrates to display NADPH consumption rates that exceeded the leak rate with the wild-type enzyme.⁴²⁰ Octane gave the highest NADPH consumption rate of the non-natural substrates employed to assay the GVQ variant (29 s⁻¹),¹¹⁸ and also its CYP102A3 equivalent.¹³⁹ 3-Methylpentane was readily accepted by engineered variants, the R47L/Y51F/I401P triple mutant giving a PFR of 50 s⁻¹.¹²⁶ Propane hydroxylation at $> 7\text{ s}^{-1}$ was accomplished using a directed-evolution strategy,³⁸⁷ and also by a variant in which three of the four component mutations were site-directed.¹²⁶ However, the optimum oxidation rate reported for ethane was three orders of magnitude lower,³²⁰ illustrating the severity of the engineering challenge presented by smaller substrates.

Methane oxidation was finally reported earlier this year—surprisingly, perhaps, by the wild-type enzyme rather than an engineered variant.²⁵¹ The experimental protocol contained two key components: a pressurised system to raise substrate saturation levels, and the participation of a perfluorocarboxylic acid co-substrate, a tightly binding but chemically inert “filler” of the type used by earlier researchers to expedite bilirubin metabolism.⁴⁰⁵ Oxidase activity towards longer-chain alkanes such as butane was similarly improved, though different substrates showed different co-substrate chain-length preferences.^{251,421} MD simulations suggested that the strategy succeeded partly because the effective volume of the access channel was reduced, and partly through induction of the SB conformation of the enzyme, including the displacement of the axial water molecule.²⁵¹ Such co-substrates could also help to flush the products from non-natural substrate oxidation out of the active site, freeing up the enzyme for the next round of catalysis (as discussed in section 3.3, it is currently unclear how this is accomplished). It is worth noting in this context that coupling in the oxidation of a selection of fluorinated octanes by a P450_{BM3} variant was significantly more efficient than in octane oxidation.³⁵³ It was suggested that this could be due to fluorine-porphyrin interactions, but it seems equally possible that the bulky substitutions helped the substrate to bind more tightly in the active site.

Cyclohexane was reported as showing no activity,⁶³ though later researchers disagreed.^{124,237} Selectivity has been redirected in the oxidation a substituted cyclohexane.²⁷⁴ Mutant A328V is more active than WT towards cyclooctane and cyclodecane, but inactive towards cyclododecane unless combined with the F87A mutation.³³⁹

6.3.2 Alkenes and alkynes. Like terpenes, alkenes typically give product mixtures dominated by allylic alcohols and epoxides when oxidised. The epoxides can be useful chiral intermediates in the synthesis of cosmetics, surfactants, industrial sterilants, and fumigants. Allylic alcohols can also be desirable end-products, particularly those formed by terminal alkenes—1-octen-3-ol, an aroma component and insect attractant also known as mushroom alcohol, being an example. Microsomal P450s are poisoned by terminal alkenes such as 1-octene (though not by styrenes), possibly as a result of N-alkylation of the porphyrin system and/or peptide

modification during epoxidation.⁴²² P450_{BM3} is noticeably less prone to inactivation, probably because the allylic hydroxylation pathway competes relatively effectively against the epoxidation pathway, with which inactivation is associated.³²¹ WT gave *ca.* 85% 1-octen-3-ol from 1-octene, for example, with <5% epoxidation,³⁵⁵ in line with the 1-hexene product distribution.³²¹ This behaviour reflects the contrasting selectivity preferences shown by the two enzyme types in the oxidation of ω -unsaturated fatty acids: P450_{BM3} favours allylic hydroxylation, while microsomal P450s typically epoxidise the terminal olefinic linkage.²⁶ Variant 139-3 gave 100% 1-hexen-3-ol from 1-hexene at an initial NADPH consumption rate of 22 s⁻¹ in an investigation that also took in cyclohexene and propylene.³⁸⁰ Variants capable of 95% terminal epoxidation with C5–C8 alkenes at *ca.* 75% *ee* have been developed.³²¹ However, these displayed lower initial NADPH consumption rates (<3 s⁻¹), and inactivation was a severe hazard. TTNs of up to 1350 were achieved, as against 200 for WT, but the same variants gave TTNs of up to 14 000 for styrene epoxidation.

As with terminal olefins, the oxidation of terminal acetylenes by P450_{BM3} took place adjacent to, rather than at, the unsaturated linkage, where the opposite occurred with microsomal P450s.²⁶ Inhibition was apparent with the C18 congener, though not with the C11 analogue.^{26,329} With hexyne and octyne, inactivation was observed when the unsaturated linkage was sub-terminal but not when it was terminal.³⁴³ With F87G, inactivation occurred irrespective of the location of the triple bond.

6.4 Aromatics

Fig. 8 shows the aromatic substrates that have been targeted by P450_{BM3} engineers. Several of these constitute environmental and human health hazards on account of their resistance to degradation, including *bêtes noires* such as polychlorinated dioxins and PAHs. The monooxygenation of such compounds is a potential method of remediation as the accompanying solubility increase allows indigenous soil-dwelling bacteria to take up the metabolites and complete the catabolic process (typically *via* dioxygenation). High-activity variants are generally employed, with enlarged active sites also being an important prerequisite for efficient oxidation if bulky substrates are involved.^{249,375,377} The oxidation of indole has been studied as a possible synthetic pathway to indigo and indirubin.^{319,349} Numerous single-ring aromatic compounds have been investigated. Styrene and *p*-chlorostyrene were the first to be identified as viable substrates for the enzyme.⁴²³ *m*-Chlorostyrene was also readily accepted for oxidation, as was propylbenzene.³³⁴ Styrenes, which are converted to epoxides rather than aldehydes,⁴²³ have been used to assay for epoxygenase activity.^{325,379} Alkylbenzenes not containing a heteroatom are relatively efficiently oxidised, particularly if the R47L/Y51F double substitution is employed, and can be used as mechanistic probes.^{254,305,337} Mutations that promote aromatic hydroxylation over benzylic hydroxylation are known,^{194,303} with potential applications that include the production of catechols and pharmaceutical precursors.⁴²⁴ Phenol formation *via* *O*-dealkylation is relatively facile, a reaction first probed using 11-phenoxyundecanoic acid.⁴²⁵

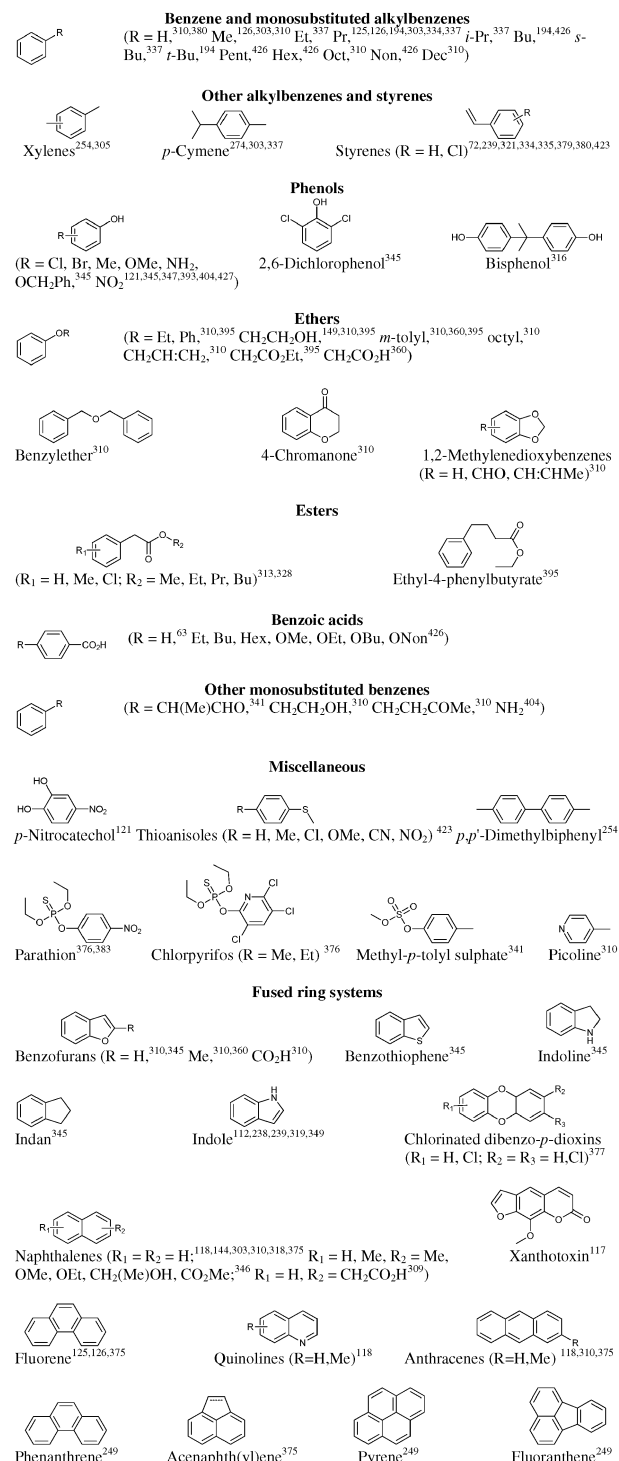


Fig. 8 Aromatic compounds targeted for oxidation by WT P450_{BM3} and variants. Coumarins and resorufins appear in Fig. 6.

However, alkoxybenzene substrates incorporating a medium- to long-chain substituent may also bind with the hydrophobic end towards the haem iron. *p*-Nonyloxybenzoic acid was hydroxylated primarily at the (*o*-2) position, for instance.⁴²⁶ Aromatics containing heteroatoms may otherwise be more resistant to oxidation by WT, but activity can usually be enhanced, whether by raising active site water levels using a space-creating mutation such as

F87A³¹⁰ or F87V,³⁴⁵ or *via* chimeragenesis.³⁹⁵ F87A has also been used to facilitate the α -hydroxylation of substituted phenylacetic acids following esterification.³²⁸

6.5 Other substrates

Miscellaneous other substrates have been investigated. These include chlorinated methanes and ethanes,^{120,329} sodium dodecyl sulphate (SDS), a surfactant towards which CYP102A1 and A2 are more active than lauric acid,^{37,120,145,146,373} methanol, ethanol, retinoic acid,⁶³ furoxan and furazan derivatives,¹²⁰ mechanistic probes such as cyclopropyl fatty acids^{8,9,80} and α - and β -thujone,⁴²⁸ synthetic intermediates such as achiral cyclopentanecarboxylic acid derivatives,³²⁷ substituted branched fatty acids, esters, alcohols and related compounds,⁴⁰ thiafatty acids,¹¹ substituted cyclopentenones, which are prostaglandin templates,³¹³ and 3,7-dimethyl-1-octanol.³²⁴

7 Production-scale approaches^{72,75,429,430}

7.1 *In vivo* biotransformation

On the basis of its unusually high activity levels, self-sufficiency, solubility and amenability to engineering strategies that facilitate non-natural substrate oxidation, P450_{BM3} is widely perceived to be the most promising member of the P450 superfamily for harnessing into production-scale applications. Like other isoforms, however, the enzyme is pyridine nucleotide-dependent, requiring the expensive co-factor NADPH to function. Numerous methods of sidestepping this obstacle have been explored.^{431–433} The most prominent is *in vivo* biotransformation (whole-cell oxidation), where the onus of co-factor production is transferred to the host organism. While this neatly addresses the cost issue, it introduces a number of separate challenges, one of the more awkward being the efficient mass transport of substrates to the point of oxidation.²⁹⁸ Many organic compounds do not readily cross cell membranes,^{434,435} sesquiterpenes being particularly recalcitrant. Counterstrategies include adding permeability-enhancing agents such as EDTA,³³³ partial lysis of the host,¹²⁰ and engineering mutant host strains with greater membrane permeability.⁴³⁶ Alternatively, the protein can be displayed on the cell surface,⁴³⁷ though this cuts off the supply of NADPH, to which the membrane is also non-permeable. Certain substrates are insoluble, and others too volatile to remain for any length of time in vigorously agitated bacterial growths. Some are harmful to the host,³⁶⁴ making it difficult to keep cultures viable and productive for longer than 48 h,³⁰⁴ while reaction products typically represent an even greater threat, being more water-soluble.

One method of mitigating cytotoxicity is to include a benign organic phase into which the reaction components can partition. Long chain alkanes, which are essentially immune to oxidation even by active P450_{BM3} variants, have been used in this role,³⁰⁰ as have esters such as diisobutyl phthalate,³⁶⁶ which offer an element of polarity. The biotransformation of cyclohexane has been carried out with the substrate forming its own second phase, a protocol in which the culture remained productive for at least 100 h.²³⁷ However, this approach is generally too stressful for the host, activity ceasing after as little as 1.5 h in the oxidation of ($-$)- α -pinene, for example.³⁶⁴

The presence of a second phase can also combat the adverse effects of high product concentrations on enzyme/substrate saturation levels. To illustrate, the apparent K_M for 12-pNCA oxidation was found to be an order of magnitude higher when determined in the presence of 1 mM ($-$)- α -pinene oxidation products.³⁶⁴ Biphasic systems can also be employed *in vitro*, though they do not always emulate the performance of monophasic systems.²⁹⁸ An alternative tactic is to vary the host system. Two metabolites generated during the biotransformation of diclofenac proved to be no impediment to cell growth in yeast, for example.³⁷⁴

Research has been undertaken to optimise fermenter-scale bacterial growth conditions and protein expression levels.^{438,439} The dissolved oxygen concentration has an important bearing on outcomes.⁴⁴⁰ Insufficient oxygenation reduces the longevity and productivity of cultures, but oxygen limitation can be used as a means of suppressing the further oxidation of target products,⁶⁰ which frequently hampers biotransformation. A balance therefore needs to be struck. Variants with enhanced activity profiles can compromise the metabolic pathways of the expression host by oxidising critical biological intermediates.¹²⁴ The productive lives of biotransformations involving variants that possess high leak rates or couple inefficiently also tend to be inferior,³¹² as the reactive oxygen species that are generated cause oxidative stress. Yields of *ca.* 90 μmol product $\text{min}^{-1} \text{g}^{-1}$ cell dry weight (90 U g^{-1} cdw) were achieved over 1.5 h in a 300 mL fermenter using a variant that showed >95% coupling with propane.³¹² For reference, AlkB gave a rate of 30 U g^{-1} cdw with 1-nonene over 5 h. There is evidence to suggest that NADPH availability is yield-limiting *in vivo*,^{304,364} an issue that can be addressed in *E. coli* by overexpressing the zwf gene responsible for the generation of NADPH *via* the pentose phosphate pathway.^{357,441} Another option is to employ knock-out mutants to suppress respiratory and fermentative pathways that also utilise this co-factor.³⁵⁷ The “product-per-glucose” yields given by the propane hydroxylase described above more than trebled as a result of such initiatives even though specific activity levels were reduced by almost 50%.

7.2 Co-factor regeneration and switching

Enzymatic co-factor regeneration is a commonly used method of supporting *in vitro* oxidation or supplementing NAD(P)H production *in vivo*, where the limited generating capacity of the host system can rapidly be overwhelmed. Dehydrogenases, which are compatible with a broad range of P450 substrates and also relatively robust, typically take the partnering role. Systems driven by glucose-6-phosphate,^{10,24,32,114,286,287} glucose,^{345,364,366} isocitrate^{29,326,328,333,442} and formate^{237,298} have all been employed to support P450_{BM3} oxidation, as has ethanol, using an alcohol dehydrogenase from *Thermoanaerobium brockii*.³²¹ *In vivo* indigo yields from indole were enhanced almost 30-fold over 8 h when glucose dehydrogenase was co-expressed with WT,⁴⁴³ while total product yields in a 500-mL α -pinene biotransformation involving a 5-mutation variant increased 4.5-fold to 320 U g^{-1} cdw over 1.5 h.³⁶⁴ A deazaflavin-dependent regeneration system driven by a 100 W lamp has been developed.⁴⁴⁴ Product generation was slower than with other approaches,

but the benign conditions resulted in higher total turnover numbers with respect to the P450 component.

P450_{BM3} has been engineered to accept NADH, which can be sourced at a fraction of the cost of NADPH, as a surrogate electron source.^{72,199,237,356,359} NADH-dependent variants are suitable for *in vivo* applications as well as *in vitro* oxidation, since NADH is produced in greater quantities by *E. coli* than NADPH, and is thus less rapidly exhausted. Introduction of the W1046A mutation produced an enzyme capable of utilising either co-factor, though still roughly twice as efficient with respect to NADPH as to NADH.^{237,359} The homologous substitution had earlier been used to bring about a comparable switch in CPR,⁴⁴⁵ whose crystal structure showed the tryptophan side-chain of the naturally occurring residue lying directly above, and parallel to, the FAD unit. The W1046S mutant was *ca.* 2.5-fold more efficient with respect to NADH in cytochrome *c* reduction than the W1046A mutant,²³⁷ while a W1046D variant was able to accept either co-factor.³⁵⁷ Mutations at other residues close to the NAD(P)H binding site were also influential,^{72,356,357} the R966D/W1046S double mutant giving the highest TTN so far reported for the enzyme (66 700), despite displaying *in vitro* activity levels four times lower than those of WT.²⁹⁸ This mutant was subsequently shown to be capable of accepting electrons from biomimetic co-factors as well as from NADH and NADPH.³⁵⁸ These artificial electron sources could be regenerated using an organorhodium complex, the TTN being *ca.* 300.

In a variation on this theme, NADPH regeneration has been accomplished using an NADH-dependent transhydrogenase harnessed to a glycerol dehydrogenase NADH-regenerating system.⁴⁴⁶ Not all hydrogenases are NADPH-dependent, of course. G6PDH from yeast accepts only NADP⁺, but that from *Leuconostoc mesenteroides* accepts both NAD⁺ and NADP⁺.⁴⁴⁷ Formate dehydrogenases (FDHs) are NAD⁺-dependent, but can be engineered to recycle NADP⁺—indeed, CYP102A2 has been used to assay the performance of an engineered FDH from *Candida boidinii*.⁴⁴⁷ The same applies to phosphite dehydrogenases.

7.3 Peroxide-dependent oxidation and other approaches

More radical approaches circumvent the use of NAD(P)H altogether. The most widely explored employs peroxide as oxidant in place of the co-factor.^{96,332} High peroxide concentrations force the peroxide shunt uncoupling pathway (section 1.2) into reverse, enabling P450s to function in the manner of peroxide-dependent enzymes such as CPO or P450BSβ. BMP is typically used in preference to the full-length enzyme, usually with mutation F87A incorporated, as this significantly enhances performance, though F87G³⁴² and F87V²³⁸ are also effective. Mutagenesis at other residues can further improve both activity and stability.^{123,297,335,372} Organic peroxides such as cumene hydroperoxide or *t*-butyl hydroperoxide may be used in lieu of hydrogen peroxide. While more expensive, these can enhance activity, cumene hydroperoxide raising the *k*_{cat} value for WT with indole by two orders of magnitude²³⁸—though, with other substrates, activity was below that shown by hydrogen peroxide.³³² The enzyme is rapidly inactivated by peroxide, particularly in the

presence of substrate,^{123,332} such that a TTN of just 1000 has been reported for a highly customised variant with 12-pNCA³³⁵—in addition to which, reaction rates are often slow.

Interest has been shown in driving P450 oxidation electrochemically, a field that has been reviewed.⁴⁴⁸ Since the haem iron is buried inside the protein to guard against electron transfer from inadvertent sources, the principal challenge is to design an effective enzyme-electrode interface. Chemical mediators such as cobalt sepulchrone can be used as electron shuttles,⁴⁴² and this approach continues to be used in the spectroelectrochemical titrations carried out to determine reduction potentials. However, confining the protein at the point of electron delivery offers practical advantages for commercial-scale applications. In P450_{BM3}, the first example involved the deposition of WT onto a graphite electrode in a multilayered film, with cyclic voltammetry (CV) being used to demonstrate electron transfer.⁴⁴⁹ Two reduction potentials were observed for the full-length enzyme, one corresponding to that shown by BMP when studied in isolation, and the other to that shown by isolated BMR. The behaviour of the enzyme under such conditions has been studied spectroscopically.⁴⁵⁰ Enhanced haem reduction rates were achieved by attaching pyrene to the Q387C BMP mutant,³⁵⁴ Gln387 being the residue to which earlier researchers had attached a ruthenium complex as a means of effecting haem reduction *via* photo-excitation.³⁴⁸ The reduction potentials of WT BMP and the haem domain of a directed-evolution variant, 1-12G were similar in the absence of CO, as determined by thin-film CV, but diverged when CO-bound, as did dioxygen reduction rates, suggesting that the high catalytic activity of 1-12G could be dioxygen binding-related.⁴⁵¹ Substrate oxidation was not observed, however, and this remained the case when BMP was immobilised using an SDS film.³⁷³ Research on P450_{cam} had suggested that film-based electrochemical oxidation took place as a result of peroxide generated by the P450-mediated reduction of dioxygen activating the peroxide shunt pathway, but variant 5H6, which had been custom-designed for use in peroxide-dependent oxidation, was also inactive under these conditions.³⁷³ CV signals tend to be dominated by the P420 component, where present.⁴⁵² Deconvolution of the electrochemical responses associated with particular system components may be possible using more sophisticated voltammetric methods.⁴⁵³

Two instances of electrochemically-driven substrate oxidation have been reported, both involving electron transfer to the haem iron *via* a protein intermediary. A BMP/flavodoxin fusion gave six times the level of *p*-nitrophenol oxidation as isolated BMP when deposited on modified glassy carbon electrodes.⁴²⁷ This construct had shown superior electrochemical properties to full-length P450_{BM3} in earlier work.²³⁰ Secondly, *p*-nitrophenolate formation was observed when a full-length enzyme variant was trapped on a glassy carbon electrode in polypyrrole and exposed to 12-pNCA.³⁶⁵ A significant increase in the PFR was achieved using a platinum electrode. Enzymes are generally unstable when absorbed directly onto electrodes, but performance can be improved by employing more sophisticated layering techniques.³⁷⁸ A BMP mutant has been immobilised on a functionalised gold electrode.¹⁹⁸

Other alternative electron sources for P450_{BM3} include hydrosulphite,⁴⁵⁴ 1,1'-dicarboxycobaltocene,⁴⁵⁵ and zinc

Published on 18 October 2011. Downloaded by The University of Manchester Library on 2/25/2021 8:45:25 AM.

powder, with cobalt sepulchrate as mediator.³³¹ Catalytic activity was reduced by 80% relative to the NADPH-driven system using the latter approach, but this compared favourably with electrochemically-driven systems, where activity was at least 8-fold lower.⁴³¹ Moreover, significant reductions in K_M values led to activity improvements of up to 50% for engineered variants over WT with NADPH.³⁰⁷ There was some uncertainty as to whether electrons passed from FMN to BMP in the usual fashion in this system.³⁰⁶

The enzyme displayed much enhanced stability ($t_{\frac{1}{2}} = 29$ days at 25 °C *vs.* 2 days in glycerol-free buffer) when co-immobilised with an engineered FDH in a gel matrix.³¹⁸ A single-mutation CYP102A2 variant was immobilised on sepharose, where it proved *ca.* 80% as active as the free enzyme.¹⁴⁵ Enzyme leaching levels were significantly reduced when the F87A mutant of BMP was immobilised on a mesoporous molecular sieve in which the pore sizes had been matched to the enzyme size. Activity towards 12-pNCA was 20% lower than with the free enzyme, but octane activity was twice as high.³³⁸

8 Summary, conclusions and outlook

Almost forty years have elapsed since the discovery of P450_{BM3}, a period during which it has become one of the most intensively studied of all enzymes. Early researchers were fascinated by the idiosyncratic mixture of specificity and promiscuity that characterised its catalytic behaviour, and eager to understand how the complexities of electron delivery were managed in a multi-domain P450 system. Fatty acids were invariably chosen as substrates in the investigations carried out to delineate its properties, and mutagenesis was undertaken only as a means of corroborating sequence alignment-based predictions that particular residues played important roles. Today, with the focus on finding and developing practical applications, it is rare to encounter new research that involves neither mutagenesis nor non-natural substrates. There is a widely shared hope that at least some of the environmentally unfriendly oxidation technologies that currently dominate the landscape can be superseded using engineered P450_{BM3} variants. And yet it would be wrong to regard the enzyme merely as a platform for commercial enterprises, as it also serves as an excellent window onto general aspects of P450 chemistry. Recent studies have reconfirmed its relevance and usefulness as a model for human and other eukaryotic isoforms, and the prodigious range of substrates that it can be adapted to oxidise makes it almost unique as a fundamental research probe in this context.

While the various engineering strategies employed to accelerate non-natural substrate oxidation have differed conceptually and identified unique mutations, most of the high-activity variants so far reported appear to be generic in reach rather than substrate-specific. This is probably because they either possess reshaped active sites that are easier to saturate, or have altered tertiary structures in which extensive substrate-induced conformational change is no longer a prerequisite for rapid inter-domain electron transfer. Only where a mutation has a specific impact on the active site—constricting it sufficiently to impede access for larger substrates or altering polarity at a crucial residue, for example—is it

unlikely to be effective across a broad range of substrates. Indeed, it is tempting to speculate that the reason high-activity variants of the type developed by protein engineers have not evolved *via* natural selection is that the associated reduction in substrate specificity is physiologically undesirable. In principle, it should be possible to develop variants with lower K_M values for non-natural substrates than those so far achieved, but rendering the active site easier to saturate can compromise substrate binding and thereby selectivity, so this is not an ideal strategy for targeting higher catalytic efficiency. Seeking to enhance k_{cat} values by raising FMN-to-haem electron transfer rates may be equally hazardous, however, since mutants with elevated k_f values more often than not show lower k_{cat} values than WT on the evidence to date. Future researchers may therefore need to focus on identifying the other catalytic steps that contribute to rate limitation in P450_{BM3}, and then search for methods of expediting them.

Regio- and stereo-selective control is proving more difficult for engineers to master, as a limited number of the residues in the substrate pocket appear to possess significant selectivity-influencing powers. Few variants capable of materially altering the product profiles given by WT have been reported that do not involve the mutation of at least one of three specific residues: Ala82, Phe87 and Ala328. The recent demonstration that the introduction of just three mutations is sufficient to bring about $\geq 95\%$ perillyl alcohol formation from (*R*)-limonene *vs.* $\leq 1\%$ for WT is an important advance, but it is possible that more radical engineering strategies will be required to produce high yields of specific oxidation products from other substrates. Chimeragenesis is starting to come of age and will surely be pursued further. Another possible approach would be to substitute proline, a conformationally demanding residue, at structurally sensitive positions throughout the protein with the aim of reshaping the active-site architecture. The remarkable proline mutations already identified suggest that, although a high incidence of enzyme misfolding would undoubtedly result, this could be an acceptable trade-off. The tactics recently used to facilitate methane oxidation may also have applications in this area, since co-substrates such as perfluorolaurate could impact not merely activity but also selectivity with certain substrates.

Much has been made of the enzyme's suitability for use in commercial-scale applications, and there is a growing incumbency on researchers to bring this potential to fruition. Bioremediation remains the most promising prospect, and recent advances such as the manipulation of the metabolic pathways of host systems confirm that progress continues to be made. However, the space-time yields and overall productivity of cultures will need to be considerably extended if process economics of the required magnitude are to be achieved. New host systems may be needed, and there are question marks over whether plasmids are sufficiently robust to fulfil the roles being demanded of them. Enhancing the longevity of the enzyme is another area of opportunity—and one that impinges on *in vitro* approaches as well as biotransformation. Total turnover numbers are limited by a range of factors, including the stability of the variants employed, intrinsic activity levels, and the response of the enzyme to specific substrates over extended periods of turnover,

including the inhibition rates associated with each product. Too little is currently known about exit channels and product release—particularly as far as non-natural substrates are concerned—and whether degradation is primarily denaturative in origin, or attributable to co-factor loss, haem modification or other factors.

With recent crystal structures giving a clearer picture of the mechanistic relevance of the conformational changes induced by directed-evolution, an understanding of how such variants enhance catalytic activity has finally begun to emerge. As more structures are solved, the significance of the various salt bridges and even some of the more complicated hydrogen bonding networks in the protein may come more sharply into focus, though rigorous analysis will be required to elucidate their exact roles. On the other hand, there is still no crystal structure for the full-length protein, or for BMP bound with a substrate in a productive conformation (*i.e.* with a C–H bond close to the haem iron), bound with a non-natural substrate, or in the ferrous, ferrous-oxy or ferrous-CO form. While the first FMN-to-haem electron transfer has been well studied, the second electron transfer remains a closed book, and dioxygen activation is still poorly understood. The complexities of palmitate binding at physiological phosphate concentrations have only recently been deciphered, reopening the debate about the physiological role of the enzyme. Slowly, this fascinating protein is revealing its secrets, but a great deal more remains to be learned.

9 Glossary of abbreviations

BMP	CYP102A1 P450 (haem) domain
BMR	CYP102A1 reductase domain
CPO	Chloroperoxidase
cdw	Cell dry weight
CPR	Cytochrome P450 reductase
CV	Cyclic voltammetry
CYP	Cytochrome P450
DTT	Dithiothreitol
FAD	Flavin adenine dinucleotide
FDH	Formate dehydrogenase
FMN	Flavin mononucleotide
G6PDH	Glucose-6-phosphate dehydrogenase
GVQ	A74G/F87V/L188Q
MD	Molecular dynamics
MDMA	3,4-methylenedioxymethylamphetamine
MMO	Methane monooxygenase
NOS	Nitric oxide synthase
NPG	<i>N</i> -palmitoyl glycine
PAH	Polyaromatic hydrocarbon
PDB	Protein data bank
PFR	Product formation rate
pNCA	<i>p</i> -Nitrophenoxycarboxylic acid
rmsd	Root mean square deviation
SB	Substrate-bound
SDS	Sodium dodecyl sulphate
SF	Substrate-free
SRS	Substrate recognition site
TTN	Total turnover number
U g ⁻¹ cdw	μmol product min ⁻¹ g ⁻¹ cell dry weight
WT	Wild-type enzyme

References

- Rupasinghe, M. A. Schuler, N. Kagawa, H. Yuan, L. Lei, B. Zhao, S. L. Kelly, M. R. Waterman and D. C. Lamb, *FEBS Lett.*, 2006, **580**, 6338–6342.
- T. L. Poulos and Y. T. Mehareenna, *Met. Ions Life Sci.*, 2007, 57–96.
- A. Souter, K. J. McLean, W. E. Smith and A. W. Munro, *J. Chem. Technol. Biotechnol.*, 2000, **75**, 933–941.
- R. L. Wright, K. Harris, B. Solow, R. H. White and P. J. Kennelly, *FEBS Lett.*, 1996, **384**, 235–239.
- P. R. Ortiz de Montellano and J. J. De Voss, in *Cytochrome P450: Structure, Mechanism and Biochemistry*, ed. P. R. Ortiz de Montellano, Plenum Publishers, New York, 3rd edn, 2005, pp. 183–246.
- J. Rittle and M. T. Green, *Science*, 2010, **330**, 933–937.
- P. J. Loida and S. G. Sligar, *Biochemistry*, 1993, **32**, 11530–11538.
- M. J. Cryle, J. M. Stuthe, P. R. Ortiz de Montellano and J. J. De Voss, *Chem. Commun.*, 2004, 512–513.
- M. J. Cryle, P. R. Ortiz de Montellano and J. J. De Voss, *J. Org. Chem.*, 2005, **70**, 2455–2469.
- T. J. Volz, D. A. Rock and J. P. Jones, *J. Am. Chem. Soc.*, 2002, **124**, 9724–9725.
- M. J. Cryle and J. J. De Voss, *Angew. Chem., Int. Ed.*, 2006, **45**, 8221–8223.
- C. Li, L. Zhang, C. Zhang, H. Hirao, W. Wu and S. Shaik, *Angew. Chem., Int. Ed.*, 2007, **46**, 8168–8170.
- C. S. Porro, M. J. Sutcliffe and S. P. de Visser, *J. Phys. Chem. A*, 2009, **113**, 11635–11642.
- L. Tian and R. A. Friesner, *J. Chem. Theory Comput.*, 2009, **5**, 1421–1431.
- X. Yuan, Q. Wang, J. H. Horner, X. Sheng and M. Newcomb, *Biochemistry*, 2009, **48**, 9140–9146.
- Y. Miura and A. J. Fulco, *J. Biol. Chem.*, 1974, **249**, 1880–1888.
- R. S. Hare and A. J. Fulco, *Biochem. Biophys. Res. Commun.*, 1975, **65**, 665–672.
- P. P. Ho and A. J. Fulco, *Biochim. Biophys. Acta*, 1976, **431**, 249–256.
- R. S. Matson, R. S. Hare and A. J. Fulco, *Biochim. Biophys. Acta*, 1977, **487**, 487–494.
- A. J. Fulco, *Annu. Rev. Pharmacol.*, 1991, **31**, 177–203.
- Y. Miura and A. J. Fulco, *Biochim. Biophys. Acta*, 1975, **388**, 305–317.
- R. S. Matson, R. A. Stein and A. J. Fulco, *Biochem. Biophys. Res. Commun.*, 1980, **97**, 955–961.
- R. S. Matson and A. J. Fulco, *Biochem. Biophys. Res. Commun.*, 1981, **103**, 531–535.
- F. Ahmed, E. H. Al-Mutairi, K. L. Avery, P. M. Cullis, W. U. Primrose, G. C. K. Roberts and C. L. Willis, *Chem. Commun.*, 1999, 2049–2050.
- S. C. Davis, Z. Sui, J. A. Peterson and P. R. Ortiz de Montellano, *Arch. Biochem. Biophys.*, 1996, **328**, 35–42.
- N. Shirane, Z. Sui, J. A. Peterson and P. R. Ortiz de Montellano, *Biochemistry*, 1993, **32**, 13732–13741.
- J. F. Buchanan and A. J. Fulco, *Biochem. Biophys. Res. Commun.*, 1978, **85**, 1254–1260.
- R. T. Ruetttinger and A. J. Fulco, *J. Biol. Chem.*, 1981, **256**, 5728–5734.
- J. H. Capdevila, S. Wei, C. Helvig, J. R. Falck, Y. Belosludtsev, G. Truan, S. E. Graham-Lorence and J. A. Peterson, *J. Biol. Chem.*, 1996, **271**, 22663–22671.
- L. O. Narhi and A. J. Fulco, *J. Biol. Chem.*, 1986, **261**, 7160–7169.
- C. F. Oliver, S. Modi, W. U. Primrose, L. Y. Lian and G. C. Roberts, *Biochem. J.*, 1997, **327**, 537–544.
- C. K. Chen, T. Shokhireva, R. E. Berry, H. Zhang and F. A. Walker, *JBIC, J. Biol. Inorg. Chem.*, 2008, **13**, 813–824.
- L. O. Narhi, B. H. Kim, P. M. Stevenson and A. J. Fulco, *Biochem. Biophys. Res. Commun.*, 1983, **116**, 851–858.
- L. O. Narhi and A. J. Fulco, *J. Biol. Chem.*, 1987, **262**, 6683–6690.
- L. P. Wen and A. J. Fulco, *J. Biol. Chem.*, 1987, **262**, 6676–6682.
- L. O. Narhi, L. P. Wen and A. J. Fulco, *Mol. Cell. Biochem.*, 1988, **79**, 63–71.
- R. T. Ruetttinger, L. P. Wen and A. J. Fulco, *J. Biol. Chem.*, 1989, **264**, 10987–10995.
- M. J. Cryle and J. J. De Voss, *Tetrahedron: Asymmetry*, 2007, **18**, 547–551.

- 39 M. J. Cryle, R. D. Espinoza, S. J. Smith, N. J. Matovic and J. J. De Voss, *Chem. Commun.*, 2006, 2353–2355.
- 40 M. Budde, M. Morr, R. D. Schmid and V. B. Urlacher, *ChemBioChem*, 2006, **7**, 789–794.
- 41 T. D. Porter, *Trends Biochem. Sci.*, 1991, **16**, 154–158.
- 42 I. F. Sevioukova and J. A. Peterson, *Biochimie*, 1995, **77**, 562–572.
- 43 D. F. Lewis, E. Watson and B. G. Lake, *Mutat. Res.*, 1998, **410**, 245–270.
- 44 B. Amarneh, C. J. Corbin, J. A. Peterson, E. R. Simpson and S. Graham-Lorence, *Mol. Endocrinol.*, 1993, **7**, 1617–1624.
- 45 P. A. Loughran, L. J. Roman, A. E. Aitken, R. T. Miller and B. S. Masters, *Biochemistry*, 2000, **39**, 15110–15120.
- 46 D. F. Lewis, *Drug Metab. Rev.*, 2002, **34**, 55–67.
- 47 S. F. Tuck, J. A. Peterson and P. R. Ortiz de Montellano, *J. Biol. Chem.*, 1992, **267**, 5614–5620.
- 48 C. A. Hasemann, R. G. Kurumbail, S. S. Boddupalli, J. A. Peterson and J. Deisenhofer, *Structure*, 1995, **3**, 41–62.
- 49 I. F. Sevioukova and J. A. Peterson, *Arch. Biochem. Biophys.*, 1995, **317**, 397–404.
- 50 S. S. Boddupalli, R. W. Estabrook and J. A. Peterson, *J. Biol. Chem.*, 1990, **265**, 4233–4239.
- 51 A. W. Munro, H. M. Girvan and K. J. McLean, *Biochim. Biophys. Acta*, 2007, **1770**, 345–359.
- 52 N. Nakayama, A. Takemae and H. Shoun, *J. Biochem.*, 1996, **119**, 435–440.
- 53 T. Kitazume, A. Tanaka, N. Takaya, A. Nakamura, S. Matsuyama, T. Suzuki and H. Shoun, *Eur. J. Biochem.*, 2002, **269**, 2075–2082.
- 54 R. De Mot and A. H. Parret, *Trends Microbiol.*, 2002, **10**, 502–508.
- 55 A. Celik, G. A. Roberts, J. H. White, S. K. Chapman, N. J. Turner and S. L. Flitsch, *Chem. Commun.*, 2006, 4492–4494.
- 56 L. Liu, R. D. Schmid and V. B. Urlacher, *Appl. Microbiol. Biotechnol.*, 2006, **72**, 876–882.
- 57 K. A. White and M. A. Marletta, *Biochemistry*, 1992, **31**, 6627–6631.
- 58 H. Y. Li, K. Darwish and T. L. Poulos, *J. Biol. Chem.*, 1991, **266**, 11909–11914.
- 59 T. Oster, S. S. Boddupalli and J. A. Peterson, *J. Biol. Chem.*, 1991, **266**, 22718–22725.
- 60 S. S. Boddupalli, B. C. Pramanik, C. A. Slaughter, R. W. Estabrook and J. A. Peterson, *Arch. Biochem. Biophys.*, 1992, **292**, 20–28.
- 61 J. S. Miles, A. W. Munro, B. N. Rospendowski, W. E. Smith, J. McKnight and A. J. Thomson, *Biochem. J.*, 1992, **288**, 503–509.
- 62 A. W. Munro, *Biochem. Soc. Trans.*, 1993, **21**, 316S.
- 63 S. D. Black, M. H. Linger, L. C. Freck, S. Kazemi and J. A. Galbraith, *Arch. Biochem. Biophys.*, 1994, **310**, 126–133.
- 64 U. Schwaneberg, A. Sprauer, C. Schmidt-Dannert and R. D. Schmid, *J. Chromatogr. A*, 1999, **848**, 149–159.
- 65 D. Rock and J. P. Jones, *Protein Expression Purif.*, 2001, **22**, 82–83.
- 66 H. Jun, M. Lehe, S. Qing, L. Dongqiang and Y. Shanjing, *Protein Pept. Lett.*, 2005, **12**, 327–331.
- 67 S. Modi, W. U. Primrose, L. Y. Lian and G. C. Roberts, *Biochem. J.*, 1995, **310**, 939–943.
- 68 J. A. Peterson, I. Sevioukova, G. Truan and S. E. Graham-Lorence, *Steroids*, 1997, **62**, 117–123.
- 69 H. Li and T. L. Poulos, *Biochim. Biophys. Acta*, 1999, **1441**, 141–149.
- 70 A. W. Munro, D. G. Leys, K. J. McLean, K. R. Marshall, T. W. Ost, S. Daff, C. S. Miles, S. K. Chapman, D. A. Lysek, C. C. Moser, C. C. Page and P. L. Dutton, *Trends Biochem. Sci.*, 2002, **27**, 250–257.
- 71 A. J. Warman, O. Roitel, R. Neeli, H. M. Girvan, H. E. Seward, S. A. Murray, K. J. McLean, M. G. Joyce, H. Toogood, R. A. Holt, D. Leys, N. S. Scrutton and A. W. Munro, *Biochem. Soc. Trans.*, 2005, **33**, 747–753.
- 72 S. Eiben, L. Kaysser, S. Maurer, K. Kuhnel, V. B. Urlacher and R. D. Schmid, *J. Biotechnol.*, 2006, **124**, 662–669.
- 73 H. M. Girvan, T. N. Waltham, R. Neeli, H. F. Collins, K. J. McLean, N. S. Scrutton, D. Leys and A. W. Munro, *Biochem. Soc. Trans.*, 2006, **34**, 1173–1177.
- 74 C. H. Yun, K. H. Kim, D. H. Kim, H. C. Jung and J. G. Pan, *Trends Biotechnol.*, 2007, **25**, 289–298.
- 75 R. Bernhardt, *J. Biotechnol.*, 2006, **124**, 128–145.
- 76 V. B. Urlacher and S. Eiben, *Trends Biotechnol.*, 2006, **24**, 324–330.
- 77 V. B. Urlacher, S. G. Bell and L. L. Wong, in *Modern Biooxidation*, ed. R. D. Schmid and V. B. Urlacher, Wiley-VCH, Weinheim, 2007, pp. 99–122.
- 78 A. W. Munro, H. M. Girvan and K. J. McLean, *Nat. Prod. Rep.*, 2007, **24**, 585–609.
- 79 S. Govindaraj and T. L. Poulos, *Biochemistry*, 1995, **34**, 11221–11226.
- 80 M. J. Cryle and J. J. De Voss, *ChemBioChem*, 2008, **9**, 261–266.
- 81 L. O. Narhi and A. J. Fulco, *J. Biol. Chem.*, 1982, **257**, 2147–2150.
- 82 N. English, V. Hughes and C. R. Wolf, *J. Biol. Chem.*, 1994, **269**, 26836–26841.
- 83 C. N. Palmer, E. Axen, V. Hughes and C. R. Wolf, *J. Biol. Chem.*, 1998, **273**, 18109–18116.
- 84 L. P. Wen, R. T. Ruettinger and A. J. Fulco, *J. Biol. Chem.*, 1989, **264**, 10996–11003.
- 85 G. C. Shaw and A. J. Fulco, *J. Biol. Chem.*, 1992, **267**, 5515–5526.
- 86 G. C. Shaw and A. J. Fulco, *J. Biol. Chem.*, 1993, **268**, 2997–3004.
- 87 Q. Liang and A. J. Fulco, *J. Biol. Chem.*, 1995, **270**, 18606–18614.
- 88 Q. Liang, J. S. He and A. J. Fulco, *J. Biol. Chem.*, 1995, **270**, 4438–4450.
- 89 Q. Liang, L. Chen and A. J. Fulco, *Biochim. Biophys. Acta*, 1998, **1380**, 183–197.
- 90 K. Makita, J. R. Falck and J. H. Capdevila, *FASEB J.*, 1996, **10**, 1456–1463.
- 91 A. J. Fulco, *Biochim. Biophys. Acta*, 1967, **144**, 701–703.
- 92 N. English, C. N. Palmer, W. L. Alworth, L. Kang, V. Hughes and C. R. Wolf, *Biochem. J.*, 1997, **327**, 363–368.
- 93 T. Kaneda, *Microbiol. Rev.*, 1991, **55**, 288–302.
- 94 S. Govindaraj and T. L. Poulos, *Protein Sci.*, 1996, **5**, 1389–1393.
- 95 S. S. Boddupalli, T. Oster, R. W. Estabrook and J. A. Peterson, *J. Biol. Chem.*, 1992, **267**, 10375–10380.
- 96 G. Truan and J. A. Peterson, *Arch. Biochem. Biophys.*, 1998, **349**, 53–64.
- 97 G. Truan, M. R. Komandla, J. R. Falck and J. A. Peterson, *Arch. Biochem. Biophys.*, 1999, **366**, 192–198.
- 98 S. Graham-Lorence, G. Truan, J. A. Peterson, J. R. Falck, S. Wei, C. Helvig and J. H. Capdevila, *J. Biol. Chem.*, 1997, **272**, 1127–1135.
- 99 L. A. Cowart, J. R. Falck and J. H. Capdevila, *Arch. Biochem. Biophys.*, 2001, **387**, 117–124.
- 100 A. Hegde, D. C. Haines, M. Bondela, B. Chen, N. Schaffer, D. R. Tomchick, M. Machius, H. Nguyen, P. K. Chowdhary, L. Stewart, C. Lopez and J. A. Peterson, *Biochemistry*, 2007, **46**, 14010–14017.
- 101 P. K. Chowdhary, N. Keshavan, H. Q. Nguyen, J. A. Peterson, J. E. Gonzalez and D. C. Haines, *Biochemistry*, 2007, **46**, 14429–14437.
- 102 A. W. Munro, K. Malarkey, J. McKnight, A. J. Thomson, S. M. Kelly, N. C. Price, J. G. Lindsay, J. R. Coggins and J. S. Miles, *Biochem. J.*, 1994, **303**, 423–428.
- 103 A. W. Munro, J. G. Lindsay, J. R. Coggins, S. M. Kelly and N. C. Price, *FEBS Lett.*, 1994, **343**, 70–74.
- 104 A. W. Munro, J. G. Lindsay, J. R. Coggins, S. M. Kelly and N. C. Price, *Biochim. Biophys. Acta*, 1995, **1231**, 255–264.
- 105 A. W. Munro, S. Daff, J. R. Coggins, J. G. Lindsay and S. K. Chapman, *Eur. J. Biochem.*, 1996, **239**, 403–409.
- 106 M. A. Noble, C. S. Miles, S. K. Chapman, D. A. Lysek, A. C. MacKay, G. A. Reid, R. P. Hanzlik and A. W. Munro, *Biochem. J.*, 1999, **339**, 371–379.
- 107 J. P. Clark, C. S. Miles, C. G. Mowat, M. D. Walkinshaw, G. A. Reid, S. N. Daff and S. K. Chapman, *J. Inorg. Biochem.*, 2006, **100**, 1075–1090.
- 108 H. M. Girvan, K. R. Marshall, R. J. Lawson, D. Leys, M. G. Joyce, J. Clarkson, W. E. Smith, M. R. Cheesman and A. W. Munro, *J. Biol. Chem.*, 2004, **279**, 23274–23286.
- 109 H. M. Girvan, H. S. Toogood, R. E. Littleford, H. E. Seward, W. E. Smith, I. S. Ekanem, D. Leys, M. R. Cheesman and A. W. Munro, *Biochem. J.*, 2009, **417**, 65–76.
- 110 S. Modi, W. U. Primrose, J. M. Boyle, C. F. Gibson, L. Y. Lian and G. C. Roberts, *Biochemistry*, 1995, **34**, 8982–8988.
- 111 C. F. Oliver, S. Modi, M. J. Sutcliffe, W. U. Primrose, L. Y. Lian and G. C. Roberts, *Biochemistry*, 1997, **36**, 1567–1572.
- 112 W. C. Huang, A. C. Westlake, J. D. Marechal, M. G. Joyce, P. C. Moody and G. C. Roberts, *J. Mol. Biol.*, 2007, **373**, 633–651.

- Published on 18 October 2011. Downloaded by The University of Manchester Library on 2/25/2021 8:45:25 AM.
- 113 M. B. Murataliev and R. Feyereisen, *Biochemistry*, 1996, **35**, 15029–15037.
- 114 M. B. Murataliev, M. Klein, A. Fulco and R. Feyereisen, *Biochemistry*, 1997, **36**, 8401–8412.
- 115 M. B. Murataliev, L. N. Trinh, L. V. Moser, R. B. Bates, R. Feyereisen and F. A. Walker, *Biochemistry*, 2004, **43**, 1771–1780.
- 116 H. Yeom and S. G. Sligar, *Arch. Biochem. Biophys.*, 1997, **337**, 209–216.
- 117 S. A. Maves, H. Yeom, M. A. McLean and S. G. Sligar, *FEBS Lett.*, 1997, **414**, 213–218.
- 118 D. Appel, S. Lutz-Wahl, P. Fischer, U. Schwaneberg and R. D. Schmid, *J. Biotechnol.*, 2001, **88**, 167–171.
- 119 M. Dietrich, T. A. Do, R. D. Schmid, J. Pleiss and V. B. Urlacher, *J. Biotechnol.*, 2009, **139**, 115–117.
- 120 G. E. Tsotsou, A. E. Cass and G. Gilardi, *Biosens. Bioelectron.*, 2002, **17**, 119–131.
- 121 G. M. Raner, J. A. Hatchell, M. U. Dixon, T. L. Joy, A. E. Haddy and E. R. Johnston, *Biochemistry*, 2002, **41**, 9601–9610.
- 122 D. A. Rock, B. N. Perkins, J. Wahlstrom and J. P. Jones, *Arch. Biochem. Biophys.*, 2003, **416**, 9–16.
- 123 P. C. Cirino and F. H. Arnold, *Adv. Synth. Catal.*, 2002, **344**, 932–937.
- 124 A. Glieder, E. T. Farinas and F. H. Arnold, *Nat. Biotechnol.*, 2002, **20**, 1135–1139.
- 125 C. J. Whitehouse, S. G. Bell, W. Yang, J. A. Yorke, C. F. Blanford, A. J. Strong, E. J. Morse, M. Bartlam, Z. Rao and L. L. Wong, *ChemBioChem*, 2009, **10**, 1654–1656.
- 126 C. J. Whitehouse, W. Yang, J. A. Yorke, B. C. Rowlett, A. J. Strong, C. F. Blanford, S. G. Bell, M. Bartlam, L. L. Wong and Z. Rao, *ChemBioChem*, 2010, **11**, 2549–2556.
- 127 B. Rowlett, J. A. Yorke, A. J. Strong, C. J. C. Whitehouse, S. G. Bell and L. L. Wong, *Protein Cell*, 2011, **2**, 656–671.
- 128 A. J. Fulco, B. H. Kim, R. S. Matson, L. O. Narhi and R. T. Ruettiger, *Mol. Cell Biochem.*, 1983, **53–54**, 155–161.
- 129 B. H. Kim and A. J. Fulco, *Biochem. Biophys. Res. Commun.*, 1983, **116**, 843–850.
- 130 R. T. Ruettiger, B. H. Kim and A. J. Fulco, *Biochim. Biophys. Acta*, 1984, **801**, 372–380.
- 131 L. P. Wen and A. J. Fulco, *Mol. Cell. Biochem.*, 1985, **67**, 77–81.
- 132 N. E. Hopkins, N. English, V. Hughes, C. W. Rowley, C. R. Wolf and W. L. Alworth, *Biochem. Biophys. Res. Commun.*, 1998, **244**, 868–872.
- 133 C. W. Rowley, R. V. Rajnarayanan, N. E. Hopkins and W. L. Alworth, *Biochem. Biophys. Res. Commun.*, 2003, **300**, 102–106.
- 134 N. English, V. Hughes and C. R. Wolf, *Biochem. J.*, 1996, **316**, 279–283.
- 135 N. T. English and L. C. Rankin, *Biochem. Pharmacol.*, 1997, **54**, 443–450.
- 136 R. V. Rajnarayanan, C. W. Rowley, N. E. Hopkins and W. L. Alworth, *J. Agric. Food Chem.*, 2001, **49**, 4930–4936.
- 137 P. K. Chowdhary, L. Stewart, C. Lopez and D. C. Haines, *J. Biotechnol.*, 2008, **135**, 374–376.
- 138 A. J. Fulco and R. T. Ruettiger, *Life Sci.*, 1987, **40**, 1769–1775.
- 139 O. Lentz, V. Urlacher and R. D. Schmid, *J. Biotechnol.*, 2004, **108**, 41–49.
- 140 M. C. Gustafsson, O. Roitel, K. R. Marshall, M. A. Noble, S. K. Chapman, A. Pessegueiro, A. J. Fulco, M. R. Cheesman, C. von Wachenfeldt and A. W. Munro, *Biochemistry*, 2004, **43**, 5474–5487.
- 141 M. Budde, S. C. Maurer, R. D. Schmid and V. B. Urlacher, *Appl. Microbiol. Biotechnol.*, 2004, **66**, 180–186.
- 142 P. K. Chowdhary, M. Alemseghehd and D. C. Haines, *Arch. Biochem. Biophys.*, 2007, **468**, 32–43.
- 143 M. Dietrich, S. Eiben, C. Asta, T. A. Do, J. Pleiss and V. B. Urlacher, *Appl. Microbiol. Biotechnol.*, 2008, **79**, 931–940.
- 144 B. S. Kim, S. Y. Kim, J. Park, W. Park, K. Y. Hwang, Y. J. Yoon, W. K. Oh, B. Y. Kim and J. S. Ahn, *J. Appl. Microbiol.*, 2007, **102**, 1392–1400.
- 145 I. Axarli, A. Prigipaki and N. E. Labrou, *Biomol. Eng.*, 2005, **22**, 81–88.
- 146 I. Axarli, A. Prigipaki and N. E. Labrou, *Enzyme Res.*, 2010, **2010**, 125429.
- 147 M. C. Gustafsson, C. N. Palmer, C. R. Wolf and C. von Wachenfeldt, *Arch. Microbiol.*, 2001, **176**, 459–464.
- 148 D. C. Lamb, L. Lei, B. Zhao, H. Yuan, C. J. Jackson, A. G. Warrilow, T. Skaug, P. J. Dyson, E. S. Dawson, S. L. Kelly, D. L. Hachey and M. R. Waterman, *Appl. Environ. Microbiol.*, 2010, **76**, 1975–1980.
- 149 C. R. Otey, M. Landwehr, J. B. Endelman, K. Hiraga, J. D. Bloom and F. H. Arnold, *PLoS Biol.*, 2006, **4**, e112.
- 150 S. Eiben, H. Bartelmas and V. B. Urlacher, *Appl. Microbiol. Biotechnol.*, 2007, **75**, 1055–1061.
- 151 D. Roccatano, T. S. Wong, U. Schwaneberg and M. Zacharias, *Biopolymers*, 2005, **78**, 259–267.
- 152 O. Lentz, A. Feenstra, T. Habicher, B. Hauer, R. D. Schmid and V. B. Urlacher, *ChemBioChem*, 2006, **7**, 345–350.
- 153 R. Weis, M. Winkler, M. Schittmayer, S. Kambourakis, M. Vink, J. R. Rozzell and A. Glieder, *Adv. Synth. Catal.*, 2009, **351**, 2140–2146.
- 154 A. Seifert, S. Vomund, K. Grohmann, S. Kriening, V. B. Urlacher, S. Laschat and J. Pleiss, *ChemBioChem*, 2009, **10**, 853–861.
- 155 H. Li and T. L. Poulos, *Nat. Struct. Biol.*, 1997, **4**, 140–146.
- 156 O. Gotoh, *J. Biol. Chem.*, 1992, **267**, 83–90.
- 157 J. Y. Kang, S. Y. Kim, D. Kim, D. H. Kim, S. M. Shin, S. H. Park, K. H. Kim, H. C. Jung, J. G. Pan, Y. Joung, Y. T. Chi, H. Chae, T. Ahn and C. H. Yun, *AMB Express*, 2011, **1**, 1.
- 158 M. Zhang and H. J. Vogel, *J. Biol. Chem.*, 1994, **269**, 981–985.
- 159 A. W. Munro, J. G. Lindsay, J. R. Coggins, S. M. Kelly and N. C. Price, *Biochim. Biophys. Acta*, 1996, **1296**, 127–137.
- 160 A. P. Jamakhandi, B. C. Jeffus, V. R. Dass and G. P. Miller, *Arch. Biochem. Biophys.*, 2005, **439**, 165–174.
- 161 S. D. Black, *Biochem. Biophys. Res. Commun.*, 1994, **203**, 162–168.
- 162 I. Sevrioukova, G. Truan and J. A. Peterson, *Biochemistry*, 1996, **35**, 7528–7535.
- 163 T. D. Porter and C. B. Kasper, *Biochemistry*, 1986, **25**, 1682–1687.
- 164 S. Govindaraj and T. L. Poulos, *J. Biol. Chem.*, 1997, **272**, 7915–7921.
- 165 J. L. Vermilion and M. J. Coon, *J. Biol. Chem.*, 1978, **253**, 8812–8819.
- 166 S. Govindaraj, H. Li and T. L. Poulos, *Biochem. Biophys. Res. Commun.*, 1994, **203**, 1745–1749.
- 167 I. Sevrioukova, G. Truan and J. A. Peterson, *Arch. Biochem. Biophys.*, 1997, **340**, 231–238.
- 168 A. W. Munro, M. A. Noble, C. S. Miles, S. N. Daff, A. J. Green, L. Quaroni, S. Rivers, T. W. Ost, G. A. Reid and S. K. Chapman, *Biochem. Soc. Trans.*, 1999, **27**, 190–196.
- 169 O. Pylypenko and I. Schlichting, *Annu. Rev. Biochem.*, 2004, **73**, 991–1018.
- 170 J. A. Peterson and S. S. Boddupalli, *Arch. Biochem. Biophys.*, 1992, **294**, 654–661.
- 171 I. Sevrioukova, C. Shaffer, D. P. Ballou and J. A. Peterson, *Biochemistry*, 1996, **35**, 7058–7068.
- 172 J. L. Vermilion, D. P. Ballou, V. Massey and M. J. Coon, *J. Biol. Chem.*, 1981, **256**, 266–277.
- 173 S. N. Daff, S. K. Chapman, K. L. Turner, R. A. Holt, S. Govindaraj, T. L. Poulos and A. W. Munro, *Biochemistry*, 1997, **36**, 13816–13823.
- 174 I. F. Sevrioukova, H. Li, H. Zhang, J. A. Peterson and T. L. Poulos, *Proc. Natl. Acad. Sci. U. S. A.*, 1999, **96**, 1863–1868.
- 175 H. C. Chen and R. P. Swenson, *Biochemistry*, 2008, **47**, 13788–13799.
- 176 H. Li, A. Das, H. Sibhatu, J. Jamal, S. G. Sligar and T. L. Poulos, *J. Biol. Chem.*, 2008, **283**, 34762–34772.
- 177 I. F. Sevrioukova, J. T. Hazzard, G. Tollin and T. L. Poulos, *J. Biol. Chem.*, 1999, **274**, 36097–36106.
- 178 S. C. Hanley, T. W. Ost and S. Daff, *Biochem. Biophys. Res. Commun.*, 2004, **325**, 1418–1423.
- 179 D. C. Haines, I. F. Sevrioukova and J. A. Peterson, *Biochemistry*, 2000, **39**, 9419–9429.
- 180 M. L. Klein and A. J. Fulco, *Biochim. Biophys. Acta*, 1994, **1201**, 245–250.
- 181 J. T. Hazzard, S. Govindaraj, T. L. Poulos and G. Tollin, *J. Biol. Chem.*, 1997, **272**, 7922–7926.
- 182 N. Kimmich, A. Das, I. Sevrioukova, Y. Mehareenna, S. G. Sligar and T. L. Poulos, *J. Biol. Chem.*, 2007, **282**, 27006–27011.

- 183 H. M. Girvan, D. J. Heyes, N. S. Scrutton and A. W. Munro, *J. Am. Chem. Soc.*, 2007, **129**, 6647–6653.
- 184 M. A. McLean, H. Yeom and S. G. Sligar, *Biochimie*, 1996, **78**, 700–705.
- 185 A. Rupenyan, J. Commandeur and M. L. Groot, *Biochemistry*, 2009, **48**, 6104–6110.
- 186 S. Marchal, H. M. Girvan, A. C. Gorren, B. Mayer, A. W. Munro, C. Balny and R. Lange, *Biophys. J.*, 2003, **85**, 3303–3309.
- 187 H. M. Girvan, A. J. Dunford, R. Neeli, I. S. Ekanem, T. N. Waltham, M. G. Joyce, D. Leys, R. A. Curtis, P. Williams, K. Fisher, M. W. Voice and A. W. Munro, *Arch. Biochem. Biophys.*, 2011, **507**, 75–85.
- 188 I. Seviroukova and J. A. Peterson, *Biochimie*, 1996, **78**, 744–751.
- 189 V. R. Dodhia, A. Fantuzzi and G. Gilardi, *JBIC, J. Biol. Inorg. Chem.*, 2006, **11**, 903–916.
- 190 M. B. Murataliev and R. Feyereisen, *Biochemistry*, 2000, **39**, 12699–12707.
- 191 O. Roitel, N. S. Scrutton and A. W. Munro, *Biochemistry*, 2003, **42**, 10809–10821.
- 192 M. J. Honeychurch, A. O. Hill and L. L. Wong, *FEBS Lett.*, 1999, **451**, 351–353.
- 193 H. M. Girvan, C. W. Levy, P. Williams, K. Fisher, M. R. Cheesman, S. E. Rigby, D. Leys and A. W. Munro, *Biochem. J.*, 2010, **427**, 455–466.
- 194 C. J. Whitehouse, W. Yang, J. A. Yorke, H. G. Tufton, L. C. Ogilvie, S. G. Bell, W. Zhou, M. Bartlam, Z. Rao and L. L. Wong, *Dalton Trans.*, 2011, DOI: 10.1039/C1DT10098J.
- 195 T. W. Ost, J. P. Clark, J. L. Anderson, L. J. Yellowlees, S. Daff and S. K. Chapman, *J. Biol. Chem.*, 2004, **279**, 48876–48882.
- 196 S. D. Black and S. T. Martin, *Biochemistry*, 1994, **33**, 12056–12062.
- 197 U. Siddhanta, A. Presta, B. Fan, D. Wolan, D. L. Rousseau and D. J. Stuehr, *J. Biol. Chem.*, 1998, **273**, 18950–18958.
- 198 V. E. Ferrero, L. Andolfi, G. Di Nardo, S. J. Sadeghi, A. Fantuzzi, S. Cannistraro and G. Gilardi, *Anal. Chem.*, 2008, **80**, 8438–8446.
- 199 T. Kitazume, D. C. Haines, R. W. Estabrook, B. Chen and J. A. Peterson, *Biochemistry*, 2007, **46**, 11892–11901.
- 200 R. Neeli, H. M. Girvan, A. Lawrence, M. J. Warren, D. Leys, N. S. Scrutton and A. W. Munro, *FEBS Lett.*, 2005, **579**, 5582–5588.
- 201 D. C. Haines, D. R. Tomchick, M. Machius and J. A. Peterson, *Biochemistry*, 2001, **40**, 13456–13465.
- 202 J. McKnight, M. R. Cheesman, A. J. Thomson, J. S. Miles and A. W. Munro, *Eur. J. Biochem.*, 1993, **213**, 683–687.
- 203 A. W. Munro, J. G. Lindsay, J. R. Coggins, I. MacDonald, W. E. Smith and B. N. Rospendowski, *Biochem. Soc. Trans.*, 1994, **22**, 54S.
- 204 I. D. Macdonald, W. E. Smith and A. W. Munro, *FEBS Lett.*, 1996, **396**, 196–200.
- 205 K. K. Khan, S. Mazumdar, S. Modi, M. Sutcliffe, G. C. Roberts and S. Mitra, *Eur. J. Biochem.*, 1997, **244**, 361–370.
- 206 J. Hudecek, V. Baumruk, P. Anzenbacher and A. W. Munro, *Biochem. Biophys. Res. Commun.*, 1998, **243**, 811–815.
- 207 I. D. Macdonald, A. W. Munro and W. E. Smith, *Biophys. J.*, 1998, **74**, 3241–3249.
- 208 T. J. Deng, L. M. Proniewicz, J. R. Kincaid, H. Yeom, I. D. Macdonald and S. G. Sligar, *Biochemistry*, 1999, **38**, 13699–13706.
- 209 I. D. G. MacDonald, W. E. Smith and A. W. Munro, *Eur. Biophys. J.*, 1999, **28**, 437–445.
- 210 J. Hudecek, E. Anzenbacherova, P. Anzenbacher, A. W. Munro and P. Hildebrandt, *Arch. Biochem. Biophys.*, 2000, **383**, 70–78.
- 211 P. Anzenbacher and J. Hudecek, *J. Inorg. Biochem.*, 2001, **87**, 209–213.
- 212 S. J. Smith, A. W. Munro and W. E. Smith, *Biopolymers*, 2003, **70**, 620–627.
- 213 Z. Chen, T. W. Ost and J. P. Schelvis, *Biochemistry*, 2004, **43**, 1798–1808.
- 214 T. Jovanovic and A. E. McDermott, *J. Am. Chem. Soc.*, 2005, **127**, 13816–13821.
- 215 D. R. Davydov, G. Hui Bon Hoa and J. A. Peterson, *Biochemistry*, 1999, **38**, 751–761.
- 216 E. Anzenbacherova, N. Bec, P. Anzenbacher, J. Hudecek, P. Soucek, C. Jung, A. W. Munro and R. Lange, *Eur. J. Biochem.*, 2000, **267**, 2916–2920.
- 217 R. Perera, M. Sono, G. M. Raner and J. H. Dawson, *Biochem. Biophys. Res. Commun.*, 2005, **338**, 365–371.
- 218 S. Modi, M. J. Sutcliffe, W. U. Primrose, L. Y. Lian and G. C. Roberts, *Nat. Struct. Biol.*, 1996, **3**, 414–417.
- 219 T. Jovanovic, R. Farid, R. A. Friesner and A. E. McDermott, *J. Am. Chem. Soc.*, 2005, **127**, 13548–13552.
- 220 S. Brenner, S. Hay, H. M. Girvan, A. W. Munro and N. S. Scrutton, *J. Phys. Chem. B*, 2007, **111**, 7879–7886.
- 221 A. Kariakin, D. Davydov, J. A. Peterson and C. Jung, *Biochemistry*, 2002, **41**, 13514–13525.
- 222 C. Jung, V. Schunemann, F. Lendzian, A. X. Trautwein, J. Contzen, M. Galander, L. H. Bottger, M. Richter and A. L. Barra, *Biol. Chem.*, 2005, **386**, 1043–1053.
- 223 G. M. Raner, J. I. Thompson, A. Haddy, V. Tangham, N. Bynum, G. Ramachandra Reddy, D. P. Ballou and J. H. Dawson, *J. Inorg. Biochem.*, 2006, **100**, 2045–2053.
- 224 R. K. Behan, L. M. Hoffart, K. L. Stone, C. Krebs and M. T. Green, *J. Am. Chem. Soc.*, 2006, **128**, 11471–11474.
- 225 R. K. Behan, L. M. Hoffart, K. L. Stone, C. Krebs and M. T. Green, *J. Am. Chem. Soc.*, 2007, **129**, 5855–5859.
- 226 N. Bec, P. Anzenbacher, E. Anzenbacherova, A. C. Gorren, A. W. Munro and R. Lange, *Biochem. Biophys. Res. Commun.*, 1999, **266**, 187–189.
- 227 T. L. Poulos, B. C. Finzel and A. J. Howard, *J. Mol. Biol.*, 1987, **195**, 687–700.
- 228 A. C. Westlake, C. F. Harford-Cross, J. Donovan and L. L. Wong, *Eur. J. Biochem.*, 2001, **265**, 929–935.
- 229 D. R. Davydov, A. A. Kariakin, N. A. Petushkova and J. A. Peterson, *Biochemistry*, 2000, **39**, 6489–6497.
- 230 G. Gilardi, Y. T. Meharennna, G. E. Tsotsou, S. J. Sadeghi, M. Fairhead and S. Giannini, *Biosens. Bioelectron.*, 2002, **17**, 133–145.
- 231 A. Fantuzzi, Y. T. Meharennna, P. B. Briscoe, F. Guerlesquin, S. J. Sadeghi and G. Gilardi, *Biochim. Biophys. Acta, Bioenerg.*, 2009, **1787**, 234–241.
- 232 G. A. Schoch, J. K. Yano, M. R. Wester, K. J. Griffin, C. D. Stout and E. F. Johnson, *J. Biol. Chem.*, 2004, **279**, 9497–9503.
- 233 M. A. Noble, L. Quaroni, G. D. Chumanov, K. L. Turner, S. K. Chapman, R. P. Hanzlik and A. W. Munro, *Biochemistry*, 1998, **37**, 15799–15807.
- 234 D. C. Haines, B. Chen, D. R. Tomchick, M. Bondlala, A. Hegde, M. Machius and J. A. Peterson, *Biochemistry*, 2008, **47**, 3662–3670.
- 235 B. M. van Vugt-Lussenburg, M. C. Damsten, D. M. Maasdijk, N. P. Vermeulen and J. N. Commandeur, *Biochem. Biophys. Res. Commun.*, 2006, **346**, 810–818.
- 236 M. C. Damsten, B. M. van Vugt-Lussenburg, T. Zeldenthuis, J. S. de Vlieger, J. N. Commandeur and N. P. Vermeulen, *Chem.-Biol. Interact.*, 2008, **171**, 96–107.
- 237 S. C. Maurer, K. Kuhnel, L. A. Kayser, S. Eiben, R. D. Schmid and V. B. Urlacher, *Adv. Synth. Catal.*, 2005, **347**, 1090–1098.
- 238 Q. S. Li, J. Ogawa, R. D. Schmid and S. Shimizu, *Biosci., Biotechnol., Biochem.*, 2005, **69**, 293–300.
- 239 W. C. Huang, P. M. Cullis, E. L. Raven and G. C. Roberts, *Metallooms*, 2011, **3**, 410–416.
- 240 M. A. Noble, H. M. Girvan, S. J. Smith, W. E. Smith, M. Murataliev, V. M. Guzov, R. Feyereisen and A. W. Munro, *Drug Metab. Rev.*, 2007, **39**, 599–617.
- 241 S. S. Boddupalli, C. A. Hasemann, K. G. Ravichandran, J. Y. Lu, E. J. Goldsmith, J. Deisenhofer and J. A. Peterson, *Proc. Natl. Acad. Sci. U. S. A.*, 1992, **89**, 5567–5571.
- 242 K. G. Ravichandran, S. S. Boddupalli, C. A. Hasemann, J. A. Peterson and J. Deisenhofer, *Science*, 1993, **261**, 731–736.
- 243 H. Li and T. L. Poulos, *Acta Crystallogr., Sect. D: Biol. Crystallogr.*, 1995, **51**, 21–32.
- 244 H. M. Girvan, H. E. Seward, H. S. Toogood, M. R. Cheesman, D. Leys and A. W. Munro, *J. Biol. Chem.*, 2006, **282**, 564–572.
- 245 D. Leys, C. G. Mowat, K. J. McLean, A. Richmond, S. K. Chapman, M. D. Walkinshaw and A. W. Munro, *J. Biol. Chem.*, 2002, **278**, 5141–5147.
- 246 H. Li and T. L. Poulos, *Biochimie*, 1996, **78**, 695–699.
- 247 J. Kuper, T. S. Wong, D. Roccatano, M. Wilmanns and U. Schwaneberg, *J. Am. Chem. Soc.*, 2007, **129**, 5786–5787.
- 248 P. A. Williams, J. Cosme, D. M. Vinkovic, A. Ward, H. C. Angove, P. J. Day, C. Vonrhein, I. J. Tickle and H. Jhoti, *Science*, 2004, **305**, 683–686.

- 249 A. B. Carmichael and L. L. Wong, *Eur. J. Biochem.*, 2001, **268**, 3117–3125.
- 250 T. W. Ost, C. S. Miles, J. Murdoch, Y. Cheung, G. A. Reid, S. K. Chapman and A. W. Munro, *FEBS Lett.*, 2000, **486**, 173–177.
- 251 F. E. Zilly, J. P. Acevedo, W. Augustyniak, A. Deege, U. W. Hausig and M. T. Reetz, *Angew. Chem., Int. Ed.*, 2011, **50**, 2720–2724.
- 252 T. Kitazume, Y. Yamazaki, S. Matsuyama, H. Shoun and N. Takaya, *Appl. Microbiol. Biotechnol.*, 2008, **79**, 981–988.
- 253 D. C. Haines, *Protein Pept. Lett.*, 2006, **13**, 977–980.
- 254 D. A. Rock, A. E. Boitano, J. L. Wahlstrom, D. A. Rock and J. P. Jones, *Bioorg. Chem.*, 2002, **30**, 107–118.
- 255 H. Yeom, S. G. Sligar, H. Li, T. L. Poulos and A. J. Fulco, *Biochemistry*, 1995, **34**, 14733–14740.
- 256 E. Stjernschantz, B. M. van Vugt-Lussenburg, A. Bonifacio, S. B. de Beer, G. van der Zwan, C. Gooijer, J. N. Commandeur, N. P. Vermeulen and C. Oostenbrink, *Proteins: Struct., Funct., Bioinf.*, 2008, **71**, 336–352.
- 257 T. W. Ost, C. S. Miles, A. W. Munro, J. Murdoch, G. A. Reid and S. K. Chapman, *Biochemistry*, 2001, **40**, 13421–13429.
- 258 T. W. Ost, J. Clark, C. G. Mowat, C. S. Miles, M. D. Walkinshaw, G. A. Reid, S. K. Chapman and S. Daff, *J. Am. Chem. Soc.*, 2003, **125**, 15010–15020.
- 259 T. W. Ost, A. W. Munro, C. G. Mowat, P. R. Taylor, A. Pesceguero, A. J. Fulco, A. K. Cho, M. A. Cheesman, M. D. Walkinshaw and S. K. Chapman, *Biochemistry*, 2001, **40**, 13430–13438.
- 260 M. L. Klein and A. J. Fulco, *J. Biol. Chem.*, 1993, **268**, 7553–7561.
- 261 M. D. Paulsen and R. L. Ornstein, *Proteins: Struct., Funct., Genet.*, 1995, **21**, 237–243.
- 262 Y. T. Chang and G. H. Loew, *J. Biomol. Struct. Dyn.*, 1999, **16**, 1189–1203.
- 263 S. K. Ludemann, V. Louannas and R. C. Wade, *J. Mol. Biol.*, 2000, **303**, 797–811.
- 264 P. J. Winn, S. K. Ludemann, R. Gauges, V. Louannas and R. C. Wade, *Proc. Natl. Acad. Sci. U. S. A.*, 2002, **99**, 5361–5366.
- 265 R. C. Wade, P. J. Winn, I. Schlichting and Sudarko, *J. Inorg. Biochem.*, 2004, **98**, 1175–1182.
- 266 T. I. Oprea, G. Hummer and A. E. Garcia, *Proc. Natl. Acad. Sci. U. S. A.*, 1997, **94**, 2133–2138.
- 267 K. H. Clodfelter, D. J. Waxman and S. Vajda, *Biochemistry*, 2006, **45**, 9393–9407.
- 268 Y. T. Chang and G. H. Loew, *Proteins: Struct., Funct., Genet.*, 1999, **34**, 403–415.
- 269 K. A. Feenstra, E. B. Starikov, V. B. Urlacher, J. N. Commandeur and N. P. Vermeulen, *Protein Sci.*, 2007, **16**, 420–431.
- 270 K. P. Ravindranathan, E. Gallicchio, R. A. Friesner, A. E. McDermott and R. M. Levy, *J. Am. Chem. Soc.*, 2006, **128**, 5786–5791.
- 271 K. P. Ravindranathan, E. Gallicchio, A. E. McDermott and R. M. Levy, *J. Am. Chem. Soc.*, 2007, **129**, 474–475.
- 272 T. S. Wong, F. H. Arnold and U. Schwaneberg, *Biotechnol. Bioeng.*, 2004, **85**, 351–358.
- 273 D. Roccatano, T. S. Wong, U. Schwaneberg and M. Zacharias, *Biopolymers*, 2006, **83**, 467–476.
- 274 A. Seifert, M. Antonovici, B. Hauer and J. Pleiss, *ChemBioChem*, 2011, **12**, 1346–1351.
- 275 R. J. Branco, A. Seifert, M. Budde, V. B. Urlacher, M. J. Ramos and J. Pleiss, *Proteins: Struct., Funct., Bioinf.*, 2008, **73**, 597–607.
- 276 C. S. Miles, T. W. Ost, M. A. Noble, A. W. Munro and S. K. Chapman, *Biochim. Biophys. Acta*, 2000, **1543**, 383–407.
- 277 V. Urlacher and R. D. Schmid, *Curr. Opin. Biotechnol.*, 2002, **13**, 557–564.
- 278 V. B. Urlacher and R. D. Schmid, *Methods Enzymol.*, 2004, **388**, 208–224.
- 279 S. G. Bell, N. Hoskins, C. J. C. Whitehouse and L. L. Wong, *Met. Ions Life Sci.*, 2007, 437–476.
- 280 S. Kumar, *Expert Opin. Drug Metab. Toxicol.*, 2010, **6**, 115–131.
- 281 S. T. Jung, R. Lauchli and F. H. Arnold, *Curr. Opin. Biotechnol.*, 2011, DOI: 10.1016/j.copbio.2011.1002.1008.
- 282 E. M. Gillam, *Clin. Exp. Pharmacol. Physiol.*, 2005, **32**, 147–152.
- 283 E. M. Gillam, *Chem. Res. Toxicol.*, 2008, **21**, 220–231.
- 284 K. Faber, *Biotransformations in Organic Chemistry*, Springer-Verlag, Berlin, 6th edn, 2011.
- 285 F. P. Guengerich, *Nat. Rev. Drug Discovery*, 2002, **1**, 359–366.
- 286 J. R. Falck, Y. K. Reddy, D. C. Haines, K. M. Reddy, U. M. Krishna, S. Graham, B. Murry and J. A. Peterson, *Tetrahedron Lett.*, 2001, **42**, 4131–4133.
- 287 A. Celik, D. Sperandio, R. E. Speight and N. J. Turner, *Org. Biomol. Chem.*, 2005, **3**, 2688–2690.
- 288 I. C. Gunsalus and G. C. Wagner, *Methods Enzymol.*, 1978, **52**, 166–188.
- 289 S. Schneider, M. G. Wubbolts, D. Sanglard and B. Witholt, *Tetrahedron: Asymmetry*, 1998, **9**, 2832–2844.
- 290 M. J. Cryle, N. J. Matovic and J. J. De Voss, *Tetrahedron Lett.*, 2007, **48**, 133–136.
- 291 S. Lutz and W. M. Patrick, *Curr. Opin. Biotechnol.*, 2004, **15**, 291–297.
- 292 J. D. Bloom, M. M. Meyer, P. Meinhold, C. R. Otey, D. MacMillan and F. H. Arnold, *Curr. Opin. Struct. Biol.*, 2005, **15**, 447–452.
- 293 M. T. Reetz, *J. Org. Chem.*, 2009, **74**, 5767–5778.
- 294 J. Sanchis, L. Fernandez, J. D. Carballeira, J. Drone, Y. Gumulya, H. Hobenreich, D. Kahakeaw, S. Kille, R. Lohmer, J. J. Peyralans, J. Podteteneff, S. Prasad, P. Soni, A. Taglieber, S. Wu, F. E. Zilly and M. T. Reetz, *Appl. Microbiol. Biotechnol.*, 2008, **81**, 387–397.
- 295 V. B. Urlacher, A. Makhsumkhanov and R. D. Schmid, *Appl. Microbiol. Biotechnol.*, 2005, **70**, 53–59.
- 296 A. M. Sawayama, M. M. Chen, P. Kulanthaivel, M. S. Kuo, H. Hemmerle and F. H. Arnold, *Chem.-Eur. J.*, 2009, **15**, 11723–11729.
- 297 C. R. Otey, G. Bandara, J. Lalonde, K. Takahashi and F. H. Arnold, *Biotechnol. Bioeng.*, 2006, **93**, 494–499.
- 298 K. Kuehnel, S. C. Maurer, Y. Galeeva, W. Frey, S. Laschat and V. Urlacher, *Adv. Synth. Catal.*, 2007, **349**, 1451–1461.
- 299 Q. S. Li, U. Schwaneberg, M. Fischer, J. Schmitt, J. Pleiss, S. Lutz-Wahl and R. D. Schmid, *Biochim. Biophys. Acta*, 2001, **1545**, 114–121.
- 300 R. J. Sowden, S. Yasmin, N. H. Rees, S. G. Bell and L. L. Wong, *Org. Biomol. Chem.*, 2005, **3**, 57–64.
- 301 B. M. Lussenburg, L. C. Babel, N. P. Vermeulen and J. N. Commandeur, *Anal. Biochem.*, 2005, **341**, 148–155.
- 302 Y. Watanabe, S. Laschat, M. Budde, O. Affolter, Y. Shimada and V. B. Urlacher, *Tetrahedron*, 2007, **63**, 9413–9422.
- 303 C. J. Whitehouse, S. G. Bell, H. G. Tufton, R. J. Kenny, L. C. Ogilvie and L. L. Wong, *Chem. Commun.*, 2008, 966–968.
- 304 J. Dietrich, Y. Yoshikuni, K. Fisher, F. Woolard, D. Ockey, D. McPhee, N. Renninger, M. Chang, D. Baker and J. D. Keasling, *ACS Chem. Biol.*, 2009, **4**, 261–267.
- 305 C. J. Whitehouse, N. H. Rees, S. G. Bell and L. L. Wong, *Chem.-Eur. J.*, 2011, **17**, 6862–6868.
- 306 J. Nazor and U. Schwaneberg, *ChemBioChem*, 2006, **7**, 638–644.
- 307 J. Nazor, S. Dannenmann, R. O. Adjei, Y. B. Fordjour, I. T. Ghompson, M. Blanusa, D. Roccatano and U. Schwaneberg, *Protein Eng., Des. Sel.*, 2007, **21**, 29–35.
- 308 J. C. Lewis, S. Bastian, C. S. Bennett, Y. Fu, Y. Mitsuda, M. M. Chen, W. A. Greenberg, C. H. Wong and F. H. Arnold, *Proc. Natl. Acad. Sci. U. S. A.*, 2009, **106**, 16550–16555.
- 309 A. Rentmeister, T. R. Brown, C. D. Snow, M. N. Carbone and F. H. Arnold, *ChemCatChem*, 2011, **3**, 1065–1071.
- 310 T. S. Wong, N. Wu, D. Roccatano, M. Zacharias and U. Schwaneberg, *J. Biomol. Screening*, 2005, **10**, 246–252.
- 311 L. G. Quaroni, H. E. Seward, K. J. McLean, H. M. Girvan, T. W. Ost, M. A. Noble, S. M. Kelly, N. C. Price, M. R. Cheesman, W. E. Smith and A. W. Munro, *Biochemistry*, 2004, **43**, 16416–16431.
- 312 R. Fasan, M. M. Chen, N. C. Crook and F. H. Arnold, *Angew. Chem., Int. Ed.*, 2007, **46**, 8414–8418.
- 313 A. Rentmeister, F. H. Arnold and R. Fasan, *Nat. Chem. Biol.*, 2008, **5**, 26–28.
- 314 M. E. Ener, Y. T. Lee, J. R. Winkler, H. B. Gray and L. Cheruzel, *Proc. Natl. Acad. Sci. U. S. A.*, 2010, **107**, 18783–18786.
- 315 J. C. Lewis, S. M. Mantovani, Y. Fu, C. D. Snow, R. S. Komor, C. H. Wong and F. H. Arnold, *ChemBioChem*, 2010, **11**, 2502–2505.
- 316 J. Reinen, S. Ferman, E. Vottero, N. P. Vermeulen and J. N. Commandeur, *J. Biomol. Screening*, 2011, **16**, 239–250.
- 317 J. Reinen, L. L. Kalma, S. Begheijn, F. Heus, J. N. Commandeur and N. P. Vermeulen, *Xenobiotica*, 2011, **41**, 59–70.

- 318 S. C. Maurer, H. Schulze, R. D. Schmid and V. B. Urlacher, *Adv. Synth. Catal.*, 2003, **345**, 802–810.
- 319 Q. S. Li, U. Schwaneberg, P. Fischer and R. D. Schmid, *Chem.–Eur. J.*, 2000, **6**, 1531–1536.
- 320 P. Meinhold, M. W. Peters, M. M. Chen, K. Takahashi and F. H. Arnold, *ChemBioChem*, 2005, **6**, 1765–1768.
- 321 T. Kubo, M. W. Peters, P. Meinhold and F. H. Arnold, *Chem.–Eur. J.*, 2006, **12**, 1216–1220.
- 322 P. Meinhold, M. W. Peters, A. Hartwick, A. R. Hernandez and F. H. Arnold, *Adv. Synth. Catal.*, 2006, **348**, 763–772.
- 323 M. G. Shapiro, G. G. Westmeyer, P. A. Romero, J. O. Szablowski, B. Kuster, A. Shah, C. R. Otey, R. Langer, F. H. Arnold and A. Jasanoff, *Nat. Biotechnol.*, 2010, **28**, 264–270.
- 324 C. K. Chen, R. E. Berry, T. Shokhireva, M. B. Murataliev, H. Zhang and F. A. Walker, *JBIC, J. Biol. Inorg. Chem.*, 2009, **15**, 159–174.
- 325 K. L. Tee and U. Schwaneberg, *Angew. Chem., Int. Ed.*, 2006, **45**, 5380–5383.
- 326 M. W. Peters, P. Meinhold, A. Glieder and F. H. Arnold, *J. Am. Chem. Soc.*, 2003, **125**, 13442–13450.
- 327 D. F. Munzer, P. Meinhold, M. W. Peters, S. Feichtenofer, H. Griengl, F. H. Arnold, A. Glieder and A. de Raadt, *Chem. Commun.*, 2005, 2597–2599.
- 328 M. Landwehr, L. Hochrein, C. R. Otey, A. Kasrayan, J. E. Backvall and F. H. Arnold, *J. Am. Chem. Soc.*, 2006, **128**, 6058–6059.
- 329 W. L. Alworth, Q. W. Xia and H. M. Liu, *FASEB J.*, 1997, **11**(9SS), 90.
- 330 U. Schwaneberg, C. Schmidt-Dannert, J. Schmitt and R. D. Schmid, *Anal. Biochem.*, 1999, **269**, 359–366.
- 331 U. Schwaneberg, D. Appel, J. Schmitt and R. D. Schmid, *J. Biotechnol.*, 2000, **84**, 249–257.
- 332 Q. S. Li, J. Ogawa and S. Shimizu, *Biochem. Biophys. Res. Commun.*, 2001, **280**, 1258–1261.
- 333 U. Schwaneberg, C. Otey, P. C. Cirino, E. Farinas and F. H. Arnold, *J. Biomol. Screening*, 2001, **6**, 111–117.
- 334 Q. S. Li, J. Ogawa, R. D. Schmid and S. Shimizu, *FEBS Lett.*, 2001, **508**, 249–252.
- 335 P. C. Cirino and F. H. Arnold, *Angew. Chem., Int. Ed.*, 2003, **42**, 3299–3301.
- 336 C. R. Otey, J. J. Silberg, C. A. Voigt, J. B. Endelman, G. Bandara and F. H. Arnold, *Chem. Biol.*, 2004, **11**, 309–318.
- 337 C. J. Whitehouse, S. G. Bell and L. L. Wong, *Chem.–Eur. J.*, 2008, **14**, 10905–10908.
- 338 E. Weber, D. Sirim, T. Schreiber, B. Thomas, J. Pleiss, M. Hunger, R. Glaser and V. B. Urlacher, *J. Mol. Catal. B: Enzym.*, 2010, **64**, 29–37.
- 339 E. Weber, A. Seifert, M. Antonovici, C. Geinitz, J. Pleiss and V. B. Urlacher, *Chem. Commun.*, 2011, **47**, 944–946.
- 340 E. Vottero, V. Rea, J. Lastdrager, M. Honing, N. P. Vermeulen and J. N. Commandeur, *JBIC, J. Biol. Inorg. Chem.*, 2011, **16**, 899–912.
- 341 M. J. Coon, D. F. McGinnity, A. D. N. Vaz, H. M. Liu, D. A. Mullin, H. Sato and T. Shimizu, *FASEB J.*, 1997, **11**(9SS), 21.
- 342 G. M. Raner, A. J. Hatchell, P. E. Morton, D. P. Ballou and M. J. Coon, *J. Inorg. Biochem.*, 2000, **81**, 153–160.
- 343 T. N. Waltham, H. M. Girvan, C. F. Butler, S. R. Rigby, A. J. Dunford, R. A. Holt and A. W. Munro, *Metalloomics*, 2011, **3**, 369–378.
- 344 A. Daiber, S. Herold, C. Schoneich, D. Namgaladze, J. A. Peterson and V. Ullrich, *Eur. J. Biochem.*, 2000, **267**, 6729–6739.
- 345 W. T. Sulistyaningdyah, J. Ogawa, Q. S. Li, C. Maeda, Y. Yano, R. D. Schmid and S. Shimizu, *Appl. Microbiol. Biotechnol.*, 2004, **67**, 556–562.
- 346 N. Misawa, M. Nodate, T. Otomatsu, K. Shimizu, C. Kaido, M. Kikuta, A. Ideno, H. Ikenaga, J. Ogawa, S. Shimizu and K. Shindo, *Appl. Microbiol. Biotechnol.*, 2010, **90**, 147–157.
- 347 S. H. Park, D. H. Kim, D. Kim, H. C. Jung, J. G. Pan, T. Ahn and C. H. Yun, *Drug Metab. Dispos.*, 2010, **38**, 732–739.
- 348 I. Sevrioukova, C. E. Immoos, T. L. Poulos and P. Farmer, *Isr. J. Chem.*, 2000, **40**, 47–53.
- 349 H. M. Li, L. H. Mei, V. B. Urlacher and R. D. Schmid, *Appl. Biochem. Biotechnol.*, 2007, **144**, 27–36.
- 350 M. C. Damsten, J. S. de Vlieger, W. M. Niessen, H. Irth, N. P. Vermeulen and J. N. Commandeur, *Chem. Res. Toxicol.*, 2008, **21**, 2181–2187.
- 351 E. T. Farinas, U. Schwaneberg, A. Glieder and F. H. Arnold, *Adv. Synth. Catal.*, 2001, **343**, 601–606.
- 352 M. G. Joyce, H. M. Girvan, A. W. Munro and D. Leys, *J. Biol. Chem.*, 2004, **279**, 23287–23293.
- 353 L. L. Wu, C. L. Yang, F. C. Lo, C. H. Chiang, C. W. Chang, K. Y. Ng, H. H. Chou, H. Y. Hung, S. I. Chan and S. S. Yu, *Chem.–Eur. J.*, 2011, **17**, 4774–4787.
- 354 A. K. Udit, M. G. Hill, V. G. Bittner, F. H. Arnold and H. B. Gray, *J. Am. Chem. Soc.*, 2004, **126**, 10218–10219.
- 355 C. J. C. Whitehouse, *D Phil Thesis*, University of Oxford, 2009.
- 356 A. J. Dunford, H. M. Girvan, N. S. Scrutton and A. W. Munro, *Biochim. Biophys. Acta Proteins Proteomics*, 2009, **1794**, 1181–1189.
- 357 R. Fasan, N. C. Crook, M. W. Peters, P. Meinhold, T. Buelter, M. Landwehr, P. C. Cirino and F. H. Arnold, *Biotechnol. Bioeng.*, 2011, **108**, 500–510.
- 358 J. D. Ryan, R. H. Fish and D. S. Clark, *ChemBioChem*, 2008, **9**, 2579–2582.
- 359 R. Neeli, O. Roitel, N. S. Scrutton and A. W. Munro, *J. Biol. Chem.*, 2004, **280**, 17634–17644.
- 360 J. D. Bloom, S. T. Labthavikul, C. R. Otey and F. H. Arnold, *Proc. Natl. Acad. Sci. U. S. A.*, 2006, **103**, 5869–5874.
- 361 J. D. Bloom, P. A. Romero, Z. Lu and F. H. Arnold, *Biol. Direct*, 2007, **2**, 17.
- 362 J. D. Bloom, Z. Lu, D. Chen, A. Raval, O. S. Venturelli and F. H. Arnold, *BMC Biol.*, 2007, **5**, 29.
- 363 O. Lentz, Q.-S. Li, U. Schwaneberg, S. Lutz-Wahl, P. Fischer and R. D. Schmid, *J. Mol. Catal. B: Enzym.*, 2001, **15**, 123–133.
- 364 H. Schewe, B. A. Kaup and J. Schrader, *Appl. Microbiol. Biotechnol.*, 2007, **78**, 55–65.
- 365 D. Holtmann, K. M. Mangold and J. Schrader, *Biotechnol. Lett.*, 2009, **31**, 765–770.
- 366 H. Schewe, D. Holtmann and J. Schrader, *Appl. Microbiol. Biotechnol.*, 2009, **83**, 849–857.
- 367 B. M. van Vugt-Lussenburg, E. Stjernschantz, J. Lastdrager, C. Oostenbrink, N. P. Vermeulen and J. N. Commandeur, *J. Med. Chem.*, 2007, **50**, 455–461.
- 368 D. H. Kim, K. H. Kim, D. H. Kim, K. H. Liu, H. C. Jung, J. G. Pan and C. H. Yun, *Drug Metab. Dispos.*, 2008, **36**, 2166–2170.
- 369 D. H. Kim, T. Ahn, H. C. Jung, J. G. Pan and C. H. Yun, *Drug Metab. Dispos.*, 2009, **37**, 932–936.
- 370 D. H. Kim, K. H. Kim, D. Kim, H. C. Jung, J. G. Pan, Y. T. Chi, T. Ahn and C. H. Yun, *J. Mol. Catal. B: Enzym.*, 2010, **63**, 179–187.
- 371 K. H. Kim, J. Y. Kang, D. H. Kim, S. H. Park, D. Kim, K. D. Park, Y. J. Lee, H. C. Jung, J. G. Pan, T. Ahn and C. H. Yun, *Drug Metab. Dispos.*, 2010, **39**, 140–150.
- 372 O. Salazar, P. C. Cirino and F. H. Arnold, *ChemBioChem*, 2003, **4**, 891–893.
- 373 A. K. Udit, M. G. Hill and H. B. Gray, *Langmuir*, 2006, **22**, 10854–10857.
- 374 J. S. van Leeuwen, G. Vredenburg, S. Dragovic, T. F. Tjong, J. C. Vos and N. P. Vermeulen, *Toxicol. Lett.*, 2011, **200**, 162–168.
- 375 Q. S. Li, J. Ogawa, R. D. Schmid and S. Shimizu, *Appl. Environ. Microbiol.*, 2001, **67**, 5735–5739.
- 376 H. Schulze, R. D. Schmid and T. T. Bachmann, *Anal. Chem.*, 2004, **76**, 1720–1725.
- 377 W. T. Sulistyaningdyah, J. Ogawa, Q. S. Li, R. Shinkyo, T. Sakaki, K. Inouye, R. D. Schmid and S. Shimizu, *Biotechnol. Lett.*, 2004, **26**, 1857–1860.
- 378 A. Pardo-Jacques, R. Basseguy and A. Bergel, *Electrochim. Acta*, 2006, **52**, 979–987.
- 379 M. Alcalde, E. T. Farinas and F. H. Arnold, *J. Biomol. Screening*, 2004, **9**, 141–146.
- 380 E. T. Farinas, M. Alcalde and F. Arnold, *Tetrahedron*, 2004, **60**, 525–528.
- 381 A. Seifert and J. Pleiss, *Proteins: Struct., Funct., Bioinf.*, 2009, **74**, 1028–1035.
- 382 E. M. Gillam, A. M. Aguinaldo, L. M. Notley, D. Kim, R. G. Mundkowski, A. A. Volkov, F. H. Arnold, P. Soucek, J. J. DeVoss and F. P. Guengerich, *Biochem. Biophys. Res. Commun.*, 1999, **265**, 469–472.

- 383 M. Waibel, H. Schulze, N. Huber and T. T. Bachmann, *Biosens. Bioelectron.*, 2006, **21**, 1132–1140.
- 384 C. R. Otey and J. M. Joern, *Methods Mol. Biol.*, 2003, **230**, 141–148.
- 385 F. H. Arnold and G. Georgiou, *Methods Mol. Biol.*, 2003, **230**, 83–183.
- 386 K. L. Tee and U. Schwaneberg, *Comb. Chem. High Throughput Screening*, 2007, **10**, 197–217.
- 387 R. Fasan, Y. T. Meharennna, C. D. Snow, T. L. Poulos and F. H. Arnold, *J. Mol. Biol.*, 2008, **383**, 1069–1080.
- 388 J. C. Lewis and F. H. Arnold, *Chimia*, 2009, **63**, 309–312.
- 389 A. W. Munro, J. R. Coggins and J. G. Lindsay, *Biochem. Soc. Trans.*, 1993, **21**, 409S.
- 390 K. J. McLean, H. M. Girvan and A. W. Munro, *Expert Opin. Drug Metab. Toxicol.*, 2007, **3**, 847–863.
- 391 S. J. Sadeghi, Y. T. Meharennna, A. Fantuzzi, F. Valetti and G. Gilardi, *Faraday Discuss.*, 2000, **116**, 135–153; discussion pp. 171–190.
- 392 C. Helvig and J. H. Capdevila, *Biochemistry*, 2000, **39**, 5196–5205.
- 393 M. Fairhead, S. Giannini, E. M. Gillam and G. Gilardi, *JBIC, J. Biol. Inorg. Chem.*, 2005, **10**, 842–853.
- 394 S. Fuziwara, I. Sagami, E. Rozhkova, D. Craig, M. A. Noble, A. W. Munro, S. K. Chapman and T. Shimizu, *J. Inorg. Biochem.*, 2002, **91**, 515–526.
- 395 M. Landwehr, M. Carbone, C. R. Otey, Y. Li and F. H. Arnold, *Chem. Biol.*, 2007, **14**, 269–278.
- 396 Y. Li, D. A. Drummond, A. M. Sawayama, C. D. Snow, J. D. Bloom and F. H. Arnold, *Nat. Biotechnol.*, 2007, **25**, 1051–1056.
- 397 P. C. Cirino, Y. Tang, K. Takahashi, D. A. Tirrell and F. H. Arnold, *Biotechnol. Bioeng.*, 2003, **83**, 729–734.
- 398 T. S. Wong, D. Roccatano and U. Schwaneberg, *Biotechnol. J.*, 2007, **2**, 133–142.
- 399 H. E. Seward, H. M. Girvan and A. W. Munro, *Dalton Trans.*, 2005, 3419–3426.
- 400 T. L. Poulos, *JBIC, J. Biol. Inorg. Chem.*, 1996, **1**, 356–359.
- 401 A. W. Munro, S. N. Daff, K. L. Turner and S. K. Chapman, *Biochem. Soc. Trans.*, 1997, **25**, S629.
- 402 M. T. Fisher and S. G. Sligar, *J. Am. Chem. Soc.*, 1985, **107**, 5018–5019.
- 403 E. J. Mueller, P. J. Loida and S. G. Sligar, in *Cytochrome P450: Structure, Mechanism and Biochemistry*, ed. P. R. Ortiz de Montellano, Plenum Publishers, New York, 2nd edn, 1995, pp. 83–124.
- 404 G. Di Nardo, A. Fantuzzi, A. Sideri, P. Panicco, C. Sassone, C. Giunta and G. Gilardi, *JBIC, J. Biol. Inorg. Chem.*, 2007, **12**, 313–323.
- 405 N. Pons, S. Pipino and F. De Matteis, *Biochem. Pharmacol.*, 2003, **66**, 405–414.
- 406 C. A. Reilly and G. S. Yost, *Drug Metab. Dispos.*, 2005, **33**, 530–536.
- 407 S. P. de Visser, *Chem.–Eur. J.*, 2006, **12**, 8168–8177.
- 408 D. Kumar, S. P. De Visser and S. Shaik, *J. Am. Chem. Soc.*, 2004, **126**, 5072–5073.
- 409 M. J. Cupp and T. S. Tracy, *Am. Fam. Physician*, 1998, **57**, 107–116.
- 410 F. P. Guengerich, *Met. Ions Life Sci.*, 2007, 561–589.
- 411 K. K. Dubey, S. Haque, A. Jawed, B. P. Singh and B. K. Behera, *Process Biochem.*, 2010, **45**, 1036–1042.
- 412 V. S. Lelyveld, E. Brustad, F. H. Arnold and A. Jasanoff, *J. Am. Chem. Soc.*, 2011, **133**, 649–651.
- 413 T. Tashiro and K. Mori, *Tetrahedron: Asymmetry*, 2005, **16**, 1801–1806.
- 414 W. A. Duetz, A. H. Fjallman, S. Ren, C. Jourdat and B. Witholt, *Appl. Environ. Microbiol.*, 2001, **67**, 2829–2832.
- 415 J. B. van Beilen, R. Holtackers, D. Luscher, U. Bauer, B. Witholt and W. A. Duetz, *Appl. Environ. Microbiol.*, 2005, **71**, 1737–1744.
- 416 J. B. van Beilen and E. G. Funhoff, *Appl. Microbiol. Biotechnol.*, 2007, **74**, 13–21.
- 417 R. Balasubramanian, S. M. Smith, S. Rawat, L. A. Yatsunyk, T. L. Stemmler and A. C. Rosenzweig, *Nature*, 2010, **465**, 115–119.
- 418 W. Adam, Z. Lukacs, C. R. Saha-Möller, B. Weckerle and P. Schreier, *Eur. J. Org. Chem.*, 2000, 2923–2926.
- 419 D. J. Koch, M. M. Chen, J. B. van Beilen and F. H. Arnold, *Appl. Environ. Microbiol.*, 2008, **75**, 337–344.
- 420 A. W. Munro, J. G. Lindsay and J. R. Coggins, *Biochem. Soc. Trans.*, 1993, **21**, 412S.
- 421 N. Kawakami, O. Shoji and Y. Watanabe, *Angew. Chem., Int. Ed.*, 2011, **50**, 5315–5318.
- 422 P. R. Ortiz de Montellano, B. L. Mangold, C. Wheeler, K. L. Kunze and N. O. Reich, *J. Biol. Chem.*, 1983, **258**, 4208–4213.
- 423 J. A. Fruetel, R. L. Mackman, J. A. Peterson and P. R. Ortiz de Montellano, *J. Biol. Chem.*, 1994, **269**, 28815–28821.
- 424 R. Ullrich and M. Hofrichter, *Cell. Mol. Life Sci.*, 2007, **64**, 271–293.
- 425 A. N. J. Shaw, C. F. Oliver, S. Modi, W. U. Primrose, L. Y. Lian and G. C. K. Roberts, *FASEB J.*, 1997, **11**(9SS), 218.
- 426 R. K. Gudiminchi and M. S. Smit, *Appl. Microbiol. Biotechnol.*, 2010, **90**, 117–126.
- 427 A. Fantuzzi, Y. T. Meharennna, P. B. Briscoe, C. Sassone, B. Borgia and G. Gilardi, *Chem. Commun.*, 2006, 1289–1291.
- 428 Y. Jiang, X. He and P. R. Ortiz de Montellano, *Biochemistry*, 2006, **45**, 533–542.
- 429 M. K. Julsing, S. Cornelissen, B. Buhler and A. Schmid, *Curr. Opin. Chem. Biol.*, 2008, **12**, 177–186.
- 430 E. O'Reilly, V. Kohler, S. L. Flitsch and N. J. Turner, *Chem. Commun.*, 2011, **47**, 2490–2501.
- 431 V. B. Urlacher, S. Lutz-Wahl and R. D. Schmid, *Appl. Microbiol. Biotechnol.*, 2004, **64**, 317–325.
- 432 R. Wichmann and D. Vasic-Racki, *Adv. Biochem. Eng. Biotechnol.*, 2005, **92**, 225–260.
- 433 F. Hollmann, K. Hofstetter and A. Schmid, *Trends Biotechnol.*, 2006, **24**, 163–171.
- 434 S. Schneider, M. G. Wubbolts, D. Sanglard and B. Witholt, *Appl. Environ. Microbiol.*, 1998, **64**, 3784–3790.
- 435 R. R. Chen, *Appl. Microbiol. Biotechnol.*, 2007, **74**, 730–738.
- 436 N. Lee, W. Y. Jang and J. Park, *Biotechnol. Bioprocess Eng.*, 2011, **16**, 7–12.
- 437 S. K. Yim, D. H. Kim, H. C. Jung, J. G. Pan, H. S. Kang, T. Ahn and C. H. Yun, *J. Microbiol. Biotechnol.*, 2010, **20**, 712–717.
- 438 Y. Lu and L. H. Mei, *J. Zhejiang Univ. Sci. B*, 2007, **8**, 27–32.
- 439 S. Pflug, S. M. Richter and V. B. Urlacher, *J. Biotechnol.*, 2007, **129**, 481–488.
- 440 S. Schneider, M. G. Wubbolts, G. Oesterhelt, D. Sanglard and B. Witholt, *Biotechnol. Bioeng.*, 1999, **64**, 333–341.
- 441 S. Lim, Y. Jung, H. Shin and Y. Lee, *J. Biosci. Bioeng.*, 2002, **93**, 543–549.
- 442 R. W. Estabrook, K. M. Faulkner, M. S. Shet and C. W. Fisher, *Methods Enzymol.*, 1996, **272**, 44–51.
- 443 Y. Lu and L. H. Mei, *J. Ind. Microbiol. Biotechnol.*, 2006, **34**, 247–253.
- 444 F. E. Zilly, A. Taglieber, F. Schulz, F. Hollmann and M. T. Reetz, *Chem. Commun.*, 2009, 7152–7154.
- 445 O. Dohr, M. J. Paine, T. Friedberg, G. C. Roberts and C. R. Wolf, *Proc. Natl. Acad. Sci. U. S. A.*, 2001, **98**, 81–86.
- 446 T. Mouri, T. Shimizu, N. Kamiya, M. Goto and H. Ichinose, *Biotechnol. Prog.*, 2009, **25**, 1372–1378.
- 447 A. Andreadeli, D. Platis, V. Tishkov, V. Popov and N. E. Labrou, *FEBS J.*, 2008, **275**, 3859–3869.
- 448 A. M. Bond, B. D. Fleming and L. L. Martin, *Met. Ions Life Sci.*, 2007, 127–155.
- 449 B. D. Fleming, Y. Tian, S. G. Bell, L. L. Wong, V. Urlacher and H. A. Hill, *Eur. J. Biochem.*, 2003, **270**, 4082–4088.
- 450 A. K. Udit, K. D. Hagen, P. J. Goldman, A. Star, J. M. Gillan, H. B. Gray and M. G. Hill, *J. Am. Chem. Soc.*, 2006, **128**, 10320–10325.
- 451 A. K. Udit, N. Hindoyan, M. G. Hill, F. H. Arnold and H. B. Gray, *Inorg. Chem.*, 2005, **44**, 4109–4111.
- 452 P. Panicco, Y. Astuti, A. Fantuzzi, J. R. Durrant and G. Gilardi, *J. Phys. Chem. B*, 2008, **112**, 14063–14068.
- 453 B. D. Fleming, J. Zhang, A. M. Bond, S. G. Bell and L. L. Wong, *Anal. Chem.*, 2005, **77**, 3502–3510.
- 454 X. Fang and J. R. Halpert, *Drug Metab. Dispos.*, 1996, **24**, 1282–1285.
- 455 A. K. Udit, F. H. Arnold and H. B. Gray, *J. Inorg. Biochem.*, 2004, **98**, 1547–1550.